Genomics, Expression and Developmental Analysis of Murine and Human Plexin B3

DISSERTATION

zur Erlangung des akademischen Grades

"Doktor der Naturwissenschaften"

am Department Biologie

der Fakultät für Mathematik, Informatik und Naturwisenschaffen

an der Universität Hamburg

vorgelegt von

Šárka Krejčová

aus Prag

Hamburg 2006

Genehmigt vom Department Biologie
der Fakultät für Mathematik, Informatik und Naturwissenschaften
an der Universität Hamburg
auf Antrag von Herrn Professor Dr. A. RODEWALD
Weiterer Gutachter der Dissertation:
Herr Professor Dr. A. GAL
Tag der Disputation: 25. November 2005

Hamburg, den 11. November 2005

Professor Dr. Arno Frühwald
Dekan

Genomics, Expression and Developmental Analysis of Murine and Human Plexin B3

Ph.D. thesis by Šárka Krejčová

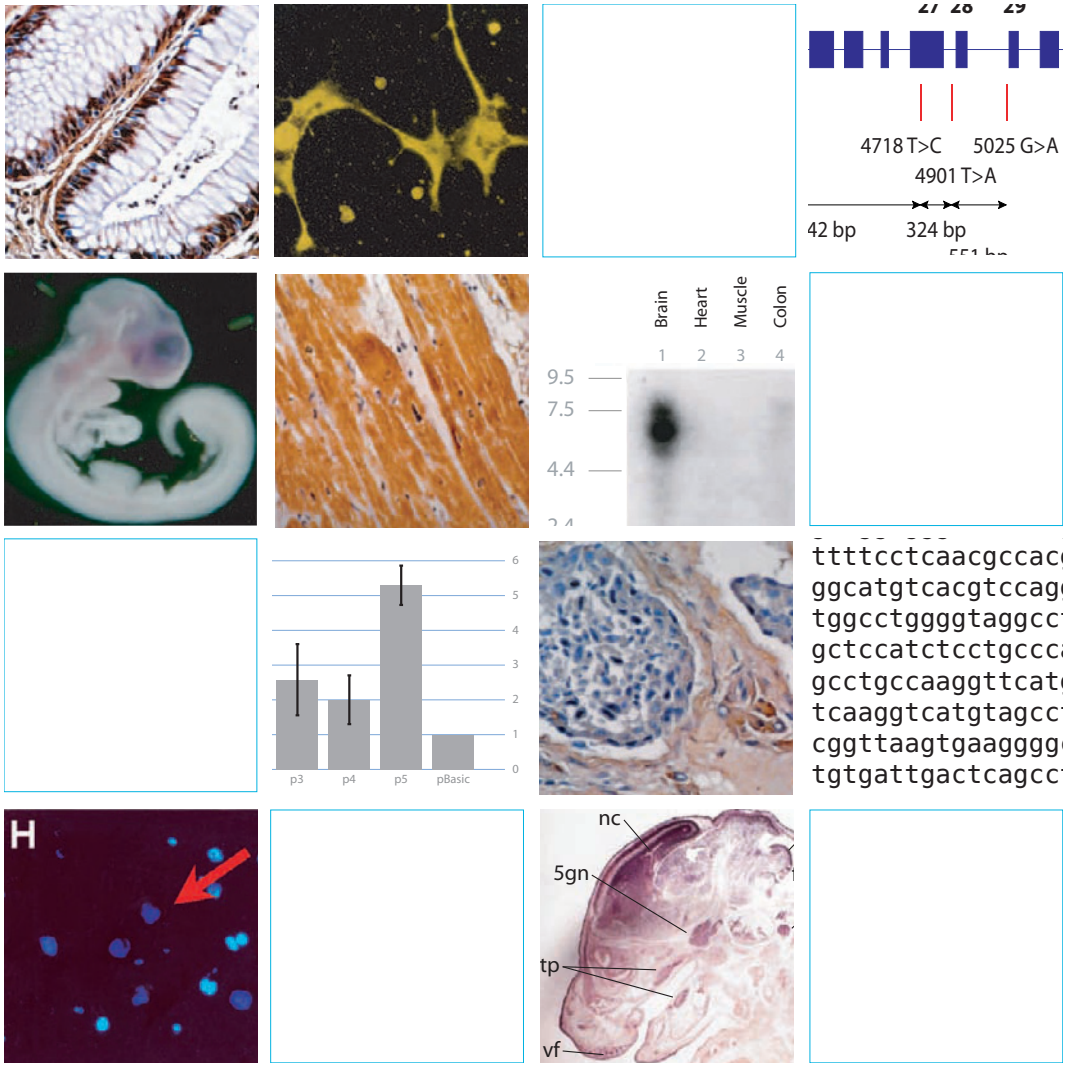

Hamburg 2006

KAISER PERMANENTE®

Kaiser Foundation Health Plan of the Northwest

August 29, 2005

Dr. Med. Sarka Krejcova
Institute of Human Genetics
University Hospital-Eppendorf
Butenfeld 42
22529 Hamburg
Germany
Telefax: +49 (040) 42803 5098

Re. Review of Dr. Sarka Krejcova's PhD thesis entitled *Genomics, expression and developmental analysis of murine and human Plexin B3.*

Dear Dr. Krejcova, and **TO WHOM IT MAY CONCERN:**

I am writing on reviewing the language content of the thesis entitled *Genomics, expression and developmental analysis of murine and human Plexin B3* by Dr. Sarka Krejcova. I have read the thesis and confirm that the English is correct and very understandable in grammar and content. The thesis is suitable for defense. If you have specific questions or concerns regarding this statement please feel free to contact me.

Sincerely,

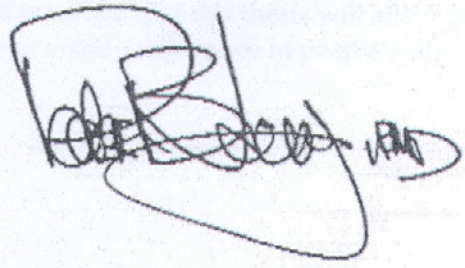

Peter Jacky, PhD, FACMG
Director Cytogenetics/Molecular Genetics
Northwest Permanente, PC, Physicians and Surgeons
Airport Way Regional Laboratory
13705 NE Airport Way, Suite C
Portland, OR 97230-1048
Tel (503) 258-6721
Fax (503) 258-6732
Email: peter.jacky@kp.org

Neboj se neúspěchu, je to tvůj přítel.

Don’t be afraid of the failure, it’s your friend.

Preface

This work was carried out at the Institute of Human Genetics, University Hospital-Eppendorf, Hamburg, during the years 2000-2005 under the supervision of Prof. Dr. Andreas Gal and Prof. Dr. Alexander Rodewald and has been submitted as Ph.D. thesis in September 2005.

It has been a long and sometimes difficult travel from my safe and wellknown background in the medical genetics in Prague to the unknown and complex destination of molecular biology in Hamburg.

Prof. Dr. Eva Seemanova was my first teacher in Prague and my first supervisor in the field of medical genetics. I remember her first genetic lectures, not in the auditorium or at the lab bench, but in front of the patients with questions about this field of science involving their lives in sometimes dramatic ways. I realized early that the goal of science is not only to satisfy our personal curiosity.

I have learned from everyday interaction with patients that behind the succes in science are still patients suffering from different genetically inherited diseases, when genes are mutated, proteins are not in proper place, enzymes are insufficient, neurons are degenerating etc. It is our goal as scientists not only to understand the complexity of life, but also to turn our knowledge into help, care and treatment for those in need.

When I was working in Neurogenetics laboratory in Institute of Biology and Medical Genetics in Prague Prof. Dr. Petr Goetz encouraged my wish and interest to study molecular biology in more depth. He sent me 'away' to get more experiences and pushed me to 'do it now!'. His personal motivation was very helpful and I am sorry that I was not able to keep my promise to come back soon...

It is my hope that this thesis will allow me to proceed my future career in a way that will allow me to make a difference in people's life.

Affidavit

I hereby declare that I have done the present work by myself, not used other than the stated sources and aids, and that any used statement from literature is noted as well. I further confirm that this dissertation is not submitted to any other institution to open the dissertation procedure.

Hamburg, September 10th, 2005 Šárka Krejčová

Abbreviations

A_{260}	absorbance at 260 nm
Amp	ampicillin
AP	alkaline phosphatase
APS	ammonium persulfate
B3	Plexin B3
BDT	Big Dye Terminator
bp	base pairs
BSA	bovine serum albumine
Ca^{2+}	Calcium
Cdc42	Cell division cycle 42
cAMP	cyclic adenosine monophosphate
cGMP	cyclic guanosine monophosphate
cDNA	complementary deoxyribonucleic acid
CP	cytoplasmatic domain
CRMP	Collapsin response mediator protein
C-Terminus	Carboxy-terminus
CHO	chinese hamster ovary
Cm	chloramphenicol
CNS	central nervous system
C-terminus	carboxy-terminus
Cy3	Cyanin3
DAPI	4′,6-diamidino-2-phenylindole
dbSNP	Database of Single Nucleotide Polymorphisms
ddH_2O	double distilled water
DEPC	diethylpyrocarbonate
D-MEM	Dulbecco's Modified Eagle Medium
DNA	deoxyribonucleic acid
dNTP	2′-desoxyribonucleotide-5′-triphosphate
DMSO	dimethylsulfoxid
DSMZ	Deutsche Sammlung von Mikroorganismen und Zellkulturen
DTT	dithiothreitol
ECM	extracellular matrix
Ecto-Domain	extracellular domain
EtOH	Ethanol
et al.	and others (*et altera*)
FGFR	Fibroblast growth factor receptor
FV/FVIII	Coagulations factor V/VIII homolog domain
E.coli	*Escherichia coli*
EDTA	ethylendiamintetraacetic acid
EST	expressed sequence tag
FCS	fetal calf serum
Fig.	figure
GAP	GTPase activating protein
GDI	Guanine nucleotide dissociation inhibitor
GEF	Guanin nucleotide exchange factor
G-P-Repeats	Glycin-Prolin-reach repeats
GPI	Glycosylphosphatidylinositol
GTPase	GDP/GTP binding protein with GTPase-activity
GDP	Guanosin-5′-diphosphat
GTP	Guanosin-5′-triphosphat

continues on next page

continued from previous page

h	hour
HPLC	high pressure liquid chromatography
ICC	immunocytochemistry
ICM	Intracellular matrix
IHC	immunohistochemistry
kb	kilobase pairs
kDa	kilodalton
Km	kanamycin sulfate
lacZBeta	gene encoding N-terminal part of Beta-galactosidase
g, mg, µg, pg	Gram, Milligram, Microgram, Picogram
HRP	horseradish peroxidase
Ig	Immunoglobulin
IPT	Immunoglobulin-like Domains in Plexin and Transcriptions factors
IC	intracellular
LARG	Leukemie associated Rho-GEF
LB	Luria Broth medium
m	milli
mAb	monoclonal antibody
µ	micro
min	minute
mRNA	messenger ribonucleic acid
n	nano
NCBI	National Center for Biotechnology Information
Neo	neomycin
N-terminus	amino-terminus
LiAc	Lithium acetat
mA	Milliampere
MAPK	mitogen activated protein kinase
Mg^{2+}	Magnesium
M, mM, µM	molar (mol/l), millimolar, micromolar
mol, mmol, µ mol	Mol, Millimol, Micromol
MRS	Met related sequences
NP1	Neuropilin 1
NP2	Neuropilin 2
NP40	non-ionized detergent P40
OD550	optical density at 550 nm
OMIM	Online Mendelian Inheritance in Man
ON	over night
OTK	Offtrack Tyrosin kinase receptor
p.a.	per analytical
PFA	paraformaldehyd
p	pico
PAA	polyacrylamide
PAGE	polyacrylamide gel electrophoresis
PBS	phosphate buffered saline
PCR	polymerase chain reaction
P/S	penicillin-streptomycin
RNA	ribonucleic acid
RNase	ribonuclease
rpm	rounds per minute
RT	room temperature
RT-PCR	reverse transcriptase polymerase chain reaction
s	second

continues on next page

continued from previous page

PNS	peripheral nervous system
PSI	Plexin, Semaphorins and Integrins domains
Rac	Protein with GTPase-activity (similar to ras-related C3 botulinum toxin substrate1)
Ras	GTPase, Rat Tumor, Sarcome-type induced (rat sarcoma)
PDZ	Protein motif, Rho protein with GTPase-activity (ras homology)
S. cerevisiae	*Saccharomyces cerevisiae* (Bake Yeast)
Sema	Semaphorin
SDS	Natriumdodecylsulfat
SE	Standard error
SD	Standart deviation
SP	Signal peptide
SP-Domain	Sex und Plexin-Domain
SSC	standard saline citrate buffer
SSCP	single strand conformation polymorphism
Tab.	table
TBE	Tris-borate-EDTA buffer
TBST	Tris-buffered saline + Tween 20
Tc	tetracycline
TE	Tris-EDTA
TEMED	N,N,N′,N′-tetramethylethylenediamine
U	unit (enzymatic activity)
UTR	untranslated region
UV	ultraviolet
TM	Transmembrane Domain
Tris	Tris-(hydroxymethyl-)aminomethan
TSP	Thrombospondin
Tween 20	Polyoxyethylensorbitan-Monolaurat
V	volt
VEGF	vascular endothelial growth factor
VEGFR2	vascular endothelial growth factor receptor 2
VESPR	viral encoded semaphorin protein receptor; Plexin C1
v/v	volume percent (volume per volume)
W	watt
w/v	weight percent (weight per volume)
wt	wilde type
X-gal	5-bromo-4-chloro-3-indolyl-beta-D-galactopyranoside

Single- and three-letter amino acid code

A	Ala	alanine	M	Met	methionine
C	Cys	cysteine	N	Asn	asparagine
D	Asp	aspartic acid	P	Pro	proline
E	Glu	glutamic acid	Q	Gln	glutamine
F	Phe	phenylalanine	R	Arg	arginine
G	Gly	glycine	S	Ser	serine
H	His	histidine	T	Thr	threonine
I	Ile	isoleucine	V	Val	valine
K	Lys	lysine	W	Trp	tryptophan
L	Leu	leucine	Y	Tyr	tyrosine

Table of Contents

Abbreviations 3

Summary 14

Zusammenfassung 16

I Introduction 18

1 How do axons navigate? 19

2 Guidance cues and their receptors 20

3 Structural domains of plexins 21

4 Semaphorins signal through the plexins 23

5 Plexin and neuropilin interplay in receptor complexes 24

6 Knock-out mouse models 27

7 Xq28 28

8 X-chromosomal genes and mental retardation 29

9 Syndromic and non-syndromic forms of XLMR 31

10 Plexin B3 32

Aims of the study 34

II Materials and methods 35

11 Materials 36

11.1 Molecular biology 36

11.2 Cell culture 37

11.3 Silver staining 38

11.4 PCR, RT-PCR, cloning and electrophoresis 39

11.5 *In situ* hybridization, immunohistochemistry 39
11.6 Buffers and solutions 40

12 Chemicals **42**
12.1 Nuclear staining 42
12.2 Bacterial strains 42
12.3 Cell lines 43
12.4 Commercial vectors used in present work 43
12.5 Primary antibodies 43
12.5.1 PLXNB3-specific primary antibodies 43
12.5.2 Commercially available primary antibodies 44
12.6 Secondary antibodies 45

13 Synthetic oligonucleotides **46**
13.1 Oligonucleotides used for sequencing/vector sequencing 46
13.2 Oligonucleotides used for Northern blot 46
13.3 Oligonucleotides used in RT-PCR analysis of *PLXNB3* isoforms 46
13.4 Oligonucleotides used for *in situ* hybridization 46
13.5 Oligonucleotides used in promoter assay 47
13.6 Oligonucleotides used in exon trapping 47
13.7 Oligonucleotides used for mutation screening 47

III Methods **49**

14 Subjects **50**

15 DNA and RNA isolation **50**
15.1 Isolation of genomic DNA from blood 50
15.2 Isolation of cytoplasmic RNA from cells 50
15.3 Isolation of plasmid DNA in small scale 51
15.4 Isolation of plasmid DNA in large scale 51

16 DNA and RNA standard methods **52**
16.1 Cutting of DNA by restriction endonucleases 52
16.2 Agarose gel electrophoresis 52
16.3 Purification and precipitation of PCR products 52
16.4 Cycle sequencing 53
16.5 Determination of DNA concentration 53

17 Molecular biology methods **53**
17.1 Generation of competent *Escherichia coli* cells for chemical transformation 53
17.2 Cloning of PCR products 54
17.3 Dephosphorylation of 5′-termini of DNA fragments 54
17.4 Ligation of DNA fragments 54
17.5 Transformation of competent cells with plasmid DNA 55

18 Polymerase Chain Reaction **56**
18.1 DNA amplification by polymerase chain reaction 56
18.2 Colony PCR of *E. coli* cells 56
18.3 cDNA synthesis and RT-PCR 57

19 Single strand conformation polymorphism analysis **57**
19.1 Polyacrylamide gel electrophoresis 57
19.2 Silver staining of DNA fragments on polyacrylamide gels 57

20 Cell biology methods **58**
20.1 Culture of adherent cells 58
20.2 Freezing and thawing of adherent cells 58
20.3 Transient transfection by liposome mediated DNA-transfer 58

21 Northern blot and RNA tissue array **59**

22 RT-PCR analysis *PLXNB3* splicing isoforms **59**

23 *In situ* hybridisation **59**
23.1 Tissue preparation 59
23.2 *In vitro* transcription (digoxigenin labelling) 59
23.3 Precipitation and preparation of cRNA probes 60
23.4 Non-radioactive *in situ* hybridization 60
23.5 Whole mount *in situ* hybridization 61
23.6 *In situ* hybridization on cultured mouse cerebellar cells 62
23.7 Cell cultures of neurons, astrocytes and oligodendrocytes 62
23.8 Immunohistochemistry on paraffin-embedded sections 63
23.9 Immunohistochemistry with fluorescent secondary antibody 63

24 Exon trapping **64**
24.1 Exon trapping constructs 64

25 Promoter assay **64**

25.1 Promoter constructs . . . 64
25.2 Transfection assay . . . 65
25.3 Cell lysate preparation and β-galactosidase assay . . . 65

26 Computer based analysis **67**

27 NCBI entries of sequences **67**

IV Results **68**

28 Expression pattern of *PlxnB3* **69**
28.1 *PlxnB3* is expressed in neurons . . . 69
28.2 In hippocampus, *PlxnB3* is expressed predominantly in NeuN-positive cells . . . 71
28.3 *PlxnB3* is expressed in cultured primary neurons . . . 71

29 Developmental expression of *PlxnB3* **73**
29.1 Analysis of the embryonic expression of *PlxnB3* by *in situ* hybridization . . . 73
29.1.1 Stage E8 . . . 73
29.1.2 Stage E9 . . . 73
29.1.3 Stage E10.5 . . . 74
29.1.4 Stage E11.5 . . . 75
29.1.5 Stage E15 . . . 75
29.2 Analysis of the expression of *PlxnB3* by whole mount *in situ* hybridization . . . 77

30 *PLXNB3* expression in human organs **78**
30.1 Northern blot and Multiple RNA dot blot array analysis . . . 78
30.2 Alternative splicing of *PLXNB3* mRNA in adult human tissues . . . 80
30.3 Predominant neuronal expression of *PLXNB3* in the human brain . . . 82
30.4 *PLXNB3* is not expressed in astrocytes and oligondendrocytes . . . 84
30.5 Immunolocalization of plexin B3 protein parallels the predominant neuronal distribution of its mRNA in the human brain . . . 85
30.6 Immunolocalization of human plexin B3 protein in non-neuronal tissues . . . 87

31 Mutation screening of *PLXNB3* **89**
31.1 Rare sequence variants . . . 90
31.2 Polymorphisms in *PLXNB3* . . . 91
31.3 Evolution of haplotypes . . . 93
31.3.1 Genotyping of *PLXNB3* . . . 93
31.3.2 Haplotypes based on single nucleotide polymorphisms . . . 93

31.4 Phylogenetic tree based on human, chimp, rat, and mouse sequences 96

32 Exon trapping **97**

32.1 Exon trapping based on pSPL3 minigene expression 97

32.2 Different splicing isoforms *in vivo* 98

33 Functional characterization of the human *PLXBN3* promoter **100**

33.1 Computer-assisted promoter sequence analysis of *PLXNB3* 100

33.2 Analysis of the 5′ region of *PLXNB3* 100

33.3 Computational analysis of conserved promoter elements 101

33.4 Functional analysis of the *PLXNB3* promoter region 101

33.5 Comparison of transient expression assays in various cell lines 102

V Discussion **110**

34 Disease causing mutation versus polymorphism **111**

35 *PLXNB3* is a candidate gene for X-linked mental retardation **112**

36 Sequence variance findings **113**

37 Sensitivity of SSCP **114**

38 Intronic mutation IVS22+21G>A **115**

39 Exon trapping assay results in different splicing isoforms *in vivo* **115**

40 Alternative splicing **116**

41 *PlxnB3* mRNA expression pattern **118**

42 *PLXNB3* expression pattern **120**

43 Non-neuronal expression of *PLXNB3* was not detected **121**

44 General aspects of *in situ* hybridization protocol **121**

45 Functional analysis of the *PLXNB3* promoter region **123**

46 Promoter assays analysis showed two major results **124**

Conclusion **126**

Publication list **127**

List of Figures

1.1 Schematic drawing of mechanism and molecular biology of axon guidance. . . . 20

3.1 Domain structure of plexins 22

4.1 Domain structure of semaphorins and neuropilins 24

7.1 Selected genes in Xq28 28

28.1 The position of the *PlxnB3* specific DIG-labelled cRNA probes relative to the *PlxnB3* mRNA 69

28.2 *In situ* hybridization of mouse brain with DIG-labelled antisense cRNA of *PlxnB3* 70

28.3 *PlxnB3* mRNA is expressed in NeuN-positive cells of the mouse hippocampus but not detectable in GFAP positive cells (astrocytes) and CNPase positive cells (oligodendrocytes). 71

28.4 Expression of *PlxnB3* in cultivated primary murine cerebellar neurons. 72

29.1 *In situ* hybridization on E8 mouse embryo section with *PlxnB3*-specific probe . . 73

29.2 *In situ* hybridization on E9 mouse embryo section with *PlxnB3* specific probe. . . 74

29.3 *In situ* hybridization on E10.5 mouse embryo section with *PlxnB3*-specific probe. 74

29.4 In situ hybridization on E11.5 mouse embryo section with *PlxnB3*-specific probe. 75

29.5 *In situ* hybridization on E15 mouse embryo sagittal section with *PlxnB3*-specific probe. 76

29.6 *In situ* hybridization on E15 mouse embryo sagittal section with *PlxnB3*-specific probe, detail view on mouse brain and internal organs 76

29.7 Whole mount *in situ* hybridization performed on E11, E15 mouse embryos with *PlxnB3*-specific probe 77

30.1 Northern blot analysis of *PLXNB3* expression in various human organs. 78

30.2 Autoradiogram of human poly(A)$^+$ RNA dot blot array. 79

30.3 Alternative splicing of *PLXNB3* mRNA in adult human tissues. 80

30.4 Possible protein structures of B3 predicted by mRNA isoforms generated through alternative splicing of exon 27. 81

30.5 *In situ* hybridization on paraffin embedded human tissues with *PLXNB3* -specific DIG-labelled antisense cRNA probe 83

30.6 Adult human neocortex showing predominant neuronal expression of *PLXNB3*. 84

30.7 Immunohistochemical detection of plexin B3 in selected areas of human adult brain. 86

30.8 Immunohistochemical distribution of plexin B3 in human non-neuronal tissues. . 89

31.1 Alignment of human intron 22 of *PLXNB3* with the corresponding intronic regions of chimp and mouse. 91

31.2 Schematic localization of ten single nucleotide polymorphisms (SNPs) and one insertion polymorphism found in *PLXNB3* 91

31.3 Schematic localization of the six polymorphisms in *PLXNB3* used for haplotyping 93

31.4 Suggested evolution of human haplotypes. 96

32.1 Structure of pSPL3 constructs used for exon trapping experiments. 97

32.2 Representative result of exon trapping experiment; nested-PCR performed with dUSA4 and dUSD2 oligonucleotides by three independent experiments. 98

32.3 Sequencing analysis of colony PCR products derived from wild type and IVS22+21G>A mutated constructs. 99

33.1 Comparison of 5′ region of *PLXNB3* in human and chimp. 104

33.2 Putative transcription factor binding sites within the 1.1 kb of the 5′ region of *PLXNB3* identified by the TFSEARCH database. 105

33.3 Reporter constructs used in the *PLXNB3* promoter assays. 106

33.4 Bar graphs showing SEAP activity of human *PLXNB3* promoter region in three different cell lines (CHO-K1, HeLa, and HEK). 106

41.1 Position of the *PlxnB3*-specific DIG-labelled cRNA probes relative to the *PlxnB3*. 119

List of Tables

5.1 Plexins are receptors for distinct semaphorins 26

7.1 Known disease genes in the neighborhood of *PLXNB3* as annotated in OMIM in April, 2005. 30

10.1 Comparison of genomic and protein characteristics of human and mouse plexin B3 33

30.1 Immunohistochemical detection of plexin B3 in paraffin-embedded human adult normal and tumour tissues 88

31.1 Nucleotide changes found in human *PLXNB3* in 191 subjects with mental retardation 92

31.2 The 11 polymorphic sequence changes found in *PLXNB3* and their relative frequencies. 92

31.3 Six human polymorphisms identified in coding regions and 5′ region of *PLXNB3*. 94

31.4 Coding differences between human and chimp PLXNB3 along with the corresponding sites in rodents. 94

31.5 Summary of 13 haplotypes and their frequency based on the five intragenic SNPs and one SNP found in the 5′ upstream region genotyped in 85 subjects. 95

31.6 Presumed recombinant haplotypes 95

33.1 Potential binding sites for transcription regulatory elements of *PLXNB3*. 103

Summary

During formation of the embryonic nervous system, axons are guided to their targets by environmental cues. Several guiding molecules have been identified, including semaphorins, a large family of soluble and transmembrane proteins sharing a common sema domain. Plexins are large single-pass transmembrane proteins that function as receptors for semaphorins, either alone or in a complex with neuropilins. In vertebrates, there are at least nine different plexins, grouped into subfamilies A-D according to their sequence similarity. Plexins are expressed widely, but differentially, in the developing central and peripheral nervous system. Semaphorins and their plexin receptors play important roles in patterning the connectivity of the developing nervous system, and they are involved in central and peripheral axon guidance. This work characterizes the expression and genetics of *PLXNB3* (NCBI/GenBank Acc. no. AF149019) the human gene of plexin B3 and *PlxnB3* (NCBI/GenBank Acc. no. NM_019587) its mouse orthologue. *PLXNB3* is located on the chromosome at Xq28. The full-length mRNA of $\sim$6.3 kb includes 36 exons and encodes a protein of 1909 amino acids. Similarity between the protein-coding mRNA sequences of *PLXNB3* and *PlxnB3* is 82.3% and reaches 83.3% on the amino acid level. This high degree of evolutionarily conservation suggests a functional relevance of plexin B3. Spatial and temporal expression of *PlxnB3* from stages E8–E15 of mouse embryonic development was analyzed by non-radioactive *in situ* hybridization (ISH). *PlxnB3* showed constant expression in the central nervous system throughout all developmental stages studied. Outside the developing nervous system, *PlxnB3* was expressed in lung bud, bronchus, forelimb bud, primordial follicles of vibrissae, primordia of upper and lower teeth, thymus, and all of the epidermis. Expression in adult mouse tissues was analyzed using two different cRNA probes. The first cRNA probe used in this work contains the major part of the 3' UTR of *PlxnB3*; it detected neuronal expression, but no expression in the white matter. The second cRNA probe used in this work, hybridizing further upstream, revealed neuronal and in addition some glial expression of *PlxnB3*. Combined ISH and immunocytochemistry performed on cultured primary cerebellar cells from six day old mice showed exclusively neuronal expression.

Tissue expression profiling of human *PLXNB3* was performed by Northern blot and multiple tissue RNA dot blot arrays. Northern blot detected the transcript predominantly in brain, although faint signals were also seen in colon and small intestine. Similarly, RNA dot blot array revealed the highest expression in various human brain regions and in addition weak signals in spleen, thymus, lymph node, leukocytes, adrenal and salivary glands have been found. ESTs analysis and allele-specific RT-PCR revealed the existence of at least four different B3-isoforms of PLXNB3 *in vivo* due to skipping various part of exon 27. These isoforms were differentially expressed in various tissues. The first isoform containing complete exon 27 was not detectable in heart, whereas an isoform detected in brain, heart and other tissues contains a frameshift, and an isoform lacking 82 residues encoded by exon 27 expressed exclusively in brain.

ISH on human cerebellum, hippocampus, cerebral neocortex, and thalamus revealed predominant neuronal expression. Combined ISH and immunohistochemistry revealed no expression

of *PLXNB3* in astrocytes or oligodendrocytes. Besides a predominant neuronal expression, *PLXNB3* was detected in vascular endothelium throughout all tissues analyzed. Furthermore, using plexin B3-specific polyclonal antibodies, plexin B3 protein was detected in neurons of the central nervous system. Immunoreactivity was also observed in skin, Langerhan's islets, myocytes, Leydig's cells, intestine, colon, and kidney. Plexin-B3 was also detected in different human tumour tissues like astrocytoma, hepatocellular carcinoma, and colon adenocarcinoma. Since, plexins are receptors implicated in axon guidance and signal transduction, both human and mouse plexin B3 showed predominant neuronal expression and due to its location on X chromosome, *PLXNB3* appeared to be a suitable candidate gene for X-linked mental retardation. Mutation screening of *PLXNB3* was performed on 191 male subjects with possible or probable X-linked mental retardation. Single strand conformation polymorphism analysis (SSCP) revealed six unique sequence variants, including three silent mutations, two intronic alterations, and one missense mutation. These variants most likely represent rare polymorphisms. Using the Exon Trapping System, an intronic sequence variant, IVS22+21G>A, was further investigated for possible effects on splicing. Both wild type and mutated constructs gave rise to various splice variants in transfected cells. However, isoforms containing exon 22 have been detected only in the wild type construct. These data suggest that the intronic mutation IVS22+21G>A may result in pathological skipping of exon 22. Futhermore, the mutation screening revealed some sequence variability of *PLXNB3*, including ten single nucleotide polymorphisms (SNPs) and a 28 bp insertion polymorphism. Genotyping of six of these SNPs in 85 males subjects revealed 13 human haplotypes. Analysis of these haplotypes in different species, including chimpanzee, mouse, and rat sequences suggested the differentiation between ancestral and modern human haplotypes.

The 1.1 kb of 5′ upstream region of *PLXNB3* along with the first 1.5 kb of the transcribed region were analyzed in order to identify the region harboring the promoter. The activity of the six promoter fusion reporter constructs including various overlapping parts of the 5′ upstream region were analyzed by reporter assay in CHO-K1, HEK, and HeLa cells. Construct p5 covering nucleotides -147 to -16 revealed the highest promoter activity in all cell lines analyzed. This region lacks any known transcription factor binding sites. Construct p4, covering nucleotides -249 to -16 (thus including construct p5 completely) showed a strongly decreased promoter activity. In this construct, binding sites for three repressor elements (RE-1/NRSE neuron restrictive silencer element, GATA-1, and Delta EF1) were predicted. These data suggest that the differential expression of *PLXNB3* is predominantly regulated by molecules binding to repressor elements located upstream in close proximity to a constitutive promoter element.

Plexins are receptors implicated in axon guidance and both human and mouse plexin B3 showed predominant neuronal expression. At the moment no human phenotype can be associated with mutations in plexin genes, but several X-linked neurodevelopmental human disorders have been mapped to Xq28. Due the localization of *PLXNB3* on Xq28, the possible role of plexin B3 in neural development, and the fact that Plexin-B3 was identified as a high-affinity receptor specific for Sema5A, this gene continued to be a functional as well as a positional candidate gene for X-linked neurological disorders or mental retardation.

Zusammenfassung

Während der Bildung des Nervensystems werden Axone durch Leitsignale der Umgebung zu ihren Zielen geführt. Verschiedene neuronale Leitsignale wurden identifiziert, darunter die Semaphorine, eine große Familie von löslichen und transmembranen Proteinen, die durch eine gemeinsame Sema-Domäne charakterisiert sind. Plexine sind große transmembrane Proteine, die als Semaphorin-Rezeptoren fungieren, entweder allein oder im Komplex mit Neuropilin 1 oder 2. Bei Vertebraten sind bisher neun verschiedene Plexine bekannt, die nach Sequenzhomologien in die Subfamilien A-D unterteilt werden. Bisher untersuchte Plexine zeigen ein breites aber differenzielles Expressionsmuster im sich entwickelnden zentralen und peripheren Nervensystem. Plexine und ihre Semaphorinliganden sind beteiligt an der zentralen und peripheren Axonwegfindung und spielen eine wichtige Rolle bei der Vernetzung des sich entwickelnden Nervensystems.

Im Rahmen dieser Arbeit wurden humanes Plexin B3 (*PLXNB3*, GeneBank Zugangsnummer AF149019) und murines Plexin B3 (*PlxnB3*, GeneBank Zugangsnummer NM_019587) charakterisiert. *PLXNB3* liegt auf Xq28. Die mRNA von ∼6,3 kb umfasst 36 Exons und kodiert für ein Protein von 1909 Aminosäuren. Auf mRNA-Ebene zeigen die *PLXNB3* und *PlxnB3* 82,3% Sequenzhomologie, auf Aminosäure-Ebene 83,3%. Dieser Grad der evolutionären Konservierung deutet auf eine funktionelle Relevanz von Plexin B3 hin. Die Expression von murinem *PlxnB3* wurde in den Stadien E8–E15 der Embryonalentwicklung der Maus mit Hilfe nicht radioaktiver in situ Hybridisierung analysiert (ISH). *PlxnB3* zeigte eine konstante Expression im zentralen Nervensystem (ZNS) in allen untersuchten Stadien. Außerhalb des Nervensystems wurde *PlxnB3* in den Anlagen der Lunge, der Bronchien, der Vorderextremitäten und der Zähne, sowie in Thymus und der gesamten Epidermis exprimiert. Die Expression im Gewebe adulter Mäuse wurde mit Hilfe zweier verschiedener cRNA-Sonden untersucht. Mit der erste Sonde, welche den größten Teil der 3' UTR von *PlxnB3* umfasst, wurde eine neuronale Expression jedoch keine Expression in der weißen Substanz des Gehirns nachgewiesen. Mit der zweiten Sonde, welche weiter stromaufwärts hybridisiert, wurde dagegen ein schwächeres neuronales und verstärktes gliales Expressionsmuster detektiert. Kombinierte ISH und Immunzytochemie an kultivierten primären cerebellären Zellen sechs Tage alter Mäuse zeigten dagegen eine ausschließlich neuronale Expression.

Die gewebespezifische Expression von *PLXNB3* wurde mit Hilfe von Northern Blot und Multiple Tissue mRNA Arrays untersucht. Das Transkript wurde im Northern Blot vorwiegend im Gehirn detektiert; schwache Signale waren auch in Dick- und Dünndarm nachweisbar. Mit dem Multiple Tissue mRNA Array konnte eine starke Expression in verschiedenen Gehirnregionen gezeigt werden (Putamen, Medulla oblongata, Corpus Callosum, Hippocampus, cerebraler Neocortex und Cerebellum). Zusätzlich wurden schwache Signale in Milz, Thymus, Lymphknoten, Leukozyten, Nebenniere und Speicheldrüse detektiert. Mi Hilfe von ISH an humanem Cerebellum, Hippocampus, cerebralem Neocortex und Thalamus konnte ebenfalls eine vorwiegend neuronale Expression nachgewiesen werden. Kombinierte ISH und Immuncytochemie zeigten keine Expression von *PLXNB3* in Astrozyten oder Oligodendrozyten.

PLXNB3 wurde predominant neuronal exprimiert und konnte zusätzlich im Gefäßendothel aller analysierter Gewebe nachgewiesen werden. Weiterhin konnte Plexin B3-Protein mit Hilfe B3-spezifischer polyklonaler Antikörper in Neuronen des ZNS sowie in verschiedenen nicht neuronalen Geweben (Haut, Langerhans-Inseln, Myozyten, Leydig-Zellen, Darm und Niere) detektiert werden. Eine Expression von Plexin B3 konnte auch in verschiedenen humanen Tumorgeweben wie Astrozytom, hepatozellulärem Karzinom und Adenokarzinom des Dickdarms gezeigt werden.

Plexine sind Rezeptoren, die an der Axonwegfindung und Signaltransduktion beteiligt sind. Beide Plexin B3 Orthologe zeigen eine vorwiegend neuronale Expression, was *PLXNB3* zu einem Kandidatengen für mentale Retardierung macht. Es wurde ein Mutationsscreening von *PLXNB3* bei 191 Patienten mit mentaler Retardierung durchgeführt. Bei diesem Mutationsscreening mit Hilfe der "single strand conformation polymorphism" (SSCP) Analyse, wurden sechs Sequenzvarianten, einschließlich dreier stiller Mutationen, zweier intronischer Veränderungen und einer missense Mutation identifiziert. Diese Varianten repräsentieren wahrscheinlich seltene Polymorphismen. Mit Hilfe von Exon Trapping wurde eine der intronischen Sequenzvarianten, IVS22+21G>A, auf mögliche Auswirkungen auf den Spleißvorgang hin untersucht. Sowohl beim Wildtyp- als auch bei dem mutierten Konstrukt wurden dabei verschiedenen Spleißvarianten identifiziert. Isoformen die Exon 22 enthielten, wurden allerdings nur beim Wildtypkonstrukt nachgewiesen. Dies deutet darauf hin, dass die intronische Mutation IVS22+21G>A möglicherweise in einem pathologischen Ausschluss von Exon 22 resultiert.

Zusätzlich konnten für *PLXNB3* zehn 'single nucleotid polymorphisms' (SNPs) und ein Polymorphismus mit einer Insertion von 28 bp identifiziert werden. Basierend auf sechs dieser SNPs, wurden durch Genotypisierung von 85 gesunden Personen 13 verschiedene humane Haplotypen identifiziert. Ein phylogenetischer Stammbaum, welcher eine Differenzierung zwischen ursprünglichen und modernen humanen Haplotypen zulässt, wurde unter Einbeziehung von Schimpansen-, Maus- und Ratten-Sequenzen konstruiert. Um die region von *PLXNB3* zu identifizieren, wurden 1,1 kb der 5' flankierenden Region und 1,5 kb der transkribierten Region von *PLXNB3* mit Hilfe eines Reporterassays auf ihre Promotoraktivität hin analysiert. Die Aktivität von sechs verschiedenen Konstrukten, die variierende Bereiche der 5' flankierenden Region enthielten, wurde in CHO-K1, HEK und HeLa-Zellen untersucht. Das Konstrukt p5, welches die Nukleotide -147 bis -16 umfasste, zeigte die höchste Promotoraktivität in allen untersuchten Zelllinien. In dieser Region konnten keine bekannten Transkriptionsfaktor-Bindungsstellen nachgewiesen werden. Das Konstrukt p4, welches die Nukleotide -249 bis -16 (und somit auch das gesamte Konstrukt p5) einschloss, zeigte eine stark verminderte Promotoraktivität. In diesem Konstrukt wurden Bindungsstellen für drei Repressor-Elemente (RE-1, GATA-1 und Delta EF1) vorhergesagt.

Part I

Introduction

Adult brain function requires precise (anatomical) connections between its different parts and with peripheral nerves. The formation of functional neuronal connections is orchestrated by a series of axon guidance decisions during embryonic development. Axonal guidance relies mainly on the motile sensory function of the most distal part of the axon, called the **growth cone**. The growth cone translates molecular cues into directed movement of axon using rearrangements of the **actin cytoskeleton**.The past decade has witnessed the identification of several conserved families of **axon guidance** molecules. Among the most prominent of these are the netrins, slits, semaphorins, and ephrins. Between those, the largest family are semaphorins. Receptors for semaphorins in the different organ systems have been identified as members of two distinct transmembrane receptor families: **plexins** and neuropilins. In addition, plexins are known to form big receptor complexes together with other molecules such as L1, Met (Scatter factor receptor) and OTK (Off Track Kinase) [Winberg et al., 2001]. This molecular receptor complex can function as a mediator for very different biological signals in such diverse physiological processes as neuronal migration [Mueller, 1999], immune response [Billard et al., 2000, Kumanogoh and Kikutani, 2003], cardiovascular organogenesis [Miao et al., 2000,Brown et al., 2001], invasive growth of tumours [Trusolino and Comoglio, 2002], and lung branching morphogenesis [Ito et al., 2000].

1 How do axons navigate?

The wiring of the nervous system is a process which occur in a stepwise manner. The first axons that develop navigate through an axon-free environment when the embryo is still relatively small, but most axons face an expanding environment crisscrossed by a scaffold of earlier projecting axons. Many later developing axons travel along preexisting axon tracts (or fascicles) for at least some of their trajectory, switching from one fascicle to another at specific choice points. This "selective fasciculation" strategy simplifies the assembly of large nervous systems such as human, in which axons extend to their targets in successive waves over a period of several months. Embryological, tissue culture and genetic experiments indicate that axons respond to the coordinate actions of four types of guidance cues: **attractive** and **repulsive** cues, which can be either **short-range** or **long-range** [Tessier-Lavigne and Goodman, 1996] (Figure 1.1).

One century ago Ramón y Cajal proposed, that axon guidance might be mediated by long-range **chemoattraction**, a process similar to the chemotaxis of motile cells, in which target cells secrete diffusible chemoattractant substances that attract axons at a distance [Tessier-Lavigne and Placzek, 1991]. *In vitro* experiments, in which neurons cultured with target cells turn toward these cells, demonstrate the existence of several chemoattractants secreted by intermediate or final targets of axons [Lumsden and Davies, 1983, Heffner et al., 1990]. Long-range **chemorepulsion** was demonstrated with the finding that axons can be repelled *in vitro* by diffusible factors secreted by tissues that these axons normally grow away from [Colamarino and Tessier-Lavigne, 1995].

Axons can also be guided at **short-range** by contact-mediated mechanisms involving non-diffusible cell surface and extracellular matrix molecules. Axon growth requires a physical substrate that is both adhesive and permissive for growth [Letourneau, 1975]. This process of contact attraction has also been implicated in selective fasciculation, in which growth cones confronted with several preexisting axon fascicles select a specific pathway. Likewise, the contact repulsion of axons, such as the contact inhibition of cell migration has been extensively documented.

Thus, axon growth can be channelled by a corridor of a permissive substrate flanked by repulsive cues that serve to hem in the axons. Local repulsive cues also can serve to block the forward progression of axons. The responses of growth cones to repulsive cues can range from simple deflection on axonal arrest, to more dramatic changes in which the growth cone collapses and retracts [Oakley and Tosney, 1993, Fan and Raper, 1995].

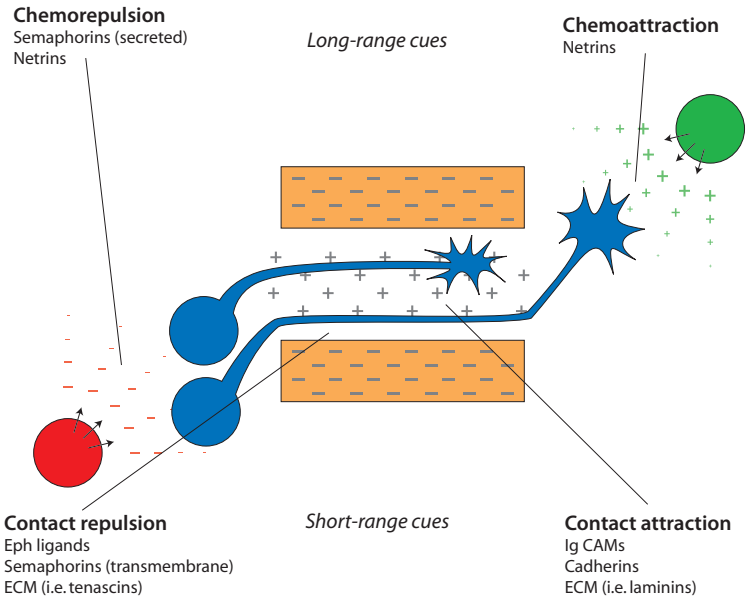

Figure 1.1. *Schematic drawing of mechanism and molecular biology of axon guidance. Four types of mechanisms contribute to guiding growth cones: contact attraction, chemoattraction, contact repulsion, and chemorepulsion. Modified from [Tessier-Lavigne and Goodman, 1996]*

2 Guidance cues and their receptors

Several families of extracellular guidance cues have been implicated in guiding neurons and axons to their appropriate destinations in the nervous system. Their receptors include secreted and transmembrane receptors, and their signal transduction pathways converge onto the Rho family of small GTPases, which control the cytoskeleton. A single guidance protein can use different mechanisms to regulate different kinds of motility or the motilities of different cell types. There is crosstalk between the signaling pathways initiated by distinct guidance cues. Studies of neuronal guidance mechanisms have shed light not only on neural development, but

also on other processes that involve the extracellular regulation of the cytoskeleton. There are several classical models of axon projection and neuronal migration in vertebrates, including the retinotectal projection, the commissural axons of the spinal cord, the radially migrating neuronal precursors in the neocortex, and the tangentially migrating neurons in the rostral migratory stream. Actin assembly is a key process that controls the growth and steering of axon growth cones, although recent evidence also supports a role for microtubules. The Rho family of small GTPases, which includes Rho, Rac and Cdc42, have important roles in regulating actin cytoskeletal dynamics and have been implicated in growth cone guidance [Kaibuchi et al., 1999].

Netrins were the first family of directional guidance cues to be found in both intervertebrate and vertebrate nervous systems. Netrin-1 and netrin-2 were identified as floor-plate-derived promoters of commissural axon outgrowth. A single netrin can be attractive to some axons and repulsive to others [Kennedy et al., 1994, Serafini et al., 1994, Stein and Tessier-Lavigne, 2001]. **Semaphorins** are a family of secreted and membrane-associates proteins that can mediate axon repulsion and growth cone collapse. They have also been implicated in responses [Kolodkin et al., 1993, Tamagnone et al., 1999]. **Ephrins** are membrane-associated guidance molecules divided into two classes (A and B) on the basis of their mechanism of membrane association. The Eph proteins were originally defined as the receptors for the ephrins, but they can also act as ephrin ligands [Gauthier and Robbins, 2003]. **Slits** are axon repellents, and they play important role in neuronal migration as well. Roundabout (Robo) are a cell surface receptors that are responsible for the repulsive effect of Slit. [Rothberg et al., 1990, Brose et al., 1999]. The chemokine stromal-derived factor 1 (**Sdf1**) is involved in axon guidance and neuronal migration. Sdf1 is expressed in the meninges surrounding the cerebellum, and it prevents premature migration of granule cells into the inner layer by anchoring them in the external layer [Rao et al., 2002, Lazarini et al., 2003]. Recent reports have implicated several well-known morphogens in axon guidance, including sonic hedgehog [Charron et al., 2003], bone morphogenetic proteins [Withers et al., 2000] and the Wnt family of secreted proteins [Yoshikawa et al., 2003].

3 Structural domains of plexins

Originally, plexins were identified through a screen for antigens expressed in the optic tectum in *Xenopus leavis* [Takagi et al., 1987]. Xenopus Plexin-1 is expressed in different groups of olfactory axons and has been shown to contain an extracellular domain related to the c-met protooncogene and to mediate calcium-dependent homophilic binding [Ohta et al., 1995]. Plexin-1 was subsequently cloned in mice and is the prototype of a family of proteins [Kameyama et al., 1996b, Kameyama et al., 1996a]. Plexins in human were cloned based on their homology to the ectodomain of the oncogene MET [Maestrini et al., 1996]. In vertebrates there are at least nine different plexin genes, grouped into four subfamilies (Plexin A, B, C, and D) according to the protein similarities [Tamagnone et al., 1999].

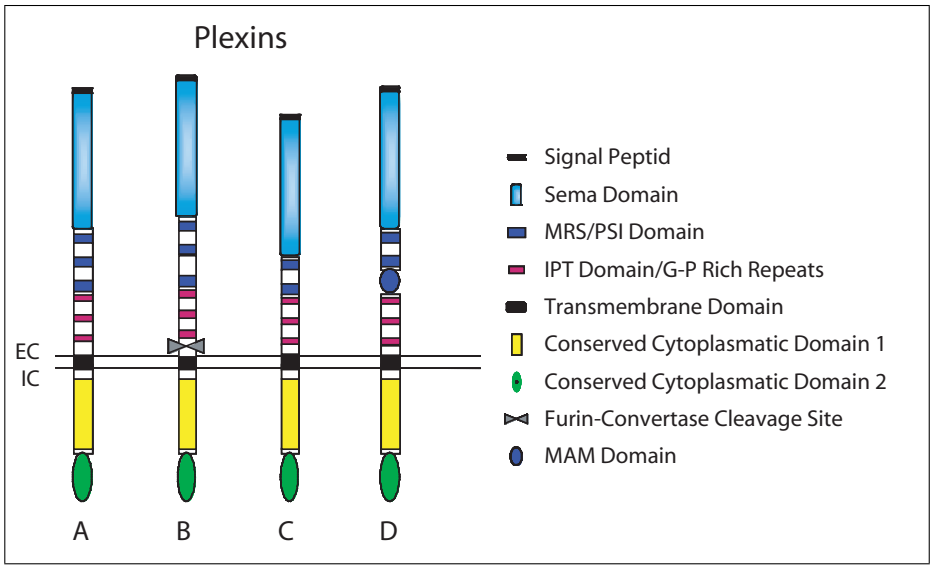

Figure 3.1. *Domain structure of plexins. EC-extracellular, IC-intracellular. Modified from [Chen et al., 1998]*

Ectodomains of all plexins contain a ∼500 amino acid *sema* domain, with 14 of the 16 conserved cysteines and many short peptide sequences that are characteristic of the semaphorin family. The sema domains of plexins share 25%-30% amino acid pairwise identity. Between plexins and semaphorins, the sema domains share 15%-20% amino acid identity and the sema domains of MET receptors share only about 10% amino acid identity with semaphorins and 15%-20% identity with plexins. Examination of phylogenetic relationships among the sema domains of plexins, semaphorins, and MET-related receptors shows that each of the three groups of proteins cluster separately [Winberg et al., 1998]. Interestingly, by considering sequence homologies and phylogenetic relationships based upon these homologies (plexins themselves contain complete semaphorin domains) plexins can be considered to be large transmembrane semaphorins or, vice versa, semaphorins can be considered as specialized plexins [Winberg et al., 1998].

The other extracellular domain of plexins include the motifs of three cysteine-rich repeats, 'MET' [Tamagnone et al., 1999], that show significant homology with the cysteine-rich domain of the cellular MET proto-oncogene and therefore are called MET-related sequences (MRS). The proteins of the MET family contain a single MRS (in their receptor beta chains), whereas in plexin family members, contain three MRS motifs. Human plexins were cloned, by using that homology to the exodomain of the MET oncogene [Maestrini et al., 1996].

The membrane-proximal regions of the plexin, ectodomain, contain another type of repeat that is rich in glycine and proline residues (G-P repeats). Three **G-P repeats** are spaced ∼50 amino acids apart. The intervening sequences are not notably similar except that each contains two conserved cysteines. All these features of the ectodomains are conserved between *Drosophila* and vertebrate plexins and also between MET-like tyrosine kinase receptors and VESPR, except that in these cases, there are different numbers of repeats [Winberg et al., 1998].

The cytoplasmic domain of plexins contains an ∼600 amino acids domain that has been termed the SP domain ('Sex and Plexins') that is highly conserved within the family (57%-97% similarity) and in evolution (over 50% similarity between invertebrates and humans). **SP domain** does not share homology with any known protein. It includes a number of potential tyrosine phosphorylation sites, but lacks the typical motifs of catalytic tyrosine kinases. Interestingly, the predicted secondary structure of the SP domain includes long conserved alpha helices typically found in protein-protein interaction modules.The cytoplasmic domain shares sequence similarity with Ras family-specific GTPase activating proteins (GAPs), however no GAP activity by plexins has been demonstrated so far [Hu et al., 2001, Oinuma et al., 2004]. The area of highest amino acid identity between the fruit fly and vertebrate Plexins is within these intracellular domains.

Expression studies of the A-subfamily plexins have focused on the late developmental stages of the nervous system (mainly from embryonic day E16.5 to adult) [Maestrini et al., 1996, Murakami et al., 2001, Suto et al., 2003, Takahashi et al., 1999, Tamagnone et al., 1999]. All four members, *PlxnA1*, *-A2*, *-A3* and *-A4* are widely, but differentially expressed in the developing central and peripheral nervous system [Murakami et al., 2001]. In addition, *PlxnA1* is expressed in the epithelium and mesenchym of the mouse lung at E11.5-E17.5 [Kagoshima and Ito, 2001], as well as in the heart at E10.5 [Toyofuku et al., 2004]. Expression of B-subfamily plexin members has also been studied in the developing murine nervous system, where they show highly specific and non-redundant patterns starting from E13.5 to adult stages [Worzfeld et al., 2004]. In contrast to Worzfeld publication, Päräla et al., 2005 described no detectable expression of *PlxnB3* mRNA in E14 mouse embryo. *PlxnD1* mRNA is most prominently expressed in the vascular endothelium (including the capillaries of the kidney glomeruli) and the central nervous system in the developing murine embryo [van der Zwaag et al., 2002].

4 Semaphorins signal through the plexins

More then 30 members of the semaphorin family have been identified to date. They are divided into eight classes according to their carboxy terminal organization and phylogeny. Semaphorins include transmembrane (classes 1, 4, 5, 6), GPI bound (class 7) and secreted (class 2, 3 and V) proteins. Class 1 and 2 are found in invertebrates, 3 to 7 in vertebrates, and class V is encoded by DNA viruses [Fiore and Püschel, 2003]. The first semaphorins were identified by searching for molecules expressed in specific axon fascicles in the grasshopper CNS [Kolodkin et al., 1992]. Receptors for semaphorins in the nervous system have been identified as members of two distinct transmembrane receptor families, plexins (Plex) and neuropilins (Np). Two neuropilin genes, phylogenetically unrelated to plexins/semaphorins, are known in the genome of birds and mammals [Kolodkin and Ginty, 1997]. Recent studies also show that integrins and several immune system receptors may function as transducers for semaphorin activities [Pasterkamp and Kolodkin, 2003, Kumanogoh and Kikutani, 2003].

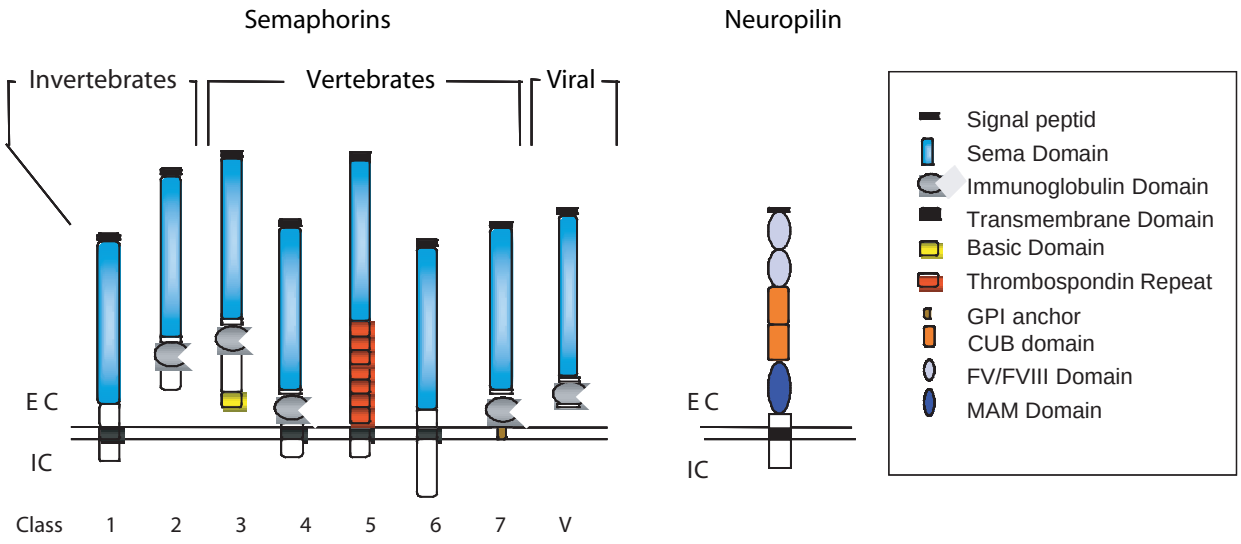

Figure 4.1: Domain structure of semaphorins and neuropilins. Modified from [Chen et al., 1998]

Semaphorin receptors belonging to the plexin family share together with semaphorins and plasminogen related growth factor receptors and conserved sema domain [Nakamura et al., 2000,Comoglio et al., 1999]. The sema domain is known to mediate receptor binding specifity of semaphorins and to be involved in autoinhibition of plexins [Takahashi and Strittmatter, 2001]. These additional conserved motifs further underline the phylogenetic relationship between the genes encoding those protein families [Winberg et al., 1998,Artigiani et al., 1999]. In vertebrates exist at least nine different plexin genes, grouped into four subfamilies (A to D) according to the protein similarities [Tamagnone et al., 1999] and at least six vertebrate plexins act directly as semaphorin receptors.

5 Plexin and neuropilin interplay in receptor complexes

As the semaphorins include both membrane-bound and secreted diffusible molecules, two distinct signaling modes might occur: cell-to-cell and long range signaling. Plexins of the A subfamily (A1-A4) and neuropilins (Np) are interacting to form receptor complexes for soluble semaphorins. Within this, plexins are providing a signal moiety whereas Np provide the ligand-binding sites [Takahashi et al., 1999]. Neuropilins can function also as cell-surface receptors for the vascular endothelial growth factor$_{165}$ (VEGF$_{165}$) and are required for developmental angiogenesis. Given that neither neuropilins nor plexins appear to be selective for individual semaphorins, and it remains unclear how the specific responses are in fact achieved. This points to the importance of additional molecules composing semaphorin receptor complexes in signaling mechanisms that mediate ligand binding and signal transduction. The cell adhesion molecule L1CAM (located in close genomic proximity to PLXNB3), directly associates with Np1, but not with Np2 controlling axonal responses to Sema3A [Castellani et al., 2002]. Similarly, an evolutionarily conserved glycoprotein off-track (OTK), was identified as a bind-

ing partner for plexins [Winberg et al., 2001]. A third protein, Met, a scatter factor/hepatocyte growth receptor with intrinsic kinase activity is required to transduce Sema4D-mediated effects in promoting epithelial cells invasive growth, and form a receptor complex with PlexB1 [Giordano et al., 2002].

The repulsive nature of semaphorin signaling during axon guidance is due the modification of the growth cone cytoskeleton following receptor activation. Because an intrinsic kinase activity of plexins is excluded, an association with tyrosine kinases has been proposed. Although the molecular mechanisms by which the semaphorins exert their effects remains has to be clarified, several intracellular Rho family small GTPases [Vikis et al., 2000, Rohm et al., 2000], PDZ-RhoGEF/LARG domain-binding motif (PDZ-Rho guanine nucleotide exchange factor/leukemia-associated Rho-GEF (LARG) via C-terminal PDZ (postsynaptic density-95/Disc large/zona occludens-1) [Swiercz et al., 2002], collapsin response mediator protein (CRMP) [Driessens et al., 2001], and cyclic nucleotide-dependent signaling [Song and Poo, 2001] have been implicated as downstream mediators for semaphorin signaling. Semaphorin signaling ultimately leads to growth cone collapse that is crucial for the formation of normal patterns of innervation by developing neurons. This process is accompanied by a rapid reorganization of the actin filaments presented in lamellipodia and filopodia, suggesting that growth cone receptor complexes interact with signaling molecules to regulate actin polymerization or cross-linking [Driessens et al., 2001, Zanata et al., 2002].

It has been shown that plexin-semaphorin interaction mediated by signaling can be bidirectional. Unlike most ligand-receptor pairs, semaphorins and their receptors mediate forward and reverse signaling. The forward signaling through plexins involves monomeric GTPases and integrins, and usually leads to the 'stop' signal, that prevents motility. In some instances, plexin may form complexes with Off-track kinases (OTK), Met or VEGFR2 (Vascular endothelial growth factor receptor 2), and this may determine whether the outcome produces 'stop' or 'go' signal. Reverse signaling, where plexins act as ligands and semaphorins as receptors has been demonstated recently by Toyofuku et al. [Toyofuku et al., 2004].

Accumulating evidence shows that some semaphorins can function as chemoattractants. It has been shown that Sema3A acts as chemoattractant for dendrites, and as chemorepellent for axons growing from these neurons [Polleux et al., 2000]. Furthemore, the Sema3A gradient apparently not only directs apical dendrite extension but also determines the site at which the dendrite forms. Behind these different response to Sema3A seems to be cyclic guanosine monophosphate (cGMP) intracellular gradient, which is established by asymmetrical distribution of guanylate cyclase [Polleux et al., 2000]. Sema3C is an other interesting example as it repels sympathetic axons but attracts cortical axons [Bagnard et al., 1998]. In the cultured *Xenopus leavis* spinal neurons repulsion to X-SemaIII can be converted to attraction by pharmacological activation of the cGMP and cAMP signaling pathways, respectively [Song et al., 1998]. Very recent studies show that semaphorin 7A directly promotes axon outgrowth acting through integrins and MAPKs [Pasterkamp and Kolodkin, 2003].

Semaphorins have been also well studied in invertebrate models such as a *C. elegans*, *D. melanogaster* and grasshopper. These each contain up to four genes encoding either transmembrane (subclass 1) or secreted semaphorins (subclass 2). Grasshopper *G-Sema1a* and *G-Sema2a* are expressed in a highly selective pattern in peripheral epithelia, where they provide cues to guide Ti1 pioneer neuron projections to discrete regions. G-Sema2a has a repelling activity [Isbister et al., 1999], whereas G-Sema1a functions as a contact-mediated attractive cue to consolidate the interactions between differentiating neurons [Wong et al., 1999]. In flies, *D-Sema1a* and its receptor *D-plexin-A* are widely expressed in the CNS and are required for defasciculation of motor axons and ventral muscle innervation [Winberg et al., 1998]. Another fly semaphorin *D-Sema2a*, is distributed selectively in neural tissues, in a single muscle and in embryonic gonads [Matthes et al., 1995]. Mutations in the *D-Sema2a* gene leads to behavioural defects and death. In worms, the mutations of the genes encoding *Ce-Sema2a* and *Ce-plexin-1* are responsible for marked defects in epidermal morphogenesis [Roy et al., 2000, Fujii et al., 2002].

In vertebrates, many semaphorins and plexins are expressed in the developing nervous system [Murakami et al., 2001, Pasterkamp and Kolodkin, 2003]. Secreted semaphorins are also found in mesoderm derived tissues and in epithelial layers of gut, lung, and kidney [Giger et al., 1998]. This expression might serve in the guidance of extending axons through layers of forming bone or skeletal muscle and in the formation of the autonomic nervous system of visceral organs, respectively. Semaphorins and their receptors often show a complementary distribution in tissues, consistent with their role as cells-repelling cues. Expression of semaphorins and their receptors is spatially and temporally regulated. The expression levels of semaphorin receptors in migratory cells or axons might change not only depending on the developmental stage but also in response to other molecular cues involved in axonal guidance. Although semaphorins and their receptors are recognized for their role in axon guidance, they are also expressed in various non-neuronal organs. Their ability to mediate cell contraction [Takahashi et al., 1999], adhesion and migration [Miao et al., 1999], as well as growth and differentiation suggests interesting parallels with the invasive growth phenotype.

Table 5.1: Plexins are receptors for distinct semaphorins

Semaphorin	Functional receptor
SemaVA,VB (viral)	Plexin C1
Sema3A	Np1 / np1 / Plexin-A1, A2
Sema3C	Plexin-D1(Np1/Np2)/Plexin-A(?)
Sema3F	Np2 / Plexin-A1, A2
Sema4A	TIM-2
Sema5A	Plexin B3
Sema6D	Plexin A1
Sema7A	Plexin C1 (VESPR) Integrins
Sema4D	CD72 and PlexinB1(CD100)

6 Knock-out mouse models

Only a limited number of plexin and increased semaphorin gene production knockouts have been analyzed in mouse embryos. The first reported knockout mouse was for *Sema3A*, where a subclass of spinal cord sensory neurons were reported to extend too far together with subsequent abnormalities in the cortex, skeletal structure, and heart development [Behar et al., 1996]. The genetic knockout of *Np-1* is an embryonic lethal and leads to axon guidance defects analogous to those seen on *Sema3A*-null mice [Taniguchi et al., 1997]. In addition *Np-1* deficiency is associated with altered vascularization of brain and heart outflow [Kawasaki et al., 1999]. The *Np-2* knockout mouse is viable, but with several defects of axon fasciculation and targeting of cranial nerves [Chen et al., 2000]. *PlxnA3* knockout mouse shows axon guidance defects in peripheral and hippocampal projections and laminar termination defects [Cheng et al., 2001].

Several class 3 semaphorins bind to the receptor neuropilin-2 (Np-2) to confer chemorepulsive reponses *in vitro*. Analysis of the CNS in *Sema3F*-null mice revealed the crucial role of Sema3F in forebrain, midbrain and hippocampus development in establishing specific neuropilin-2 expressing limbic tracts. Sema3F is the principal ligand for Np-2 mediated axon guidance events *in vivo*, and is critical for development of limbic circuitry [Sahay et al., 2005].

Analysis of *Sema3C* mutant mice generated by targeted mutagenesis revealed severe congenital cardiovascular defects, consisting of persistent truncus arteriosus, interruption of the aortic arch, and improper septation of the cardiac outflow tracts. Disruption of the *Sema3C* mouse gene and subsequent phenotype is similar to ablation of the cardial neural crest in chick embryos, and also resembles congenital heart defects seen in humans [Feiner et al., 2001].

Signaling by semaphorin 3E and its receptor plexin-D1 control endothelial cells positioning and the patterning of developing vasculature in mouse. Genetic ablation of *Sema3E* or *PlxnD1* leads to disruption of vascular patterning independent from neuropilin-mediated signaling [Gu et al., 2005]. The sema4D/CD100 differentially utilizes two distinct receptors: plexin-B1 (in non-lymphoid tissues such as kidney and brain) and CD72 (in lymphoid tissues). The *sema4D/CD100*–deficient mice show functional defects in their immune system, and activation of defective B and T cells, but without abnormalities in other tissues [Shi et al., 2000].

Results were recently published of inactivation of the *Sema5a* gene. Plexin-B3 is a high affinity receptor specific for Sema5A. Homozygous *Sema5A* null mutants died during embryonic development, indicating an essential role of Sema5A during embryogenesis. However, mutant embryos did not show any morphological defects that could explain lethality of the mutation, in fact the detailed analysis of the vascular system of *Sema5A* null mouse mutant uncovered a role of *Sema5A* in the remodeling of the cranial blood vessels [Fiore et al., 2005]).

There is at the moment **no human phenotype**, which can be associated with mutations in plexin genes, although Lalani et al. (2004) reported one patient with CHARGE syndrome with muta-

tion in the *Sema3E* gene. It has been shown that some semaphorins act as tumor supressor genes and in contrast to neuropilins and other semaphorins have a important role in the cancerogenesis [Neufeld et al., 2005]. As mentioned above different semaphorins and their receptor complexes are playing a variety of roles during the development of nerve, cardiovascular and pulmonary systems, and in maintenance of the integrity of different organ systems.

7 Xq28

This selected region of the human genome has been analysed systematically to identify genes causing monogenic diseases. Many of the found genes mapped to the region of Xq28 subchromosomal band cause very different diseases, e.g. hemophilia A (factor VIII deficiency, *F8C*; MIM 306700), X-linked mental retardation associated with fragile site FRAXE (*FMR2*, MIM 309548), colorblindness, (*OPN1MW*, MIM 303800 and *OPN1LW*, MIM 303900), glucose-6-phosphatase dehydrogenase deficiency (*G6PD*, MIM 305900) causing hemolytic anemia, incontinentia pigmenti (*IKBKG*, MIM 308300), and plenty of other genes. Based on genetic maps of the chromosomal band Xq28 various novel candidate genes for genetic disorders have been isolated. The systematic generation of physical and transcription maps has allowed the identification of most genes localized to this region, supporting the hunt for new disease genes and making Xq28 one of the best characterized regions of the human genome [Aradhya et al., 2002, McPherson et al., 2001, Nadeau et al., 2001]. The analysis of the chromosomal band Xq28 serves as a model system for analysis of the whole human genome. The importance of this region arises from the high gene density and the large number of genetic disorders linked to the 8 Mb region.

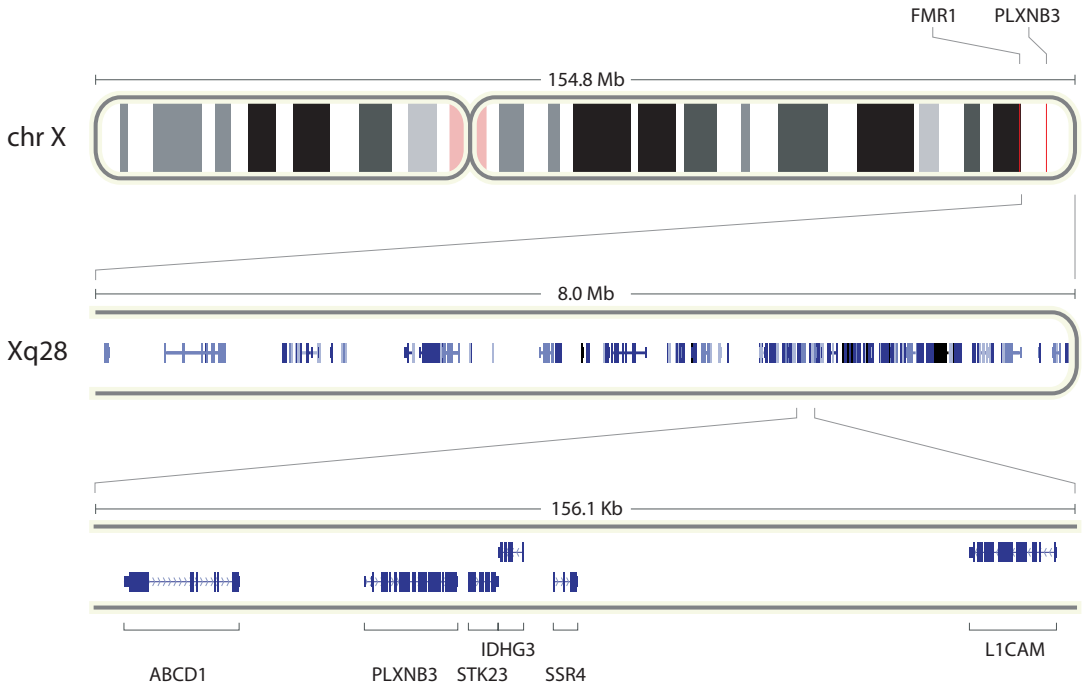

Figure 7.1: Selected genes in Xq28

PLXNB3 is located in Xq28 in close proximity to *L1CAM* (Figure 7.1). L1-disease is a group of overlapping clinical phenotypes including X-linked hydrocephalus or hydrocephalus due to stenosis of the aqueduct of Sylvius (HSAS, MIM 308840, 307000), MASA syndrome (mental retardation, aphasia, shuffling gait, adducted thumbs, MIM 303350), spastic paraparesis type 1 (SP1, MIM 312900), and X-linked agenesis of the corpus callosum (ACC, MIM 217990). All these syndromes are caused by mutations in the *L1CAM* gene (MIM 308840) and have been summarized as L1-disease [Fransen et al., 1997, reviewed in]. The responsible gene, *L1CAM* encodes the L1 protein which is a member of immunoglobulin superfamily of neuronal cell adhesion molecules [Walsh and Doherty, 1997]. The L1 protein is expressed in neurons and Schwann cells and seems to be essential for nervous system development and function. The overall mechanisms by which L1 gene mutations impair the development of the central nervous system are still under study. For example, in the development of the corticospinal tract L1 seems to be responsible for axonal pathfinding at a time when the axons are required to grow across the midline [Cohen et al., 1998]. At this point in axon guidance, L1 is required as an attractive or repulsive cue, substrate, or neuronal receptor. The underdeveloped corticospinal tract observed in the *L1*-deficient mouse and L1-disease patients could result from degeneration of neurons that could not be connected by synapse with the appropriate target [Kenwrick et al., 2000, reviewed in].

8 X-chromosomal genes and mental retardation

Besides trisomy of the chromosome 21, X-linked mental retardation (XLMR) is considered to be the most frequent type of mental handicap in males. It has been estimated that mutations in X-chromosomal genes account for 25 to 50% of all cases of mental retardation [Kerr et al., 1991]. A small part of XLMR can be attributed to recognizable syndromes be known as syndromic XLMR (S-XLMR). More often, however, the mental retardation is not associated with additional phenotypic characteristics and is referred to as non-syndromic XLMR (NS-XLMR). The prevalence of mental retardation in developed countries is thought to be on the order of 2-3% [Leonard and Wen, 2002]. X-linked gene defects have been considered to be important causes of mental retardation, on the basis of the observation that mental retardation is significantly more common in males than in females [Lehrke, 1974]. Clinical observations and linkage studies in families revealed that XLMR has a highly heterogeneous condition. The most common form of XLMR syndrome is Fragile X mental retardation syndrome associated with a cytogenetic fragile site in the distal region of the long arm of the X chromosome, which was shown to coincide with the map position of the underlying gene defect, and eventually led to the cloning of the *FMR1* gene [Verkerk et al., 1991]. Since then, the number of cloned XLMR genes has been increasing exponentially and about 140 syndromic forms of XLMR have been described so far [Ropers and Hamel, 2005].

Table 7.1: Known disease genes in the neighborhood of PLXNB3 as annotated in OMIM in April, 2005.

	OMIM	Disorder
FMR1	309548	X-linked mental retardation, FRAXE type
GDI1	309541	GDP1 dissociation inhibitor/MRX3
IDS	309900	Mucopolysaccharidosis II
MTM1	310400	Myotubular myopathy, X-linked
SLC6A8	300036	Creatine deficiency syndrome
ABCD1	300100	Adrenoleukodystrophy
PLXNB3	300214	**???**
IDH3G	30089	Isocitrate dehydrogenase-3
L1CAM	307000	Hydrocephalus due aqueductal stenosis
	303350	MASA syndrome
	312900	Spastic paraplegia
AVPR2	304800	Diabetes insipidus, nephrogenic
MECP2	312750	Rett syndrome
FLNA	300049	Periventricular heterotopia
EMD	310300	Emery-Dreifuss muscular dystrophy
TAZ	302060	Barth syndrome
	300069	Cardiomyopathy, X-linked dilated
	305300	Endocardial fibroelastosis-2
	300183	Noncompaction of left ventricular myocardium
PLXNA3	300022	???
FMR2	309548	X-linked MR, FRAXE type
G6PD	305900	Hemolytic anemia due G6PD deficiency
IKBKG	308300	Incontinentia pigmenti
DKC1	305000	Dyskeratosis congenita-1

9 Syndromic and non-syndromic forms of XLMR

XLMR is subdivided into syndromic (S-XLMR) and non-syndromic (NS-XLMR) forms, depending on whether further abnormalities (in addition to mental retardation) are found on physical examination, laboratory investigation and brain imaging. Roughly two thirds of XLMR cases are thought to be non-syndromic [Fishburn et al., 1983]. Moreover, mutations in several XLMR genes can give rise to both non-syndromic and syndromic forms, indicating that there is no reliable molecular basis for strictly distinguishing between genes for S-XLMR and NS-XLMR. About 140 syndromic forms of XLMR have been described so far. 66 of these, including several that have been found to be allelic, the causative genetic defects have been identified and in about 50, the underlying defects have been mapped to specific regions of the X chromosome. By contrast, for NS-XLMR, less than 50% of the causative gene defects have been identified. Different strategies have led to the identification of those genes. For example, *FMR2* was found due of its association with a fragile site (FRAXE), analogous to the association of *FMR1* with another such site (FRAXA) in mentally retarded males [Gecz et al., 1996,Gu et al., 1996].

Some genes were identified by breakpoint mapping and cloning in mentally retarded patients with balanced rearrangements that involve the X chromosome, or by molecular characterization of small X-chromosomal deletions. Mental retardation (MR) occurs significantly more often in males than in females. This male bias is largely due to the involvement of X-linked genes that play a role in brain differentiation and function [Turner et al., 1970]. Finding the molecular causes of NS-XLMR has turned out to be much more difficult because of genetic heterogeneity, and therefore, mapping intervals have remained comparatively wide. In most of the genes known to play a role in NS-XLMR, mutations have turned out to be very rare. Extrapolation of these findings suggests that close to 100 different genes might be involved in non-syndromic XLMR, 5-10 times more than previously thought. By contrast, mutations in the recently isolated *ARX* gene, the human homologue of the Drosophila gene *aristaless*, seem to be relatively common in NS-XLMR and various syndromic forms such as XLMR with epilepsy or dystonic movements of the hands. This observation has opened up the possibility that there are still other, until now unrecognized genes that play a major role in the etiology of XLMR.

At Xq28 four genes limited to non-syndromic XLMR and seven genes linked to syndromic XLMR has been identified [Ropers and Hamel, 2005, reviewed in]. The *FMR2* (FRAXE) gene was identified as a second site of chromosome fragility at Xq28. The gene *GDI1* (GDP-dissociation inhibitor) has a role in Rab GDP-dissociation inhibitor and is involved in synaptic vesicle fusion and neuronal mophogenesis. *GDI1* mutations have been shown to reduce the concentration of several Rab GTPases, including Rab4 and Rab5, which in turn seems to result in a reduction of the synaptic vesicle pool. The third gene *MECP2* (Methyl CpG-binding protein) which has role in chromatin remodelling and gene silencing. Mutations in *MECP2* give rise to a wide range

of disorders, including female-specific Rett syndrome which is characterized by cessation and regression of development in early childhood, ataxia, stereotypic hand movements, and other neurological features. The fouth one *SLC6A8* (Solute carrier family 6, member 8) is a creatine transporter required for maintenance of (phospho) creatine pools in the brain. The genes *FMR1* (FRAXA), *IDS* (mucopolysacharidosis II), *ABCD1* (adrenoleukodystrophy), *L1CAM* (L1-disease), *FLNA* (periventricular heterotopia), *IKBKG* (incontinentia pigmenti), *DKC1* (dyskeratosis congenita) are located in or near Xq28 and cause syndromic-XLMR. Most of the genes identified to date are very rare causes of NS-XLMR. Therefore, there remain a large number of NS-XLMR families in which the causative mutation has not yet been identified yet. On the present there is no doubt that additional genes on the X chromosome remain to be assigned to a mental retardation phenotype.

In 1996, the European XLMR Consortium has been found with the aim to elucidate all major forms of X-linked mental retardation with a focus on non-syndromic XLMR [XLMR, 2005]. Activities of the Consortium include the systematic collection and clinical characterisation of families and patients, linkage studies to define the map position of the underlying gene defect(s), and keep gene identification as well as functional studies to shed light on the pathogenesis of these disorders. The European XLMR Consortium has collected blood and DNA from 450 families with established or probable XLMR, and its resources help in identifying novel genes causing mental retardation.

10 Plexin B3

Human *PLXNB3* (NCBI/GenBank Acc. no. AF14019) is located in Xq28 in close vicinity to *L1CAM* and *ABCD1* genes. *PLXNB3* spans more than 15 kb of genomic DNA and contains 36 exons. The 5′ UTR extends to exon 2, which also encodes the initial 15 amino acids. The third exon encompasses more than 1 kb and encodes the major part of the sema domain [Kolodkin et al., 1993]. The predicted exon/intron boundaries are in agreement with the GT/AG rule, with adjacent intronic sequences following the consensus pattern. Conceptual translation of the full-lengh isoform of *PLXNB3* cDNA predicts a protein of 1909 amino acids, a calculated weight of 207 kDa (prior to any protein modification), and an estimated isoelectric point of 6.21. The expression pattern of *PLXNB3* has not yet been characterized.

The mouse orthologue for human *PLXNB3*, *PlxnB3* previously known as plexin 6, contains 36 exons and spans more than 19.9 kb (NCBI/GenBank Acc. no. NM_019587). On the nucleotide level the similarity between the ORF of *PlxnB3* and of *PLXNB3* is 82.8%, reaching 83.8% at the amino acid level, along with an overall identical domain structure. The expression and function of plexin B3 in neuronal and non-neuronal tissues has been poorly characterized, although there exist somewhat controversial data. The *PlxnB3* was detected using RT-PCR in different mouse fetal tissues, such as brain, dorsal root ganglia, heart, kidney, liver, and lung [Artigiani et al., 2004]. Cheng et al., (2001) demonstrated exclusive neuronal expression and Wortzfeld et al. (2004) showed *PlxnB3* expression pattern selectively localized to the white matter. By *in situ*

hybridization at embryonic mouse stage E14, *PlxnB3* expression was not detected [Perälä et al., 2005]. Plexin B3 was identified as a receptor for semaphorin 5A. After binding to plexin B3, sema5A triggers the collapsing response, consistent with its function as a repelling cue in axon guidance [Artigiani et al., 2004]. *Sema5A* is one of the genes lost in the Cri-du-chat gene deletion syndrome, associated with severe mental retardation, further suggesting the important role of this semaphorin in brain development [Simmons et al., 1998]. Several X-linked neurodevelopmental human disorders have been mapped to Xq28, the region harboring *PLXNB3* include L1-disease caused by mutations in the gene *L1CAM*, responsible for neuronal cell adhesion molecule L1 that is involved in axon guidance and fasciculation. Mutations in *L1CAM* reduce or abolish L1-dependent neurite outgrowth *in vitro* [Michelson et al., 2002]. Due the localization of *PLXNB3* on Xq28, the possible role of plexin B3 in neural development, and the fact that Plexin-B3 was identified as a high-affinity receptor specific for Sema5A, *PLXNB3* appears to be a functional as well as a positional candidate gene for X-linked neurological disorders or mental retardation.

Table 10.1: Comparison of genomic and protein characteristics of human and mouse plexin B3

	Human *PLXNB3*	**Mouse *PlxnB3***
Localization	Xq28	XqA6
Gene	$>$ 15 kb	19.9 kb
Exons	36 exons	36 exons
mRNA	6.2 kb	6.9 kb
ORF	5730 bp	5943 bp
Protein	1909 aa	1892 aa
Splice variants	$\geq$4 variants	$\geq$2 variants
Domains	**Residues**	**Residues**
Sema	54 - 454	34 - 434
PSI	473 - 526	453 - 505
PSI	787 - 833	766 - 812
IPT	835 - 925	814 - 904
IPT	927 - 1012	906 - 991
IPT	1014 - 1145	994 -1124

Aims of the study

At least nine different plexin genes are present in vertebrates. Based on protein similarities plexins are grouped into four subfamilies, plexins A-D. Members of the plexin family are receptors for different semaphorins and most plexins have been shown to be expressed in the central and peripheral nervous system. Plexins are involved in control of axon guidance during development.

The present work focused on the human and mouse plexin genes *PLXNB3* (NCBI/GenBank Acc. no. AF149019 and PlxnB3 (NCBI/GenBank Acc. no. NM_019587). Human *PLXNB3* is located on the X chromosome, in the q28 band. *PLXNB3* appears to be a candidate gene for neurological disorders because plexins are expressed in the central nervous system and are involved in axon guidance events during the embryogenesis and maintenance of the brain homeostasis in the adulthood. Plexin B3 is physically linked to the another cell adhesion molecule L1 molecule, which in mutated form is involved in development of L1-disease. In addition other candidate genes for mental retardation have been mapped to this chromosomal region.

The aim of the present work can be outlined as follows:

1. Characterize of the spatial and temporal expression pattern of *PLXNB3* and its mouse orthologue *PlxnB3* at the mRNA and protein level.
2. Identify tissues and cell types which express human *PLXNB3* and murine *PlxnB3* at different stages of development
3. Create of specific polyclonal antibodies to human and mouse Plexin-B3, and assess their use in assays of immunohistochemistry, immunocytochemistry and molecular biology.
4. Screen patients with mental retardation for *PLXNB3* mutations.
5. Characterize promoter and regulatory elements of *PLXNB3*.

Part II

Materials and methods

11 Materials

All enzymes and chemicals were obtained, if not indicated otherwise, from companies Amersham Biosciences (Freiburg), BD Biosciences (Heidelberg), Biorad (München), Calbiochem (Schwabach), Dianova (Hamburg), Eurogentec (Köln), Falcon (Oxnard, USA), Fluka (Neu-Ulm), Genomed (Löhne), ICN (Eschwege), Invitrogen/Gibco (Karlsruhe), MBI Fermentas (St. Leon-Rot), Merck (Darmstadt), Metabion (Planegg-Martinsried), Millipore (Eschborn), Molecular Probes (Göttingen), New England Biolabs (NEB, Frankfurt a.M.), Novagen (Darmstadt), Pierce/Perbio (Bonn), Promega (Mannheim), Qbiogene (Heidelberg), Qiagen (Hilden), Roche (Mannheim), Roth (Karlsruhe), Serva (Heidelberg), Sigma (Taufkirchen), Stratagene (Heidelberg) and Vector Laboratories (Burlingame, USA), and were analysis quality grade.

11.1 Molecular biology

Agarose	Invitrogen (Karlsruhe)
TOPO® TA PCR Cloning Kit	Invitrogen (Karlsruhe)
Zero Blunt™ PCR Cloning Kit	Invitrogen (Karlsruhe)
1 kb DNA Ladder	MBI Fermentas (St. Leon-Rot)
6×Loading Dye	MBI Fermentas (St. Leon-Rot)
Alkaline Phosphatase	Roche (Mannheim)
Restriction endonuclease	Promega (Mannheim)
Restriction endonuclease	NEB (Frankfurt)
Quick T4 DNA Ligase	NEB (Frankfurt)
T4 DNA Ligase	Gibco (Karlsruhe)
dNTPs' (dATP, dCTP, dGTP, dTTP)	Qiagen (Hilden)
PfuTurbo® DNA Polymerase	Stratagene (Heidelberg)
PfuUltra™ HF DNA Polymerase	Stratagene (Heidelberg)
Taq DNA Polymerase	Qiagen (Hilden)
QIAquick Gel Extraction Kit	Qiagen (Hilden)
QIAGEN Plasmid Midi Kit	Qiagen, (Hilden)
QIAGEN Plasmid Maxi Kit	Qiagen, (Hilden)
JETQUICK PCR Product Purification Spin Kit	Genomed (Löhne)
Bacto Tryptone	BD (Heidelberg)
Mangandichlorid ($MnCl_2$)	Sigma (Taufkrichen)
Yeast extract	Sigma (Taufkrichen)
Spectinomycin	Sigma (Taufkrichen)
Ampicillin	Sigma (Taufkirchen)
Chloramphenicol	Sigma (Taufkirchen)
Kanamycin sulfate	Fluka (Steinheim)
Ethidiumbromide	Merck (Darmstadt)
Acidum Boricum	Merck (Darmstadt)
ABI Prism Big Dye Terminator	Applied Biosystems
Acrylamide/bisacrylamide	BioRad (München)
Bacto™ Tryptone	BD (Heidelberg)
Bovine serum albumine	Sigma (Taufkirchen)

continued on next page

continued from previous page

Bromphenolblue	Sigma (Taufkirchen)
DAPI	Sigma (Taufkirchen)
Dimethyl Sulphoxide (DMSO) Hybri-Max®	Sigma (Taufkirchen)
Formaldehyde solution 36.5%	Fluka (Steinheim)
Formamide	Merck (Darmstadt)
Glucose	Sigma (Taufkirchen)
Glycerol	Fluka (Steinheim)
Glycin	Merck (Darmstadt)
Goat serum	Sigma (Taufkirchen)
HPLC water LiChrosolv®	Merck (Darmstadt)
Orange G	Sigma (Taufkirchen)
Paraformaldehyde	Sigma (Taufkirchen)
Phenol	Roth (Karlsruhe)
Select agar	Invitrogen (Karlsruhe)
Sodium dodecyl sulfate	Sigma (Taufkirchen)
TEMED	Sigma (Taufkirchen)
Tetracycline	Sigma (Taufkirchen)
TRIZMA® BASE (Tris)	Sigma (Taufkirchen)
X-Gal	Invitrogen (Karlsruhe)
Xylene cyanol FF	Sigma (Taufkirchen)
N,N,N′,N′-Tetramethylethylendiamin (TEMED)	Sigma (Taufkirchen)
Ammoniumpersulfat (APS)	Sigma (Taufkirchen)
β-Mercaptoethanol	Merck (Darmstadt)
Methanol	Roth (Karlsruhe)
Isopropyl β-D-1-thiogalactopyranosid (IPTG)	Sigma (Taufkirchen)
Sucrose	Sigma (Taufkirchen)
L-(+)-Arabinose	Sigma (Taufkirchen)
Polyoxyethylensorbitan Monolaurat (Tween 20)	Biorad (München)
Nonidet P40 / Igepal	ICN (Eschwege)
Triton X-100	Sigma (Taufkirchen)

11.2 Cell culture

Lipofectamine™ 2000 Reagent	Invitrogen (Karlsruhe)
FuGENE 6	Roche (Indianopolis)
Poly-L-Lysine 0.01%	Sigma® (Darmstadt)
Polyethylenimine	Sigma® (Darmstadt)
Poly-L-ornithine	Sigma® (Darmstadt)
Sodium bicarbonate 7.5%	Invitrogen (Karlsruhe)
BME medium (10×)	Invitrogen (Karlsruhe)
DMEM Minimum essential medium	Invitrogen (Karlsruhe)
Opti-mem I	Invitrogen (Karlsruhe)
Putrescine	Sigma® (Taufkirchen)
Progesterone	Sigma® (Taufkirchen)
3,3′, 5-triiodo-L-Thyronine	Sigma® (Taufkirchen)

continued on next page

continued from previous page

basicFGF	Sigma® (Taufkirchen)
D(+) glukose	Sigma® (Taufkirchen)
Transferrin	Roche (Mannheim)
Sodium selenite	Sigma® (Taufkirchen)
Insulin	Sigma® (Taufkirchen)
L-thyroxine	Sigma® (Taufkirchen)
Aprotinin	Sigma® (Taufkirchen)
Penicilin/Streptomycim	Gibco (Karlsruhe)
Geneticin (G418 sulfat)	Gibco (Karlsruhe)
100 mm Polystyrene tissue culture dishes	Falcon (Oxnard, USA)
6- and 24 wells culture dishes	Falcon (Oxnard, USA)
2 Chamber polystyrene treated glass slides	Falcon (Oxnard, USA)
F-12 Nutrient Mixture (Ham)	Gibco (Karlsruhe)
Dulbecco's modified Eagle Medium (DMEM)	Gibco (Karlsruhe)
Bovine serum albumin	Sigma® (Taufkirchen)
Fetal bovine serum (FBS)	Gibco (Karlsruhe)
Fungizone (Amphotericin B)	Gibco (Karlsruhe)
Phosphate buffered saline (pH 7,4)	Gibco (Karlsruhe)
Dulbecco's Phosphate buffer (D-PBS)	Gibco (Karlsruhe)
Phosphate buffer$^{+/+}$ (PBS$^{+/+}$)	Gibco (Karlsruhe)
10x Trypsin-EDTA (0,5 %)	Gibco (Karlsruhe)
Dimethyl Sulphoxide (DMSO)	Merck (Darmstadt)
Phosphatase alkaline conjugated streptavidin	Dianova (Hamburg)
Paraformaldehyd	Sigma (Taufkirchen)
Glycerol-Gelatine	Sigma (Taufkirchen)
VECTASHIELD® Mounting Medium	Vector Laboratories
Hank's buffered salt solution(HBSS)	Gibco (Karlsruhe)
DNAse	Roche (Mannheim)
Basalmedium Eagle (BME, 1×)	Gibco (Karlsruhe)
Aprotinin	Sigma (Taufkirchen)
Insulin	Sigma (Taufkirchen)
Na_2SeO_3	Sigma (Taufkirchen)

11.3 Silver staining

Acetic acid	Merck VWR (Darmstadt)
Ammonium persulfat (APS)	Serva (Heidelberg)
Formaldehyde 37%	Sigma (Taufkirchen)
Glycerine	Roth (Karlsruhe)
N,N,N,N'-Tetramethylethylendiamin (TEMED)	Sigma (Taufkirchen)
Nitric acid 65%	Merck (Darmstadt)
Rotiphorese Gel 30	Roth (Karlsruhe)
Silver nitrate	Merck (Darmstadt)
Sodium carbonate	Merck (Darmstadt)

11.4 PCR, RT-PCR, cloning and electrophoresis

PBR322 DNA (MspI digested)	Invitrogen (Karlsruhe)
ϕX-174 (HaeIII digested)	Invitrogen (Karlsruhe)
RNA Molecular Weight Marker set II	Invitrogen (Karlsruhe)
Agarose, ultra pure	Invitrogen (Karlsruhe)
Bromphenolblue	Merck (Darmstadt)
Q solution	Qiagen (Hilden)
Perfect Match	Stratagene (Heildelberg)
SP6 RNA polymerasis-Plus™ 20U/µl	Ambion (Austin,Texas)
Superscript II Reverse Transcriptase	Invitrogen (Karlsruhe)
Oligo d(T) primer	Invitrogen (Karlsruhe)
Random primer	Invitrogen (Karlsruhe)
Platinum Pfx Polymerase	Invitrogen (Karlsruhe)
Dimethylsulfoxid (DMSO)	Serva (Heidelberg)
Ethidiumbromide	Merck (Darmstadt)
Ethylen-diamin-tetraacetate (EDTA)	Merck (Darmstadt)
Ficoll Type 400	Amersham Biosciences (Freiburg)
Ampicilin	Sigma (Darmstadt)
Kanamycin	Sigma (Darmstadt)
Chloramphenicol	Sigma (Darmstadt)
T4 polynucleotide-kinase	Roche (Mannheim)
T4 DNA ligase	BD Biosciences (Heidelberg)

11.5 *In situ* hybridization, immunohistochemistry

Anti-Digoxigenin-AP, Fab fragment	Roche (Mannheim)
DIG RNA labeling Mix (10×)	Roche (Mannheim)
Proteinase K	Sigma (Darmstadt)
Chloroform	Merck (Darmstadt)
Diethylpyrocarbonate (DEPC)	Sigma (Darmstadt)
Isoamylalcohol	Merck (Darmstadt)
RNase	Ambion (Austin, USA)
DNase I, RNA-free	Roche (Mannheim)
Heparin, sodium salt	Sigma (Darmstadt)
CHAPS	Sigma (Darmstadt)
Tissue Tek OCT Compound	Sakura, Finetek
Triethanolamin	Merck (Darmstadt)
Acetic anhydride	Merck (Darmstadt)
Blocking reagent	Roche (Mannheim)
Magnesiumchlorid-Hexahydrat	Merck (Darmstadt)
Clarion mounting medium	Biomeda (Foster City, CA)
Dextransulfate	Sigma (Darmstadt)
Ethanol, absolute	Roth (Karlsruhe)
Formamide	Merck (Darmstadt)
Glycogen	Roche (Mannheim)

continued on next page

continued from previous page

Mixed Bed Resin TMD-8	Sigma (Darmstadt)
Mercaptoethanol	Sigma (Darmstadt)
NBT/BCIP	Roche (Mannheim)
Levamisol	ICN (Mannheim)
Paraffin, liquid	Merck (Darmstadt)
Paraformaldehyde	Aldrich (San Francisco)
Phenol	Merck (Darmstadt)
Polysialic acid 5'	Sigma (Darmstadt)
tRNA	Roche (Mannheim)
Maleic acid	Invitrogen Life Sciences
Hydrogen peroxide 30%	Sigma (Darmstadt)
Ethanol, absolute	Roth (Karlsruhe)
Methanol	Roth (Karlsruhe)
Acetone	Sigma (Darmstadt)
Xylol	Merck (Darmstadt)
Sheep serum	Sigma (Darmstadt)
Goat serum	Vector Labs. (Burlingame, CA)
Hoechst No.33258	Sigma (Darmstadt)
DAPI	Sigma (Darmstadt)
Protease type XXIV	Sigma (Darmstadt)
Mayer's Hemathoxylin	Merck (Darmstadt)
DAKO liquid DAB	DAKO (Glostrup, DK)
Naphtol-ASMX-phosphate	Sigma (Darmstadt)
Fast Red TR salt	Sigma (Darmstadt)
Sigma Fast red tablets	Sigma (Darmstadt)
Clarion Mounting Medium	Biomeda (Foster City, CA)
Crystal/Mount™	Biomeda (Foster City, CA)
Prolong antifade,	Molecular Probes (Leiden, NL)
Triton X-100	Sigma (Darmstadt)

11.6 Buffers and solutions

Antibody solution (IHC)	3% (v/v) goat serum 2% (v/v) BSA 0.3% (v/v) Triton X-100 in 1×PBS$^{+/+}$
Blocking solution (ISH)	3% (v/v) goat serum 1% (v/v) blocking medium 1% (v/v) fetal calf serum in TBS buffer
DNA-loading buffer I	25 ml glycerol 100% 25 ml 1×TBE $\sim$ 20 mg orange G
DNA-loading buffer II (6×)	30% (v/v) glycerol in ddH_2O

continued on next page

continued from previous page

	0.25% (w/v) bromphenol blue 0.25% (w/v) xylene cyanol FF
SSCP-loading buffer	98% (v/v) formamid 10 mM EDTA 0.025% (w/v) bromphenol blue 0.025% (w/v) xylene cyanol FF
PBS (20×)	137mM NaCl 2.7 mM KCl 8.1 mM Na_2HPO_4 1.5 mM KH_2PO_4 pH 7.4 for $PBS^{+/+}$ add 0.5 mM $MgCl_2$ and 1 mM $CaCl_2$
$PBS^{+/+}$ high salt	add 500 mM NaCl
SSC (20×)	3 M NaCl 300 mM sodium citrat; pH 7.0
TBS buffer (10×)	50 mM Tris-HCl 150 mM NaCl; pH 7.5
TBST buffer (10×)	200 mM Tris-HCl, pH 7.4 1500 mM NaCl 1% (v/v) Tween 20 in 1000 ml ddH_2O; pH 7.5
Denhardt's solution (50×)	5 g Ficoll 400 5 g polyvinylpyrrolidon 5 g BSA to 500 ml water
Dextransulfat (50%)	10 g dextransulfate 100 ml dd -water
DEPC-water	0,1% DEPC in bi-dist. water Incubation at 37°C for 12 hours
Ethidiumbromide solution	10mg/ml in distilled water
4% Paraformaldehyde	4 g parafolmaldehyde 100 ml 1×PBS buffer
TNM buffer	100 mM Tris 100 mM NaCl 50 mM $MgCl_2$; pH 9.5
Triethanolamine buffer	0.25% acetic anhydride

continued on next page

continued from previous page

	100 mM TEA buffer; pH 8.0
Maleic acid buffer	100 mM Maleic acid 150 mM NaCl; pH 7.5
10% Blocking reagent	10g (v/w) Blocking reagent 100 ml maleic acid buffer
Staining solution (AP- reaction)	200µl of NBT/BCIP 10 ml TNM buffer
Dithithreitol (DTT)	2 M DTT 0.01 M sodium acetate (pH 5.2)
Deionized formamide	100 mg of Mixed Bed Resin TMD-8 100 ml formamide
MAB-T Buffer	100 mM Maleic acid 150 mM NaCl, pH 7.5 0.5% Tween 20
TNM buffer	100 mM Tris 100 mM NaCl 50 mM $MgCl_2$, pH 9.5
X-gal	2% (w/v) X-Gal in dimethylformamid Storage at -20ąC

12 Chemicals

12.1 Nuclear staining

DAPI (4',6-Diamidine-2'-phenylindoline dihydrochloride)	1mg/ml	Roche
Accustain Haematoxylin		Sigma

12.2 Bacterial strains

Name		Source	Reference
DH10B	F$^-$ *mcr*A Δ(*mrr-hsd*RMS-*mcr*BC) ϕ80*lac*ZΔM15 Δ*lac*X74 *deo*R *rec*A1 *end*A1 *ara*D139 Δ(ara, leu)7697 *gal*U *gal*K λ-*rps*L (Str^R) *nup*G	Invitrogen (Karlsruhe)	
TOP10	F$^-$ Δ(*mrr-hsd*RMS-*mcr*BC) ϕ80d*lac*ZΔM15 Δ*lac*X74 *deo*R *rec*A1 *ara*D139 Δ(*ara*, *leu*)7697 *gal*U *gal*K *rps*L (Str^R) *end*A1 *nup*	Invitrogen (Karlsruhe)	

12.3 Cell lines

Name		Source	Reference
COS-7	African green monkey kidney; fibroblast-like cells growing as monolayers	DSMZ (Braunschweig) ACC 60	[Gluzman, 1981]
CHO-K1	Chinese hamster ovary cells; Adherent, fibroblastoid cells	DSMZ (Braunschweig) ACC 110	[Puck, 1965]
Kelly	Human neuroblastoma; Adherent round to spindle-shaped cells	Nitsch, UKE, Hamburg (DSMZ ACC 355)	[Schwab et al., 1983]
SH-SY5Y	Human, bone marrow, neuroblastoma, Epithelial-like cells	DSMZ (Braunschweig) No ACC 209	
HeLa	Human cervix adenocarcinoma, Epithelial-like cells	DSMZ (Braunschweig) ACC 57	
HEK 293	Human embryonal kidney cells, adherent, fibroblastoid cells	DSMZ (Braunschweig) ACC 305	
U2OS	Human Bone Osteosarcoma Epithelial Cells, epithelial adherent morphology	Pette Institut UKE, Hamburg	
SW 1353	Human chondrosarcoma	Pette Institut UKE, Hamburg	

12.4 Commercial vectors used in present work

Cloning Vector	Characters	Source
pCR® 2.1-TOPO	Km^r , Amp^r	Invitrogen (Karlsruhe)
pCR®- Blunt TOPO	Km^r , Zeo^r	Invitrogen (Karlsruhe)
pCR®-XL- TOPO	Km^r , Zeo^r	Invitrogen (Karlsruhe)
pBluescript® SK	$Spec^r$	Stratagene (Heidelberg)
pBluescript® II KS	Amp^r	Stratagene (Heidelberg)
pSPL3	Amp^r	Gibco BRL (Karlsruhe)
pAPM10	Amp^r	Gibco BRL (Karlsruhe)
pGEM®-5fz(+)	Amp^r	Promega (Manheim)
pSEAP2-Basic	Amp^r	BD Clontech (Heidelberg)
pSEAP2-Control	Amp^r	BD Clontech (Heidelberg)
pSV-β-galactosidase	Amp^r	Promega (Manheim)

12.5 Primary antibodies

12.5.1 PLXNB3-specific primary antibodies

In this work the following purchased polyclonal primary antibodies were used:

pAbhB3-A Rabbit polyclonal antibodies (pAb) against the extracellular domains of human B3 were produced by immunization with KLH-coupled peptides `TSRCVTLPLDSPESYP` (human sema domain, aa 354–369). The antibody was produced by the Eurogentec company. Affinity-purified antisera were diluted 1:50 for IHC and ICC.

pAbhB3-B rabbit polyclonal antibodies (pAb) against the third IPT-domain of human B3 were produced by immunization with KLH-coupled peptides `VQASRAQPQDPQPRRS` (third IPT–domain, aa 1058–1074). The antibody was produced by the Eurogentec company. Affinity-purified antisera were diluted 1:500 for IHC and ICC.

Name	Antigen	Work. Conc.	Source
Anti-CNPase mAb	Purified human 2′,3′-cyclic nucleotide 3′phoshodiesterase	IHC 1:500 ICC 1:1000	Sigma
Anti-myelin associated glycoprotein (MAG)	L2 epitope glycoprotein extract of 1-2 day old chicken brain	IHC 1:500	Chemicon
Anti-oligodendrocyte marker O4 mAb	White matter of corpus callosum from bovine brain	IHC 1:100	Chemicon
Anti-Neuronal Nuclei (NeuN) mAb	Purified mouse brain cell nuclei	IHC 1:50 ICC 1:100	Chemicon
Anti-neuromodulin/GAP-43 mAb	Synthetic Peptid Human Neuromodulin	IHC 1:100 ICC 1:100	Transduction Lab./ BD
Anti-human β-tubulin, clas III,(TU-20) mAb	Class III β-isoform of tubulin	IHC 1:200 ICC 1:200	BMA
Anti-GFAP mAb	Mouse glial fibrillary acidic protein	IHC 1:500 ICC 1:1000	Transduction Lab./ BD
Anti-mouse CD11b	T cell enriched splenocyts from b10 mice	IHC 1:50	Serotec
Biotinylated Ricinus comunis Agglutinin I	Biotynilated Lectin	IHC 1:100	Vector Laboratoties

Name	Antigen	Conjugate	Conc.	Source
Biotin-SP-conjugated AffiniPure goat Anti-Mouse IgG (H+L)	Goat Imunoglobulin	Biotin	IHC 1:1000	Dianova
Cy™ 3-conjugated AffiniPure F(ab')−2 Fragment	Mouse Immunglobulin	Cyanin 3	IF 1:100	Dianova
Fluorescein (FITC)-konjugiertes AffiniPure Anti-Rabbit IgG	Rabbit Immunglobulin	Fluorescein	IF 1:100	Dianova
Alexa Fluor® 488 Goat-anti-Rabbit	Rabbit Imunoglobulin	Alexa-Fluor® 488	ICH 1:1000 ICC 1:2000	Molecular Probes
Alexa Fluor® 488 Goat-Anti-Mouse	Mouse Immunglobulin	Alexa-Fluor® 488	IF 1:1.000	Molecular Probes
CY™ 3-conjugated AffiniPure Goat anti-Rabbit IgG	Rabbit Imunoglobulin	Cyanin 3	IF 1:100	Dianova
Alexa Fluor® 546 Goat anti-Rabbit IgG	Rabbit Imunoglobulin	Alexa-Fluor® 546	IF 1:1500	Molecular Probes
Alexa-Fluor® 568 Goat-anti-Mouse	Mouse Immunglobulin	Alexa-Fluor® 568	IF 1:1.000	Molecular Probes
Streptavidin Texas Red®- X conjugate		Streptavidin	IHC 1:1000	Molecular Probes
StreptaABComplex/HRP Duet, Mouse/Rabbit	Mouse/Rabbit Imuno-globulin	Streptavidin	IHC 1:1000	DAKO
Vectastain ABC kit				

13 Synthetic oligonucleotides

Oligonucleotides were supplied from Sigma (Taufkirchen) or Metabion (Planegg-Martinsried), lyophilized and desalted. All oligonucleotides were resuspended in 1×TE to 100 pmol/µl concentration before use. When needed, aliquots from this stock solution were diluted with sterile water to 10 pmol/µl.

13.1 Oligonucleotides used for sequencing/vector sequencing

m13uni	5′—GTAAAACGACGGCCAG—′3
m13rev	5′—CAGGAAACAGCTATGAC—′3
T7 Promotor Fw	5′—TAATACGACTCACTATAGGGC—′3
T7 Terminator Rv	5′—TGCTAGTTATTGCTCAGCGGT—′3
T3 Rv	5′—AATTAACCCTCACTAAACCC—′3
M13 Fw	5′—GTAAAACGACGGCCAGT—′3
M13 Rv	5′—GGAAACAGCTATGACCATG—′3

13.2 Oligonucleotides used for Northern blot

NB-hB3Fw	5′—ACGCCCGCTCCGCCTACTTC—′3
NB-hB3Rv	5′—TAGTCCCCGAACGACAATG—′3

13.3 Oligonucleotides used in RT-PCR analysis of *PLXNB3* isoforms

Splice junctions are marked by bar.

ASFw	5′—TTCCTCCTCACG|CTCATCCACAC—′3
AS(698)Rv	5′—TCTGGGAC|CTTGTAGTGTTG—′3
AS(536)Rv	5′—CAGGCCTGAGCGCCACT|CTTCTC—′3
AS(356)Rv	5′—AGGCCTGAGCGCCACT|CTGTCAC—′3

13.4 Oligonucleotides used for *in situ* hybridization

Mouse

mb3-4647Fw	5′—CTCCCAGAGGCCTTCAGTGCAC—′3
mb3-5936Rv	5′—GATGTGTTTCTACTTTATTT—′3
mb3-3744Fw	5′—GCTGATTGCTGCGGTGCTCCTC—′3
mb3-5679Rv	5′—GTGGCCCTAGTTCACAGGTCAGTC—′3

Human

hB3-4496Fw	5′—GCCTGTACGCCTTCCTGAGG—′3
hB3-5550Rv	5′—GTAGAGCAGTTTGTTCACTG—′3
hB3-1793Fw	5′—ATTGTGCGTTCGGGGACTATG—′3
hB3-2320Rv	5′—GCCTGAATCCCCTGCTGTCTC—′3

13.5 Oligonucleotides used in promoter assay

Primer sequences with included Xho I site (CTCGAG) and EcoR I (GAATTC) site used for cloning in the promoter assay. Recognition sequences for restriction endonucleases are underlined.

B3PF	5′—CTGGAGGGTGCTTCGTGCCAGGTTATG—′3
B3PR+R	5′—GAATTCTGGGACATACGCTCAGTTCAG—′3
B3PR	5′—GAATTCCCAGCCTCCCTCCCCACAATG—′3
B3P1F	5′—CTCGAGCCTCTGTGCCCCATTTCTCTC—′3
B3P2F	5′—CTCGAGCCCCTCAGTCTTACCGTCCTC—′3
B3P3F	5′—CTCGAGACCCCACCTGATTTGCTGACC—′3
B3P4F	5′—CTCGAGGGTGCTTCGTGCCAGGTTATG—′3
B3P5F	5′—CTCGAGCCAGCAGAGGGCAGCAACATC—′3

13.6 Oligonucleotides used in exon trapping

Primer sequences with included BamH I site (GGATCC) and EcoR I (GAATTC) site used for cloning in the exon trapping experiment. Recognition sequences for restriction endonucleases are underlined.

SPLBR	5′—GGATCCGCCAGGAGGCGCCGAGGTGTG—′3
SPLER	5′—GAATTCGCCAGGAGGCGCCGAGGTGTG—′3
SPLEF	5′—GAATTCACAGCAGAGCCCAGCTCACTC—′3
SPLBF	5′—GGATCCACAGCAGAGCCCAGCTCACTC—′3
SD6	5′—TCTGAGTCACCTGGACAACC—′3
SA2	5′—ATCTCAGTGGTATTTGTGAGC—′3
SD2	5′—GTGAACTGCACTGTGACAAGCTGC—′3
dUSD2	5′—CUACUACUACUAGTGAACTGCACTGTGACAAAGCTGC—′3
dUSA4	5′—CUACUACUACUACACCTGAGGAGTGAATTGGTCG—′3

13.7 Oligonucleotides used for mutation screening

Ex.	5′	3′	Ta (°C)		PCR product (bp)
2	GGCTGAGCCTGGCGACTGTCTC	ACCCTGCCCCTCCCAGGAAC	59	+	216
3a	TCCGCTCACTCTCTCTCATTC	GTGGTTGAGAGTGGTATTAGG	57	-	271
3b	CGCTTCTCCGCACCTAATACC	CTCACCAGCAGCAGCTGGTTG	59	-	233
3c	GTGCCCACAGGCCCAGCTCAC	CGGCCCAGGCCCTCGCTGGAG	59	+	333
3d	GGGGTGCCACCCCTGGCCATC	GCGAGGGGGACCTCCACGTAG	59	+	251
3e	CTCCTACGTGGCCCGCGTCTG	AAAGATGCCAGCCATCCACAG	58	+	358
4	CTCTTCCGGGGGCTGATTCTC	GTTGCTGGGGGCTTTCCTGAG	59	+	289
5	AGGAGGGCGTGTCCCTGGAAC	GCCGCGTGTGCTGGCCCCTTC	58	-	233
6	GTCTCGTGCCCATTGCCTCTC	CACCCGTTGGCCCTAGCCTAG	59	+	181
7	GTCTAGGACCCCCACGGTGAC	GGGAGGCAGGCGGGTTCATG	59	+	250
8	CCCCCTCTCTCTGGCTACATC	ATTACCCCTCCAGCCTCCATC	59	+	254
9	ATGGAGGCTGGAGGGGTAATG	AACTGAGTGCCCTCTGGGGTC	58	+	216
10	GCGACCCCAGAGGGCACTCAG	GGAAGGGTGGAGAAGGGACAG	59	+	215
11+12	TCCCAGACCCGCCCAGCAGTA	ACGGAAGCTTGGGGGCAAGAG	59	+	431
13	GCACCCAGCCTGACCCCACAC	GTGCTGAGCGCCTCCTGTCTG	58	+	189
14	CAGGAGGCGCTCAGCACACTG	CACTGCGGGGCAGGAGAAGTG	59	+	263
15	GACCCCATCTGCCATCATTTG	CCGAGTGCCCCAGGTTTCTTG	55	-	280
16	CCTCCCCTGCGTAGGGCACAC	CAAGAAACCTGGGGCACTCGG	58	-	196

Continued on next page

Continued from previous page

Ex.	5′	3′	Ta (°C)		PCR product (bp)
17	CCTACCCAGCCTGCGCTGTTC	GCCACAGCAACCACTTCTCTA	58	+	234
18	GGGTGGTAGAGCCGAGATGAG	GGCGGGCGGTGGGCAACATAG	59	+	306
19	CCGCCCGCCCACACCCGACTG	GGACAGCCTTGTCGCCTGCTG	59	+	265
20	AGCCCAGCTCACTCCACCTG	CGTGGCGGGGCAGGGTTGAAG	58	+	305
21	CTGTGGGGGCCAGCAGCTTAG	TGGCGGCACCCGGTCCACCTG	58	+	242
22	GTGCCGCCAGCATGCACTCAG	AATGGCGAGGAGGGAAGTGTG	57	+	235
23	CGGCCCTGGCTGATGAAGCTG	GAGTTCAGGCCTCGTGGGTAC	57	+	182
24	GGGTACCCACGAGGCCTGAAC	GTAGTTCCCCAGCCCCACCTC	59	+	331
25	AGTGGGGCTTCCCAGGATGAG	CACCCCCGCCACCGGGTCCAG	59	+	251
26	AGCAGGGACACAGGCACAAAG	TGGCAAGAGGGGAGGAGTCTG	57	+	176
27a	TCATCAATCCTCCCTCGCTTG	CTCCAGGTGCCGGAGGGGTAG	54	-	440
27b	GAGGCGAGAAGGGCTATCATC	GGTGCCGGAGGGGTAGGGAAG	59	+	456
28	AGCCCCTCAACTGTGTCTTAC	CCCGCCCTGCCTCGCCCCGTC	57	+	227
29	CGGTGTAGGCGCCTGGCTAG	TGGGGTGGGGGATGAAGTTG	57	-	256
30	CTCCTTCCTTTCTTCCAGTC	GTCCCTGGCTGAGCCTGGTC	55	+	335
31	TGCCCTCCACACAGCCCTTAT	GGCGCATCCACCCTGGGAATG	59	+	28
32a	GCCAGTAGGCTGGAGTACATG	CTGCCACTGCCCACCCAGAG	55	-	299
32b	GCCAGTAGGCTGGAGTACATG	CTGCCACTGCCCACCCAGAG	56	-	332
33	GGTGGGCAGTGGCAGCATCAT	TGGAGGAGCAGACTTCGTTAG	57	+	216
34+35	CCCCACCCCTAACGAAGTCTG	CTGTGCCTCCCCTCCGGAGTG	57	+	343
36	AGAGGGGCAGGCTCAGACAG	TCCAGCAGGCAAATAAATAC	55	+	405

Part III

Methods

14 Subjects

DNA or blood samples were collected from 191 patients with clinically diagnosed mental retardation. The group of subjects included of 17 subjects with suspected L1-disease but without mutation in *L1CAM*, and 8 subjects with nonsyndromic X-linked mental retardation (Institute of Human Genetics, Hamburg). From the European X-linked Mental Retardation Consortium samples of DNA from 166 subjects with mental retardation were obtained.

15 DNA and RNA isolation

15.1 Isolation of genomic DNA from blood

Genomic DNA was isolated from peripheral blood. The method of isolation used in this study was a modification of Miller et al. (1988) and involves preparation of nuclei, digestion of nuclei with a combination of proteinase K and SDS, deproteinization with organic reagents and high concentration of salt, and precipitation of DNA with ethanol. When genomic DNA was isolated, DNA concentration was determined by UV spectrophotometry and quantitative analysis on agarose gel. Genomic DNA was stored at 4˚C.

Nuclei were prepared by mixing 10 ml whole blood with 30 ml cold Leidener solution and centrifugation at 1900 rpm for 10 min at 4˚C. The pellet was washed with the same solution twice and resuspended in 5 ml cold lysis solution by vortexing, and incubated subsequently with 500 µl 10% SDS and 100 µl 10 mg/ml Proteinase K for 2.5 h at 55˚C or over-night at 37˚C. After digestion, 1.5 ml saturated NaCl solution was added and shaken vigorously, followed by centrifugation at 6200 rpm for 15 min. The supernatant containing the DNA was transferred to a new tube and mixed with 2 volumes of absolute ethanol. The precipitated DNA was transferred to a new tube containing 0.5 ml 1×TE buffer and dissolved.

Leidener solution	155 mM NH_4Cl 10 mM $KHCO_3$ 0.1 mM EDTA; pH 7.4
Lysis solution	10 mM Tris-HCl 400 nM NaCl 2 mM EDTA; pH 8.2
TE-buffer (1×)	10 mM Tris 1 mM EDTA; pH 8.0

15.2 Isolation of cytoplasmic RNA from cells

Approximately 10^6 cells in monolayer culture were lysed directly in the culture dish. RNA extraction was carried out according to Qiagen RNasy Midi Kit manual. For cDNA synthesis 2 µl of isolated cytoplasmic RNA was used. The concentration of RNA was estimated by agarose gel electrophoresis with a known standard RNA, or by spectrophotometry, and RNA was kept at -80˚C.

15.3 Isolation of plasmid DNA in small scale

For isolation of plasmid DNA, the mini-preparation method of Birnboim and Doly (1979) [Birnboim and Doly, 1979] based on alkaline lysis was used. One single colony was inoculated in 2 ml LB-medium containing the appropriate selective antibiotic and incubated overnight at 37˚C with constant agitation (220 rpm). The culture was transferred into a 1.5 ml Eppendorf tube and the cells were pelleted by centrifugation (8,000 rpm / 4 min). The pellet was resuspended in 100 µl Solution I by vortexing. 200 µl Solution II was added and the sample was mixed by inverting and incubated for 3-5 min at RT to lyse the bacterial cells and denature genomic DNA. 300 µl Solution III was added to precipitate genomic DNA and most of the proteins. The suspension was inverted several times in the tube, incubated for 5–10 min on ice, and then centrifuged at 13,000 rpm for 10 min. The plasmid DNA in the supernatant was precipitated by adding 350 µl isopropanol and subsequently centrifuged (13,000 rpm / 10 min). RNA was removed by digestion with 100 µl 1×TE-buffer containing 100 µg/ml RNase for 20 min at 37˚C. The plasmid DNA was precipitated by adding 120 µl 88% (v/v) isopropanol/0.2 M potassium acetate with incubation of the sample for 10 min at RT. After a final centrifugation step at 13,000 rpm for 10 min, the pellet was resuspended in 20 µl sterile water and plasmid DNA was kept at -20˚C.

Solution I	50 mM glucose 25 mM Tris-HCl, pH 8.0 10 mM EDTA
Solution II	0.2 M NaOH 1% (w/v) SDS
Solution III	4 M potassium acetate 2 M acetic acid (glacial)
TE/Rnase buffer	RnaseA (100 µg/ml) in 1x TE
1×TE-buffer	10 mM Tris 1 mM EDTA pH 8.0

15.4 Isolation of plasmid DNA in large scale

Large and pure amounts of plasmid DNA used for either transfection of eukaryotic cells, or for translation *in vitro* later use for *in situ* hybridization were isolated by using the QIAGEN Plasmid Midi- or Maxi- Kit (Qiagen, Hilden) according to the manufacturer's instructions. The protocol is based on a modified alkaline lysis procedure, followed by binding of plasmid DNA to a column under appropriate conditions. RNA, proteins, etc. were removed by a medium-salt wash. Plasmid DNA was eluted in high-salt buffer and then concentrated and desalted by isopropanol precipitation. The DNA pellet was redissolved in sterile water and stored at -20˚C. The concentration of DNA was determined by UV spectrophotometry.

16 DNA and RNA standard methods

16.1 Cutting of DNA by restriction endonucleases

Type II restriction endonucleases are DNases that recognize specific oligonucleotide sequences, make double stranded cleavages, and generate unique equal molar fragments from a DNA molecule [Smith and Birnstiel, 1976]. By the nature of their controllable, predictable, infrequent and site-specific cleavage of DNA, restriction endonuclases prove to be extremely useful tools in confirming different alleles if there is any difference between them in the restriction map. In the present study, nucleic acid changes detected by sequencing were confirmed, whenever possible, by using appropriate restriction endonucleases. Plasmid DNA and PCR products were incubated with 0.5–1 U of restriction enzymes in appropriate buffers (Promega, New England Biolabs) in the presence of 1×BSA (bovine serum albumine) according to the manufacturer's protocol. When necessary, restriction was terminated by heat inactivation at 65˚C for 20 min or by freezing the sample at -20˚C, and examined by electrophoresis in 1–2% agarose. 10 µl of digested sample was mixed with 3 µl 6 × Ficoll gel loading buffer.

16.2 Agarose gel electrophoresis

Separation of DNA fragments was performed on non-denaturing agarose gels in a horizontal chamber (BioRad, Munich). Agarose gel was prepared by heating 0.8-2.5% (w/v) agarose (Invitrogen, Karlsruhe) in 1×TBE buffer or 1×TAE buffer, depending on the size of the DNA fragments to be separated. DNA-loading buffer I was mixed with the probe in a 1:3 ratio and the gel was run at constant voltage between 100–120 Volts. Afterwards, the agarose gel was stained in an ethidium bromide solution (Merck, Darmstadt; 1 ml/2 l water) for 5 min and washed in water for 10 min. Finally; the gel was documented under UV-light using Herolab UVT-28M Videosystem (Wiesloch). For determination of the size of DNA fragments, 100 bp and 1 Kb DNA Ladders (Invitrogen, Karlsruhe) were used. Low and High DNA Mass Ladders (Invitrogen, Karlsruhe) were used to estimate the quantity of DNA samples. The separation of RNA molecules was also done by non-denaturing horizontal agarose gel electrophoresis in 0.8–1% (w/v) agarose gel. The equipment used for electrophoresis of RNA was treated with RNase ERASE (ICN Biomedicals, USA) to render it ribonuclease-free.

10×TBE	Tris	890 mM
	Boric acid	890 mM
	EDTA	20 mM
10×TAE	Tris	400 mM
	Acetic acid	400 mM
	EDTA	10 mM

16.3 Purification and precipitation of PCR products

PCR products were purified from residual nucleotides, primers and salt using Spin collumns according to manufacture's description (Genomed, Qiagen). Afterward purified PCR products were subjected to 1-2% agarose gel electrophoresis to estimate yield and concentration of eluted DNA. Alternatively, for purification of PCR products NH_4OAc/ethanol precipitation was used. 1 volume of 4 M ammonium acetate and 6 volumes of absolute ethanol were added to the

sample and the samples were centrifuged at 13,000 rpm for 25 min. The pellet was washed with 70% (v/v) ethanol, centrifuged again for 10 min, dried, and resuspended in 20 µl sterile water. After sequencing reactions, DNA was precipitated by addition of 1/10 volume of 3 M ammonium acetate (pH 5.2) and 2.5 volumes of absolute ethanol. After 25 min centrifugation at 13,000 rpm, the pellet was washed with 70% (v/v) ethanol, centrifuged, and dried.

16.4 Cycle sequencing

DNA sequencing was performed at the Institute of Human Genetics by the dideoxy method [Sanger et al., 1977]. Automatic sequencing analysis was done using ABI Prism™ Big Dye Terminator Kit and an ABI Prism 377 DNA Sequencer (PE Applied Biosystems, Weiterstadt) according to the supplier's instructions. Cycle sequencing using dye-labelled terminators is a rapid and convenient method for performing the enzymatic extension reaction for DNA sequencing. For each reaction the following reagents were mixed in a 0.2 ml PCR tubes: terminator ready reaction mix (2 µl), double stranded purified PCR products (2–5 µl) or plasmid DNA (1µl), primer 1 µl (3.2 pmol), and distilled water to 10 µl. When a high GC content was expected (>75%), denaturation time was increased to 30 seconds and 5% DMSO was added to the cycle sequencing reaction. Cycle sequencing reaction was carried out on the GeneAmp PCR system 9600 using the following thermoprofile:

Sequencing reaction:	Thermoprofile:	
5 µl PCR product or 1-3 µl plasmid DNA	1. 96˚C	5 min
2 µl Big Dye Terminator (BDT)	2. 96˚C	30 s
1 µl primer (10 pmol/µl)	3. 55˚C	15 s
sterile H_2O ad 10 µl	4. 60˚C	4 min
	5. repeat steps 2-4	24-29 times

16.5 Determination of DNA concentration

DNA concentration was determined by UV spectrophotometry using a photometer Ultrospec® 2000 (Pharmacia Biotech, Freiburg). The absolute volume necessary for measurement was 50 µl and DNA was diluted 1:5 with water. Concentration was determined by measuring the absorbance at 260 nm (A_{260}). A ratio A_{260}/A_{280} between 1.8 and 2 showed a sufficiently pure DNA preparation.

17 Molecular biology methods

17.1 Generation of competent *Escherichia coli* cells for chemical transformation

Competent *E. coli* cells (DH10B) were prepared by the rubidium method [Sambrook and Russell, 2001]. One single colony was inoculated in 2 ml ψB-medium and incubated overnight at 37˚C with constant agitation at 2200 rpm. 1 ml from this culture was inoculated in 100 ml ψB-medium and incubated until the optical density at 550 nm (OD_{550}) was 0.3-0.4. To generate 500 ml final volume, 5x 5 ml from the 100 ml culture were inoculated in 100 ml fresh ψB-medium and incubated at 37˚C until OD_{550} 0.3–0.4. The bacterial suspension was transferred to 50 ml tubes, incubated in ice water for 5 min, then centrifuged at 4˚C at 2,500 rpm for 8 min. The supernatant was decanted and the pellet was resuspended in 15 ml cold TfBI. The cells were incubated in ice water for 30 min. After another centrifugation step at 4˚C at 2,500 rpm for 8 min, the cells were resuspended in 2 ml cold TfBII. 200 µl aliquots were made and the bacterial cells were immediately frozen in liquid nitrogen. Competent cells were kept at -80˚C

and thawed on ice immediately before use. One Shot TOP10 Chemically Competent cells were supplied with TOPO TA Cloning® Kit (Invitrogen, Karlsruhe).

ψB-medium (1.000 ml)	5 g yeast extract 20 g bactotryptone 0.75 g KCl pH 7.6 with KOH; autoclave add 34 ml sterile 1M $MgSO_4$/l
TfBI (500 ml)	1.47 g potassium acetate 4.95 g $MnCl_2$ 6.05 g RbCl 0.74 g $CaCl_2$ 75 ml glycerol pH 5.8 with 0.2 M acetic acid filter, sterilize, and store at +5˚C
TfBII (100 ml)	10 ml 100 mM MOPS (pH 7.0) 1.10 g $CaCl_2$ 0.12 g RbCl 15 ml glycerol filter, sterilize, and store at +5˚C in the dark

17.2 Cloning of PCR products

PCR amplicons were cloned in pCR® 2.1-TOPO® vector from TOPO TA Cloning® Kit according to the manufacturer's instructions.

17.3 Dephosphorylation of 5′-termini of DNA fragments

Calf Intestine Alkaline Phosphatase (CIAP) catalyzes the release of 5′- and 3′-phosphate groups from linearized DNA, RNA, deoxyribonucleoside and ribonucleoside mono-, di- and triphosphates. During ligation, DNA ligase catalyzes the formation of a phosphodiester bond between adjacent nucleotides only if one nucleotide contains a 5′-phosphate group and the other a 3′-hydroxyl group. Because circular DNA transforms much more efficiently than linear plasmid DNA, most of the transformants will contain recombinant plasmids. Recircularization of plasmid DNA can be minimized by removing the 5′ phosphates from both ends of the linear DNA with calf intestinal phosphatase. For dephosphorylation, 1µg of the vector digest, 2µl (2U) of alkaline phosphatase (AP), 3 µl 10×dephosphorylated buffer were added to an end volume of 30µl and incubated at 37˚C for 3 hours. The dephosphorylation was followed by inactivation of alkaline phosphatase by adding EGTA solution and heating at 65˚C for 10 min.

17.4 Ligation of DNA fragments

Ligation is the process where a DNA fragment is inserted into an appropriate plasmid [Dugaiczyk et al., 1975]. Most plasmids have been engineered to contain a multiple cloning site (MCS) which have keep a *lacZ* gene inserted. When inserted into a suitable bacterial cell, a functional MCS (*lacZ* gene) will produce β-galactosidase, which in turn produces blue colonies. Therefore, if DNA (the fragment being incorporated) ligates successfully into the MCS, the *lacZ* gene is disrupted, and the host bacteria appear as white colonies.

In general a 3:1 to 2:1 (insert : vector) ratio is recommended for the ligation reaction. To calculate the ratio for different sizes of inserts, the following formula is used:

$$\frac{\text{vector(ng)} \times \text{insert(kb)}}{\text{vector(kb)}} \times \frac{\text{ratio of insert}}{\text{vector}} = \text{insert}(X \text{ ng})$$

T4 DNA ligase covalently combines double stranded DNA fragments with blunt- or cohesive-compatible ends. The ligation was catalyzed by 1 U T4 DNA Ligase (Invitrogen, Karlsruhe) in ligation buffer at RT for 4–6 h or at 16˚C overnight, or with 1 U Quick T4 DNA Ligase (New England Biolabs, USA) in ligase buffer at RT for 20 min. 2–4 µl of the ligation mix was used directly for transformation.

17.5 Transformation of competent cells with plasmid DNA

For transformation of competent *E. coli* cells [Hanahan, 1983], one vial of TOP10 or 100 µl DH10B cells was gently mixed with 2 µl of the TOPO TA cloning reaction or 2–3 µl of ligation mix, respectively, and incubated on ice for 20-30 min. After a heat-shock at 42˚C for 0.5-1.5 min and incubation on ice for 5 min, 250 µl SOC-medium was added and the suspension was incubated at 37˚C for 1 h. Different volumes of the suspension were then plated on prewarmed agar plates containing the appropriate antibiotic (eventually also X-gal) and incubated overnight at 37˚C. Due to the insertion of foreign DNA into the multiple cloning site of the TOPO vector, the *lacZ* gene encoding the N-terminal part of β-galactosidase is disrupted. Due to the inactivation of the *lacZ* gene in recombinant clones, X-gal is not degraded and bacteria carrying recombinant plasmids form white colonies.

SOC-medium	20 g trypton 5 g yeast extract 0.5 g NaCl in 980 ml ddH_2O; pH 7.0; autoclave 10 ml sterile 1 M $MgSO_4$ 10 ml sterile 1 M $MgCl_2$ 10 ml sterile 40% glucose
LB (Luria Bertani) medium (1000 ml)	10 g trypton 5 g yeast extract 10 g NaCl in 1000 ml ddH_2O; pH 7.0
LB (Luria Bertani)-Agar (1000 ml)	15 g select agar in 1000 ml LB-medium; autoclave add antibiotic and/or X-gal
Antibiotics concentration for *E. coli* medium	Ampicillin 250 µg/ml Kanamycin 50 µg/ml Chloramphenicol 25 µg/ml Spectinomycin 100 µg/ml

18 Polymerase Chain Reaction

18.1 DNA amplification by polymerase chain reaction

Polymerase chain reaction (PCR) [Mullis and Faloona, 1987] was performed in 25 µl reaction volume containing 50–100 ng genomic or plasmid DNA, 0.5 U Taq DNA Polymerase (Qiagen, Hilden), 5 pmol of primer, 0.2 mM of each dNTP (Invitrogen, Karlsruhe) and 1×PCR Buffer containing 1.5 mM $MgCl_2$ (Qiagen, Hilden). PCR conditions were optimized by addition of 5% (v/v) DMSO, $MgCl_2$, 5% formamide or 20% Q solution (Qiagen), if necessary. (It has been proposed that the additives listed above may affect the melting temperature of primers, the thermal activity profile of thermostable DNA polymerases, the degree of product strand separation, or facilitate primer annealing by altering primer secondary structure). In the present study, for long and accurate PCR, high fidelity Pfu DNA-polymerase or Pfx Platinum-polymerase were used. In some special cases, nested-PCR was used. (Products from an initial PCR were highly diluted in water and used as template for a second round PCR with primers located more proximal to the first set of primers). PCR amplification was done in GeneAmp® PCR System 9700 (Applied Biosystems) thermocycler using the following programs; initial denaturation at 95˚C for 2 min followed by 5 cycles of denaturation for 10 sec at 94˚C, annealing for 15 sec at an optimal annealing temperature +4˚C, elongation for 30 sec at 72˚C, followed by 5 cycles for 15 sec at 94˚C, annealing for 15 sec at an optimal annealing temperature +2˚C, followed by 28-35 cycles at optimal annealing temperature. PCR was ended with a single elongation step for 5 min at 72˚C [Don et al., 1991]). The quality of the PCR product was examined by agarose gel electrophoresis.

The principle of PCR is based on the use of two specific oligonucleotide primers to direct the synthesis of specific sequences of DNA between them. One primer anneals to the coding strand of DNA and the other one to the anticoding strand. Primer binding sites are typically separated by a few hundred base pairs to several kilobases. A typical PCR contains 30 to 40 repeated cycles including denaturation (94˚C), annealing (50–72˚C), and elongation (72˚C) steps that will lead to an exponential increase in the sequence defined by the primers. Generally the termostable Taq-DNA polymerase from thermophile Thermus aquaticus is employed in PCR reactions.

18.2 Colony PCR of *E. coli* cells

To screen a large amount of bacterial colonies for a desired insert, single colonies were picked from a transformation plate with a sterile tooth pick and spotted on selective agar. The rest of the colony on the tooth pick is used as template for a PCR reaction. Primers m13uni and m13rev were used for the amplification of fragments cloned into TA cloning vector, and primer SD2 using pAMP10 cloning vector.

Single colony PCR:	Thermoprofile:
0.5 µl dNTPs (10 mM)	1. 95˚C 5 min
0.5 µl primer 1 (10 pmol/µl)	2. 95˚C 45 s
0.5 µl primer 2 (10 pmol/µl)	3. 55˚C 30 s
3.25 µl 10×PCR Buffer	4. 72˚C 30-90 s
0.1 µl Taq DNA Polymerase	5. steps 2–4 repeat 34 times
20.15 µl HPLC H_2O	6. 72˚C 10 min

18.3 cDNA synthesis and RT-PCR

For cDNA synthesis 2–6 µl of the isolated RNA was used. Primers for first strand cDNA synthesis were oligo dT or random hexanucleotides primers (Invitrogen, Karlsruhe). Samples of purified RNA (2–6 µl) were mixed with 5 µl of 5× cDNA synthesis buffer, 1 µl of each dNTPs (20 pmol), 1 µl of placental RNase inhibitor (10 U/µl), 1 µl of 20 pmol first strand synthesis primer (random hexamers or oligo dT) and 39 µl of DEPC water, heated at 65˚C for 5 min and transferred to ice for 5 min. 200 U SuperScript™ II RNase H^- Reverse Transcriptase (Invitrogen, Karlsruhe), were used. Mixture was first incubated at 70˚C for 10 min and afterwards chilled on ice for 2 min. The mixture was reverse transcribed to first-strand cDNA by adding 200 U Superscript Rnase H^- reverse transcriptase (Invitrogen Life Sciences) at 37˚C. Following incubation at 42˚C for 50 min, then 1 min at 50˚C and finally 65˚C for 5 min. Obtained cDNAs were stored at -20˚C. The cDNA was further used as template for PCR or nested-PCR.

19 Single strand conformation polymorphism analysis

19.1 Polyacrylamide gel electrophoresis

Non-denaturing polyacrylamide gels (PAA-gel) were used for separation of DNA fragments during single strand conformation analysis (SSCP) [Orita et al., 1989a]. PCR products (3-5 µl) were mixed with 5 µl SSCP-loading buffer, denatured at 95˚C for 10 min, placed on ice, and loaded on PAA-gel. Two different types of PAA-gels were used (See below). Polyacrylamide gel electrophoresis (PAGE) was performed using 1×TBE buffer overnight at 5–8 Watts for 8% PAA-gels, or at ∼18 Watts for 8% PAA-gels with glycerol depending on the size of PCR amplicons. To visualise the bands, a silver-staining technique was used.

	PAA-gel (8%)	PAA-gel (8%) with glycerol
ddH_2O	80.0 ml	67.5 ml
Acrylamide/bisacrylamide (30%)	33.0 ml	33.0 ml
10×TBE	12.5 ml	12.5 ml
Glycerol (100%)	-	12.5 ml
10% APS	1.0 ml	1.0 ml
TEMED	24.0 µl	24.0 µl

19.2 Silver staining of DNA fragments on polyacrylamide gels

For visualization of DNA, silver staining is more sensitive than staining with ethidium bromide. This is especially true for single-stranded DNA. All subsequent staining steps were performed on a shaker. Gels were transferred from glass plates to glass dishes and fixed in 10% ethanol for 5 min. Liquid was removed by vacuum pump, and gels were oxidized in 1% nitric acid for 3 min. Gels were again washed twice in deionised water for 1 min and silver stained in 0.012M silver nitrate solution (2.02 g/l), for 20 min. Gels were washed again twice in distilled water for 1 min and developed in 0.28 M sodium carbonate, 0.019% formaldehyde. Developer with silver precipitate was removed immediately and fresh developer was added. When the desired staining intensity was reached, developer was removed and reaction was stopped by adding 10% acetic acid (5 min). Gels were rinsed in distilled water for 5 minutes and sealed in a plastic bag.

Silver nitrate solution	2.02 g silver nitrate in 1000 ml ddH_2O
Reducer solution	29.6 g sodium carbonate anhydrous 540 µl formaldehyde solution 36.5% in 1000 ml ddH_2O

20 Cell biology methods

20.1 Culture of adherent cells

All cells were cultured in Dulbecco's Modified Eagle Medium (D-MEM) supplemented with 10% (v/v) fetal calf serum (FCS) and 1% (v/v) penicillin-streptomycin (P/S) (all Gibco, Karlsruhe) at 37˚C, with relative humidity of 95% and 5% CO_2 concentration (NUaire™CO_2 Water Jacketed Incubator; Zapf, Sarstedt). Cells were passaged until 90-95% confluence, medium was removed and cells were washed in $PBS^{-/-}$ (without $MgCl_2$ and $CaCl_2$), and detached by incubation with Trypsin-EDTA-Solution (2 ml/10-cm plate; Gibco, Karlsruhe). Trypsin was inactivated by the addition of 8 ml fresh pre-warmed complete medium. Resuspended cells were split either 1/10 or 1/20 for maintenance, or cells were seeded in 24-, 6-well or 10-cm plates for transfection experiments.

20.2 Freezing and thawing of adherent cells

Freezing medium was composed of 9 volumes of medium and 1 volume of dimethyl sulfoxide (DMSO). Cells were grown in 10-cm plates or flasks until 90-95% confluence. After trypsination, 10 ml fresh pre-warmed medium was added and the cell suspension was centrifuged at 950 rpm for 5 min. The pellet was carefully resuspended in 3 ml chilled freezing medium and 1 ml aliquots of the cell suspension were pipetted into cryovials (Nalgene). Cells were frozen in steps (4˚C, -80˚C) and kept in liquid nitrogen for long-term storage. Thawing of the cells was done by incubation in a water bath at 37˚C, and the suspension was immediately then transferred to pre-warmed medium.

20.3 Transient transfection by liposome mediated DNA-transfer

Negatively-loaded nucleic acids and synthetic, positively-loaded liposomes form a complex that is brought near to cells and fuses with the cell membrane. 24 h before transfection, 3×10^4 or 1.2×10^5 cells were plated in a 10 cm culture dish or 6-well and 24-well plates. Cells were grown in D-MEM medium and 80–90% confluent cells were used for transfection with the fusion constructs using Lipofectamine™ 2000 (Invitrogen, Karlsruhe) or FuGENE™ 6 Transfection Reagent (Roche) according to the manufacturer's instructions. The plasmids and Lipofectamine™ 2000 or FuGENE™ 6 Transfection Reagent were separately diluted with serum- and antibiotic-free medium Opti-MEM® I (Gibco, Karlsruhe), incubated 5 min (Lipofectamine™ 2000) and 15 min (FuGENE™ 6 Transfection Reagent) at RT, combined, and left at RT for 20-30 min. Meanwhile, cells were washed with $PBS^{-/-}$ (without $MgCl_2$ and $CaCl_2$) and left in Opti-MEM® I medium until transfection. DNA-transfection complexes were carefully added to each well and incubated for 5–6 h at 37˚C. After this cells were washed once with pre-warmed complete medium D-MEM and cultivated in the medium overnight.

	Culture vessel	DNA	Transfection agent	Opti-MEM® I	Plating medium
Lipofectamine	24-well	0.5 µg/well	1 µl/well	50 µl	500 µl
FuGENE		0.5 µg/well	1 µl/well	100 µl	500 µl
Lipofectamine	6-well	1 µg/well	5-6 µl/well	250 µl	2 ml
FuGENE		1 µg/well	3-6 µl/well	100 µl	2 ml
Lipofectamine	10-cm	4-10 µg	12-20 µl	400 µl	10 ml
FuGENE		4-10 µg	6 µl	100 µl	10 ml

21 Northern blot and RNA tissue array

As probe template, the fragment of *PLXNB3* cDNA corresponding to nucleotide 833–1814 (NCBI GenBank Acc. no. AF149019) was amplified by RT-PCR using primers NB-hB3Fw and NB-hB3Rv and cloned into pCRII®-TOPO (Invitrogen, Karlsruhe). The probe was randomly labeled with [α32P] d-CTP (RadPrime DNA labeling system, Invitrogen). After purification using DNA columns (QiatexII, Qiagen) the probe was hybridized to normalized Multiple Tissue Northern Blot (BD Biosciences) with 12 different human tissues. The blot was hybridized with *PLXNB3* ^{32}P-dCTP labelled cDNA probe at 65˚C overnight. After stringent washing the membrane was exposed to X-ray film at -70˚C. The Northern blot was stripped and re-hybridized with a β-actin control probe.

Multiple Tissue Expression Array hybridization was performed according to the manufacturer's instructions (BD Biosciences). The filter was hybridized overnight with ^{32}P-dCTP-labelled cDNA plexin B3 probe, washed with 2 × SSC, 1% SDS at 65˚C, and 0.1 × SSC, 0.5% SDS at 55˚C, and exposed to the X-ray film.

22 RT-PCR analysis *PLXNB3* splicing isoforms

The distribution of three isoforms of *PLXNB3* due to alternative splicing of the 3'- part of exon 27 was analyzed by RT-PCR form various human organs using forward primer ASFw and isoform-specific reverse primers. A 698 bp fragment containing full length exon 27 was amplified using reverse primer AS(698)Rv. A 536 bp fragment lacking the 3'-terminal part of exon 27 and coding for a C-terminally truncated B3 was amplified using reverse primer AS(536)Rv. A 356 bp fragment lacking (in-frame) 246 bp of exon 27 was amplified using reverse primer AS(356)Rv.

23 *In situ* hybridisation

23.1 Tissue preparation

Mice were kept on normal laboratory diet and water *ad libidum*. They were housed in cages in compliance with the guidelines for the humane care and use of laboratory animals in the Federal Republic of Germany. The mice were sacrificed by CO_2. Tissue samples of interest were rapidly dissected surgically from mice, wrapped in aluminum foil and immediately immersed for 1 min in liquid nitrogen . The frozen tissues were placed on dry ice and stored at -80˚C until usage. Prior to slide preparation using a cryomicrotome, tissues were equilibrated for 20 min at -20˚C. 5–10 µm sections were cut and mounted on slides. Slides were dried approximately 2 min and heated on a heating plate for 2 min at 55˚C. After RNA fixation by heating, slides were fixated in 1×PBS (pH 8-9) buffered paraformaldehyde at least 1 hour.

23.2 *In vitro* transcription (digoxigenin labelling)

RNA probes were produced by *in vitro* transcription. DNA generated by PCR was first subcloned into a pCR®-2.1-TOPO® vector and then using restriction sites (See table below) sub-

sequently cloned into a pGEM®-5fz(+) vector. Isolation of plasmid DNA in large scale was performed and the identity of the probes used for *in vitro* transcription was continued by DNA sequencing. For preparation of human (*PLXNB3*) and mouse (*PlxnB3*) specific probes plasmid DNAs were linearized with the appropriate restriction endonuclease (See table below). Riboprobes were transcribed from 1 µg linearized plasmid for 2h at 37˚C using 2µl DIG RNA Labeling Mix (Roche), 40 units T7 or Sp6 phage RNA polymerases (5U/µl), and 2 µl 10×transcription buffer (all Ambion) in a final volume of 20 µl. Below are given the combination of primers, restriction sites for cloning, and localization of probes used for *PlxnB3*-specific or *PLXNB3*-specific probes for *in situ* hybridization.

Mouse probe	Subcloning vector (Restriction sites)	Target vector (Restriction sites)	Primers	Template GenBank/Acces. Nr.
Probe A	pCR®-2.1-TOPO® Spe I/Not I	pGEM®-5fz(+) Spe I/Not I	mb3-4647Fw mb3-5936Rv	NM019587
Probe B	pCR®-2.1-TOPO® Spe I/Not I	pGEM®-5fz(+) Spe I/Not I	mb3-3744Fw mb3-5679Rv	NM019587
Human probe				
Probe A	pCR®-2.1-TOPO® Sal I/Not I	pGEM®-5fz(+) Sal I/Not I	hB3-4515Fw hB3-5552Rv	AF149019
Probe B	pCR®-2.1-TOPO® Sal I/Not I	pGEM®-5fz(+) Sal I/Not I	hB3-1793Fw hB3-2320Rv	AF149019

23.3 Precipitation and preparation of cRNA probes

To remove the DNA template prior to using the transcript as a probe, DNase I, RNase-free (Roche) was added and incubated at 37˚C for 15 min. Then 5 µl of 5 M ammonium acetate and 165 µl of pre-chilled 100% ethanol was added, and the solution was chilled at -20˚C for 30 min. Centrifugation was performed at 4˚C for 15 min at 14,000 rpm. The supernatant was removed and the pellet was washed with 70% ethanol. The RNA probe was air-dried for 5–10 min and dissolved in 50 µl of nuclease-free water. For complete removal of unincorporated dNTPs all steps were repeated once again. The RNA probe was aliquoted and stored at -20˚C until usage for *in situ* hybridization.

23.4 Non-radioactive *in situ* hybridization

In situ hybridization was performed on sectioned paraffin-embedded human tissues (Human Hybrid-Ready Tissue Set; Novagen, Schwalbach) or on human brain tissues stored at – 80˚C (Institute of Neurosurgery, UKE, Hamburg). ISH experiments were performed on the wild-type mouse, *Mus Musculus*, line C57BL/6J tissues.

Before deparaffinization, slides were dried horizontally for 1h at 58˚C. Slides were deparaffinized using xylol (Merck) three times for 5 minutes and hydrated in stepwise descending ethanol concentrations for 4 minutes (100%, 95%, 80%, 70%, 50%, 25%, water) and subsequently postfixed for 15 min with 4% paraformaldehyde (pH 8–9). After postfixation the slides were washed three times for 7 min in PBS buffer. The hybridization mixture used for ISH contained 1-3 ng/µl riboprobe, 50% (v/v) formamide, 0.33 M NaCl, 0.1 M dithithreitol (DTT), 10% dextransulfat, 0.2 M TrisHCl (pH 7.5), 10 mM EDTA, 10×Denhardt's reagent, 5mg/ml yeast tRNA, and 1mg/ml polyadenylic acid (polyAMP 5', Sigma).

Sections were fixed in 4% paraformaldehyde and washed three times for 7 min in TBS buffer. Prior to hybridization, sections were pretreated for 10 min with 200 mM HCl and washed.

Sections were acetylated in freshly prepared 0.25% (v/v) acetic acid anhydride in 0.1 M triethanolamin (pH 8.0), followed by stepwise dehydratation in ascending ethanol concentrations and air-dried for 20 min under laminar hood.

The sections were covered with 80–100 µl of hybridization mixture containing cRNA probe, covered with coverslips and denaturated on a heating plate for 4 min at 94˚C. The hybridisation was carried out in a humid chamber for 12–16 h at 55˚C or 65˚C. After hybridization, the sections were treated with ribonuclease A (20µl/ml, Roche) at 37˚C for 30 min. The slides were washed at high stringency in 0.2×SSC at 55˚C twice to remove coverslips, and three times in 0.2×SSC/50% formamide (v/v) at 55˚C for 1 h, followed by two times for 10 min in 0.2×SSC at RT. The final equilibration of slides was performed in TBS (10min). Before digoxigenin detection, non-specific binding sites were blocked with 1% (w/v) blocking medium (Roche, Manheim) and 1% (w/v) fetal calf serum (GibcoBRL) in TBS buffer. The sections were incubated at 4˚C overnight (16-20h) with alkaline phosphatase conjugated anti-digoxigenin Fab fragments (Roche) diluted 1:1500 in blocking buffer. The staining reaction was performed at RT in darkness with TNM buffer containing 275 µM nitroblue tetrazolium salt (NBT) and 400 µM 5-bromo-4-chloro-3-indolyl phosphate (BCIP) (Roche). When sufficient purple colour appeared reaction was stopped by washing in water. Finally, the sections were mounted with Clarion Mounting Medium (Biomeda Corp.)

23.5 Whole mount *in situ* hybridization

Embryos were isolated from pregnant C57BL/6J mice at the time indicated in the text. The day of plug detection was considered to be 0.5 dpc (day post conception).

Embryos from day 9 p.c. until 15 p.c. were dissected from decidua, yolk sac and amnion in DEPC-treated PBS (4˚C) and briefly washed in PBS and fixed by rocking for 1–2 h at RT or 4˚C overnight in 4% PFA. After fixation embryos were twice washed (inverting tube several times) in PBS (4˚C) containing 0.1%Tween (PBST). Bleaching by 100% methanol/30% hydrogen peroxide 5:1 for 5–6 h was followed by several washes in methanol and finally embryos were rehydratated (allowing embryos to settle) in methanol/PBST. Prior to hybridization, digestion for 15–30 min with 10 µg/ml Proteinase K dissolved in PBST was performed, followed by rinsing with 0.2% glycin/PBST and with PBST. A 20 min fixation was performed in 4% PFA/0.2% glutaraldehyde resolved in PBST. Postfixation the embryos were rinsed in PBST and transferred in 2 ml cryotubes (Nunc). After rinsing with PBST/hybridization solution 1:1 (50% formamide, 1.3×SSC (pH5), 5mM EDTA (pH 8), 50µg/ml yeast tRNA, 0.2% Tween-20, 0.5% CHAPS, 100µg/ml heparin all diluted in H_2O-DEPC water) was added. After prehybridization for 1 hour at 70˚C, 0.75 ml 70˚C pre-warmed hybridization solution with 1µg/ml DIG-labelled RNA probe was added. Embryos were hybridized at 70˚C horizontally with rocking overnight. After hybridization embryos were rinsed twice with pre-warmed 70˚C hybridization solution without the probe and subsequently washed twice for 30 min with 1ml pre-warmed 1:1 diluted hybridization solution and MABT buffer (MABT: 100 mM maleic acid, 150 mM NaCl, 0.5% Tween 20). After rinsing three times with 1 ml MABT buffer the embryos were incubated for 1 h with successive solutions: MABT buffer/2% Blocking reagent/2 mM levamisol, MABT buffer/2% Blocking reagent/20% heat-treated sheep serum/2 mM levamisol, and finally overnight at 4˚C in MABT buffer/2% Blocking reagent/20% heat-treated sheep serum/2 mM levamisol solution with AP-anti-DIG antibodies Fab fragment (dilution 1:2000). Before colour reaction embryos were rinsed three times with MABT buffer and transferred into 5 ml transparent glass vials. In those vials embryos were washed by rolling three times for 1h with 5 ml MABT buffer/2 mM levamisol, followed by washing twice for 10 min in NTMT buffer (100 mM Tris-HCl pH 9.5, 50 mM $MgCl_2$., 100 M NaCl; 0.1% Tween 20. To start the color reaction embryos were incubated with 5ml NTMT buffer with 200µl NBT/BCIP first by rocking for 20

min, and then incubated at RT for an additional 30 min to 3 h. After the colour was developed to the desired, embryos were rinsed and washed in PBST buffer and subsequently re-fixed for 2 h in 4% PFA/0.1% glutaraldehyde diluted in PBST buffer. Finally embryos were rinsed twice for 20 min in PBST buffer and stored at 4˚C in PBST buffer containing 0.1% natriumazide.

23.6 *In situ* hybridization on cultured mouse cerebellar cells

In situ hybridization was performed as described in section (23.4 with some modifications. After removal of culture medium, cells were rinsed in PBS and fixed in 4% PFA for 20 min at RT. Cells were rinsed with PBS and treated with 0.1 M HCl for 10 min at RT and subsequently acetylated with 0.25% (v/v) acetic anhydride in 0.1 M triethanolamine (pH 8.0) for 10 min, followed by dehydratation in a graded series of ethanol concentration and airdrying. Hybridization was performed overnight at 55˚C in hybridization solution as described in section 23.4. After hybridization cells were incubated twice for 15 min in 2×SSC at 55˚C and 1×SSC/50% formamide for 30 min at 55˚C, and subsequently incubated twice in 0.5×SSC for 10 min and once in 0.2×SSC for 10 min at RT. Finally cells were rinsed in PBS and then ISH was performed as describe in section 23.4.

23.7 Cell cultures of neurons, astrocytes and oligodendrocytes

The neurons, astrocytes and oligodendrocytes were prepared from primary mixed cell cultures of 6 day mouse cerebellum. The below described procedures are necessary to eliminate neurons and astrocytes [Itoh et al., 2000].

Oligodendocytes Cerebellum was mechanically dissociated in 10% fetal calf serum in Eagle's MEM (FCS/EMEM). The dissociated cells were centrifuged for 10 min, 100 rpm at 4˚C. Cells were resuspended in FCS/EMEM and were seeded on poly-L-lysine (PLL; 100 µg/ml; Sigma) coated 90 mm-diameter culture dishes (Griner, Germany) at density of 1×10^7 cells/dish. After 7 days of culture, the cells were passaged with 0.05% trypsin in D-PBS (1^{st} passage). Cells were resuspended in FCS/EMEM and were cultured for 7 days at density of 8×10^6 on non-coated culture dishes. After 7 days of culture, cells were passaged with 0.05% trypsin in D-PBS (2^{nd} passage), resuspended in FCS/EMEM and cultured for 2 days at a density 3×10^6 on non-coated culture dishes. On the second day of culture, the medium was exchanged by serum-free DMEM (Invitrogen) suplemented with 5.6 mg/ml glucose, 5 µg/ml insulin, 0.5 µg/ml transferin, 100 mg/ml bovine serum albumin, 0.06 ng/ml progesterone, 16 µg/ml putrescine, 40 ng/ml sodium selenite, 40 ng/ml thyroxine, 30 ng/ml triiodthyronine, 2 ng/ml basic fibroblast growth factor (bFGF; all ingredients from Sigma). After 5 days of culture, cells were passaged with 0.05% trypsin in D-PBS (3^{rd} passage) and were resuspended in serum-free DMEM at a density of 2×10^6 cells on a non-coated petri dish in the absence of bFGF. The cells were cultured 1 month before ISH and immunocytochemical staining was performed.

Neurons The cerebellar mechanically dissociated cells were resuspended in serum-free DMEM supplemented with 25 µg/ml insulin, 100 µg/ml transferin, 100µg/ml BSA, 20 nM progesterone, 60 µM putrescine, 30 ng/ml sodium selenite to eliminate oligodendrocytes and astrocytes and were seeded on PLL (100 µg/ml) coated dishes at a density of 2×10^6. After 7 days of culture, neurons were used for experiments.

Astrocytes The cells were resuspended in 10% FCS/DMEM and were seeded on PLL (100 µg/ml) coated culture dishes at a density of 1×10^6. After 7 days of culture, cells were passaged with 0.05% trypsin in D-PBS to eliminate other cells. After resuspension in 10% FCS/DMEM, astrocytes were seeded and cultured for 7 days.

23.8 Immunohistochemistry on paraffin-embedded sections

Sections were stained by standard immunohistochemical techniques. Primary antibodies were detected with an avidin-biotin peroxidase system (Vector Laboratories, CA, USA) with diaminobenzidine as the chromogen or by fluorochrome conjugated secondary antibodies. All antibodies were diluted in PBS with 3% goat serum, 2% BSA, 0.3% Triton X-100 with working concentration pAbhB3-A 1:50 and pAbhB3-B, 1:500. Endogenous peroxidase was inhibited by incubation with 3% H_2O_2 in methanol for 30 min. Slides were rinsed in water, and for antigen retrieval and improved accessibility of epitopes sections were subjected to 0.1 M glycin/6 M Urea (pH 3.5) solution for 10 min. The nuclei of cells were counterstained for 30 sec with haematoxylin and after drying slides were mounted in Clarion mounting medium. Control sections were incubated either with non-immune serum or by omitting the primary antibodies.

PBS	8.1 mM Na_2HPO_4 1.5 mM KH_2PO_4 137 mM NaCl 2.7 mM KCl pH 7.3 with HCl adjusted
PBST	PBS with 0.05% Tween 20
$PBS^{+/+}$	PBS with 0.5 mM $CaCl_2$ 1 mM $MgCl_2$
High-salt-$PBS^{+/+}$	$PBS^{+/+}$ with 500 mM NaCl
PFA-solution	4% Paraformaldehyd in $PBS^{+/+}$
Blocking solution	$PBS^{+/+}$ with 2% BSA; 3% Goat serum; 0.3% Triton X-100
Antibody solution	$PBS^{+/+}$ with 3% Goat serum; 2% BSA

23.9 Immunohistochemistry with fluorescent secondary antibody

Sections of 4-6 µm-thickness were dried at least one and a half hours under laminar flow containment and after fixation in methanol or acetone again followed by two hours drying. Sections were blocked to prevent non-specific binding of antibody for 30 min in blocking solution consisting of 3% goat serum, 2% BSA, and 0.3% Triton X-100 in PBS buffer. Primary antibodies were diluted in 3% goat serum in PBS buffer and applied on sections and incubated overnight at 4˚C in a humid chamber. After incubation sections were washed in PBS buffer and secondary antibody Cy3-anti-rabbit or Cy3-anti-mouse (Dianova) were applied. Incubation was performed for 45 min in a protected light area followed by three washing with 0.1% Tween 20 in PBS. Slides were mounted using Clarion mounting medium and analysed with the Zeiss Axioplan fluorescence microscope.

24 Exon trapping

24.1 Exon trapping constructs

An Exon Trapping System (Gibco, BRL) was used to investigate, whether the intronic mutation IVS22+21G>A has an influence on splicing. A sample of DNA with the mutation was obtained from patient no.1378. From the patient and wild-type DNA using a primer combination of SPLEF and SPLBR, a 1065 bp fragment containing 57 bp of intron 19, exon 20, intron 20, exon 21, intron 21, exon 22, intron 22, exon 23, and 72 bp of intron 2 was amplified and subcloned into a pCR®-2.1-TOPO® plasmid and sequenced using m13uni and m13rev primers. Control construct containing the genomic DNA fragment in reverse orientation was used and amplified using primers SPLBF and SPLER. Reverse orientation of fragment did not allow splicing and therefore served as a negative control. The mutant, wild type, and negative control were subcloned into exon trapping vector pSPL3 (GIBCO, BRL). Constructs were transfected into COS-7 cells, and cytoplasmatic RNA was extracted. DNA constructs which contained exons in the proper orientation (wild type and mutant construct) allowed splicing between the vector and insert. cDNA synthesis was performed using SA2 primer, and for primary PCR primers SA2, SD6 were used, and for secondary PCR dUSA4 and dUSD2 were used. To eliminate vector-derived products the primary PCR products were treated with Bstx I. The putative insert-specific RT-PCR amplification products were subcloned either into a pAMP10 vector or into pCR®-2.1-TOPO® and plated. Colony PCR products were sequenced using dUSD2 or m13uni and m13rev primers and analyzed. All three constructs, and an empty pSPL3 vector with no genomic insert serving as a negative control, were included in each experiment in order to control for the presence of vector-derived PCR products.

Construct	Subcloning vector (Restriction sites)	Target vector (Restriction sites)	Primers
pSPL3wt	pCR®-2.1-TOPO®	pSPL3	SPLEF
	EcoR I/BamH I	EcoR I/BamH I	SPLBR
pSPL3mut	pCR®-2.1-TOPO®	pSPL3	SPLEF
	EcoR I/BamH I	EcoR I/BamH I	SPLBR
pSPL3neg	pCR®-2.1-TOPO®	pSPL3	SPLBF
	EcoR I/BamH I	EcoR I/BamH I	SPLER

25 Promoter assay

25.1 Promoter constructs

For functional analysis of the promoter region of *PLXNB3* the commercially available Great EscAPE system (Great EscAPE™ SEAP, Clontech) was used. SEAP, used as reporter molecule, is secreted alkaline phosphatase, and encodes a truncated form of the placental enzyme. This protein lacks the membrane-anchoring domain; thereby the protein is efficiently secreted from the transfected cells into medium and allows monitoring activity of promoters and enhancers or silencers. Using human DNA as template, PCR was used to amplify 5 different regions of putative promoter with Platinum Pfx DNA Polymerase. PCR products were subcloned into pCR2.1®-TOPO® vector using a TOPO TA Cloning Kit®. Constructs were sequenced to confirm correct position and orientation of cloned fragments in the pCR2.1®-TOPO® vector. Constructs pex1+2, p1, p2, p3, p4 and p5 were recloned to a pSEAP2-basic vector. This vector

lacks eukaryotic promoter and enhancer sequences and has a multiple cloning site (MCS) that allows promoter DNA fragments to be inserted upstream of the *SEAP* gene. The constructs were co-transfected with β-galactosidase plasmid in CHO-K1, HeLa and HEK cells. Control plasmid containing the SV40 early promoter inserted upstream and SV40 enhancer inserted downstream driving the expression of *SEAP* gene (pSEAP2-Control), and the promoter-less plasmid pSEAP2-Basic were co-transfected as well.

Construct	Subcloning vector (Restriction sites)	Target vector (Restriction sites)	Primers	NCBI/GenBank Acc. no. U52111
pex1+2	pCR®-2.1-TOPO®	pSEAP2-Basic	B3PF	U52111
	EcoRI/XhoI	EcoR I/Xho I	B3P+R	
p1	pCR®-2.1-TOPO®	pSEAP2-Basic	B3P1F	U52111
	EcoRI/XhoI	EcoR I/Xho I	B3PR	
p2	pCR®-2.1-TOPO®	pSEAP2-Basic	P2F	U52111
	EcoRI/XhoI	EcoR I/Xho I	B3PR	
p3	pCR®-2.1-TOPO®	pSEAP2-Basic	B3P3F	U52111
	EcoRI/XhoI	EcoR I/Xho I	B3PR	
p4	pCR®-2.1-TOPO®	pSEAP2-Basic	B3P4F	U52111
	EcoRI/XhoI	EcoR I/Xho I	B3PR	
p5	pCR®-2.1-TOPO®	pSEAP2-Basic	B3P5F	U52111
	EcoRI/XhoI	EcoR I/Xho I	B3PR	

25.2 Transfection assay

The Great EscAPE system (Great EscAPE™ SEAP, Clontech) uses SEAP, a secreted form of human placental alkaline phosphatase, as a reporter molecule to monitor the activity of potential promoters and enhancers. Secreted alkaline phoshatase activity was measured in the growth medium. 110 µl of cell culture medium was removed 72 h after transfection from appropriate cells. Medium was centrifuged for 1 min at 12,000 rpm to remove any cells present in the medium. To block endogenous alkaline phosphatase, 25 µl of supernatant was diluted with 25 µl of 1x dilution buffer and incubated for 30 min at 65˚C. The samples were cooled down on ice for 2-3 min and then equilibrated at RT for 5 min. 97 µl of Assay Buffer was added and incubated at RT for an additional 5 min. Finally 3 µl of 1 mM MUP Fluorescent Substrate solution was added and incubated for 60 min at RT protected from light (all buffers and chemical Clontech). The excitation and emission peaks of MUP fluorescence are 360 nm and 449 nm, respectively. The assay was performed in black 96-well flat bottom microtiter plates suitable for plate fluorometers. The fluorescent emission was detected using plate fluorometer FluoroCount with Filter Wheels. The obtained data were analysed using PlateReader 3.0 for Windows software.

25.3 Cell lysate preparation and β-galactosidase assay

β-galactosidase was used in the promoter assay as the reporter molecule to evaluate the efficiency of cell transfection. The β-galactosidase Enzyme Assay System with Reporter lysis Buffer (Promega) was the method used for assaying of β-galactosidase activity in lysates prepared from cells co-transfected with β-galactosidase reporter vector (Promega).

Fluorescence data (fluorescent counts) obtained from SEAP activity measurement were normalized with β-galactosidase activity, which was measured in the same cell lysates. 72 hours after transfection cell growth medium was removed. Cells were washed twice with 1×PBS

(Mg^{2+}, Ca^{2+}) and 400 µl of Reporter Lysis Buffer (Promega) was added to the culture dish. The dish was slowly rocked during incubation for 15 min. Cell lysate was scraped from the culture dish and transferred to tubes. Tubes were vortexed for 15 sec and then centrifuge for 2 min/14,000 rpm at 4˚C. Supernatant was transferred to a new tube and lysate was assayed directly or stored at -70˚C prior to measurement.

The β-galactosidase assay was performed directly in 96-well plates, and absorbance of each sample was measured using a plate reader. A negative control was prepared using the same dilution of cell lysate made from cells that had not been transfected with β-galactosidase vector. 50 µl of cell lysate was added to a 96-well plate; when necessary, cell lysate was diluted (e.g. 30 µl of cell lysate + 20 µl RLB) in 1×Reporter Lysis Buffer (Promega). 2×Assay Buffer (Promega) was added to 50 µl protein lysate and mixed. The 96-well plate was covered and incubated at 37˚C for 30 min to 3 h, until a faint yellow colour had developed. The reaction was stopped by adding 150 µl of 1 M Sodium carbonate. Reading of absorbance of the sample at 420 nm was performed in a plate reader.

26 Computer based analysis

NCBI (National Center for Biotechnology) GenBank contains a genetic sequence database, with an annotated collection of all publicly available DNA sequences. http://www.ncbi.nlm.nih.gov/GenBank/

BLAST (Basic Local Alignment Search Tool) For homology searches and alignment of nucleotide sequences.http://www.ncbi.nlm.nih.gov/BLAST [Altschul et al., 1990].

OMIM (Online Mendelian Inheritance in Man) McKusick-Nathans Institute for Genetic Medicine, Johns Hopkins University (Baltimore, MD) and National Center for Biotechnology Information, National Library of Medicine (Bethesda, MD). http://www.ncbi.nlm.nih.gov/omim/ /Searching in database and a catalog of human genes and genetic disorders.

GENESCAN For predicting the locations and exon-intron structures of genes in genomic sequences from a variety of organisms. http://genes.mit.edu/GENSCAN.html [Burge and Karlin, 1997].

ClustalW For alignment of homologous sequences. http://searchlauncher.bcm.tmc.edu/multi-align/multi-align.html and Human Genome Sequencing Center, One Baylor Plaza, Houston, TX.

BOXSHADE http://www.ch.embnet.org/software/BOX_form.html. Shading of or pretty-printing multiple alignment output. Swiss Institute of Bioinformatics (SIB).

Promoter prediction and seaching for Transcription Factor Binding Sites
http://www.genomatix.de/
http://www.cbrc.jp/research/db/TFSEARCH.html
http://www.cbs.dtu.dk/services/ProtFun/
http://rvista.dcode.org
http://ecrbrowser.dcode.org

Splice Site Prediction
http://palsdb.ym.edu.tw/
http://www.cbs.dtu.dk/services/NetGene2/
http://l25.itba.mi.cnr.it/~webgene/wwwspliceview.html
http://www.fruitfly.org/seq_tools/splice.html

27 NCBI entries of sequences

All human, chimp, mouse and rat sequences were obtained from NCBI GenBank entries with following accession numbers:

Homo sapiens	AF149019, U52111, NM_005393
Pan troglotydes	AC151486
Rattus norvegicus	XM_343841
Mus musculus	NM_019587

Part IV

Results

28 Expression pattern of *PlxnB3*

28.1 *PlxnB3* is expressed in neurons

In order to examine expression of *PlxnB3* at the cellular level, non-radioactive *in situ* hybridization (ISH) was performed in murine embryonic and adult tissues. The two cRNA probes (A and B) corresponding to the most specific plexin B3 region were used (Figure 28.1) and were complementary to 1.2–1.9 kb of the 3′ region of the *PlxnB3* mRNA. ISH probe A, corresponding to *PlxnB3* nucleotides from 4,647–5,936 and probe B corresponding to nucleotides from 3,744–5,702 (numbering of nucleotides is according to NCBI/GenBank Acc. no. NM_019587), were synthesized and controlled for usability by comparing the hybridization results of the antisense probes with those of the corresponding sense probes, i.e. the negative control probes (Figure 28.2.F).

Figure 28.1. *The position of the PlxnB3-specific DIG-labelled cRNA probes relative to the PlxnB3 mRNA. Probe A extends from exon 25 to exon 36 and contains also 245 bp of the 3′ UTR, probe B extends from exon 20 to exon 36.*

ISH using probe A performed on specimens of various adult mouse organs resulted in strong hybridization signals in several brain areas and suggested the predominant neuronal expression of *PlxnB3* (Figure 28.2). Neurons of all six layers of the cerebral cortex appeared to stain positive (Figure 28.2.B). Especially, strong signals were obtained in the hippocampus (dentate gyrus and pyramidal cells of cornu ammonis (Figure 28.2.A). Other brain areas, such as the granular cells of the granular layer and Purkinje cells of the cerebellum were also positive (Figure 28.2.C). At higher magnification, expression of *PlxnB3* in distinct hypothalamic and thalamic nuclei was detected (data not shown). No specific expression could be demonstrated in the white matter or in plexus chorioideus (Figure 28.2.D and E). ISH using probe B showed neuronal expression of *PlxnB3* but in addition, also expression in oligodendrocytes. Positive signal was seen in oligodendrocytes of the white matter, e.g. distinct cell populations of oligodendrocytes in the stratum moleculare of the cerebellum.

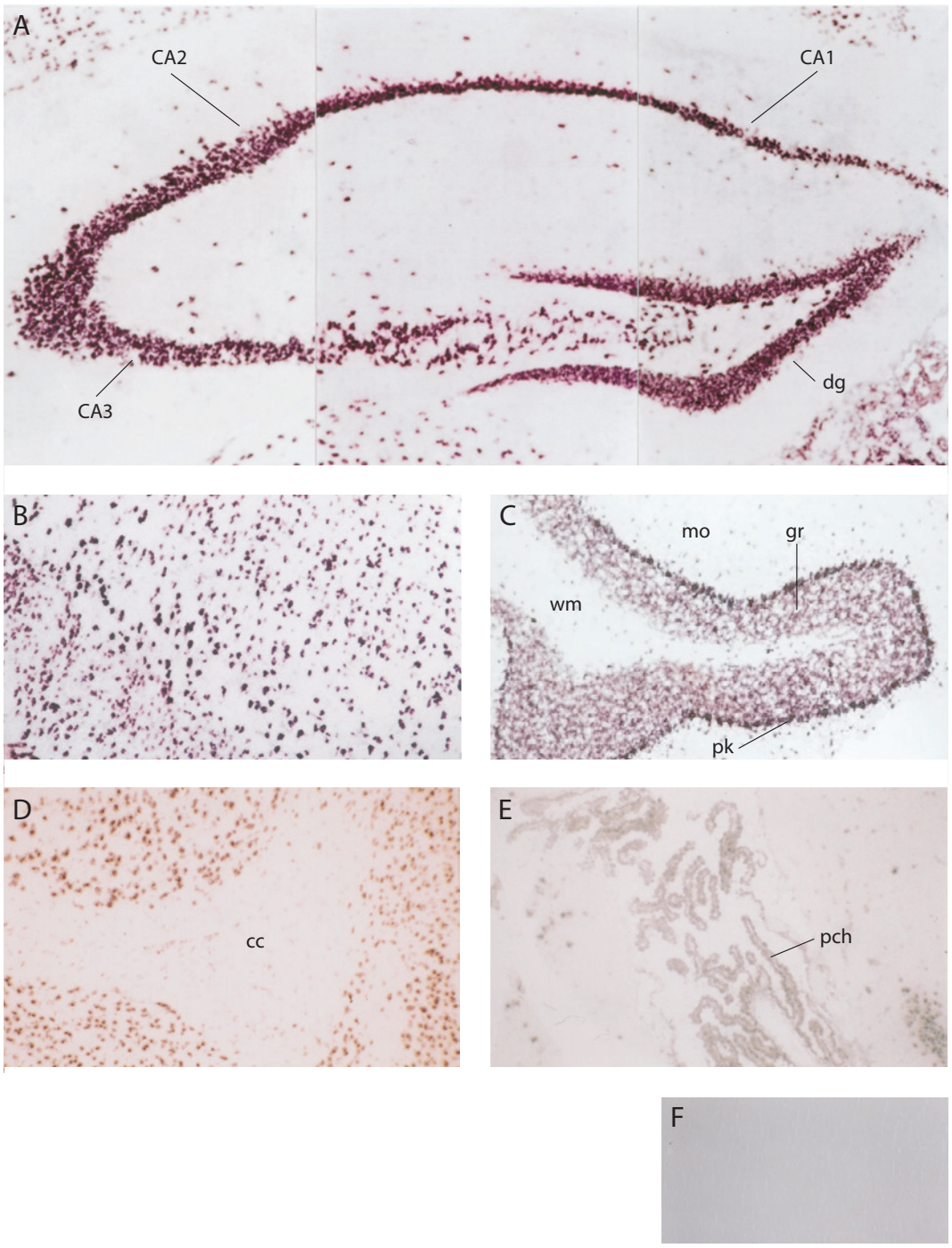

Figure 28.2. *In situ hybridization of mouse brain with DIG-labelled antisense cRNA of PlxnB3. Tissue sections were hybridized with the antisense DIG-labelled cRNA probe A (A-E). An example of the control experiments using the corresponding sense probe is shown in F. (A) Hippocampus: strong positivity is seen in the pyramidal neurons of cornu ammonis, CA1, CA2, CA3 regions and dentate gyrus. (B) Cortex: positive neuronal signals are visible throughout all six layers of the grey matter. (C) Cerebellum: most intense staining is seen in the Purkinje cells and granular cells. No positive signal is seen in the white matter of the corpus callosum in (D) and in the plexus chorioideus in (E). (F) Lack of signal obtained when the sections were hybridized with the sense probe. Original magnification 200×. Abbreviations are as follows:* ***CA1-3*** *of cornu ammonis;* **dg** *dentate gyrus,* **mo***, molecular layer;* ***pk****, Purkinje layer;* ***gr****, granule layer;* ***cc****, corpus callosum;* ***pch****, plexus choroideus;* ***wm****, white matter.*

28.2 In hippocampus, *PlxnB3* is expressed predominantly in NeuN-positive cells

In order to investigate whether *PlxnB3* is expressed predominantly in neurons, ISH on sagittal sections of the hippocampus was combined with immunohistochemistry. To distinguish neurons, astrocytes and oligodendrocytes, cell type-specific antibodies were used against NeuN (neuron-specific), GFAP (astrocyte-specific) and CNPase (oligodendrocytes-specific). ISH using DIG-labelled antisense probe A was followed by fluorescent immunohistochemistry using the cell-type specific monoclonal antibodies. Only the NeuN positive cells appeared to express *PlxnB3*, strongly supporting the above-mentioned result of the predominant neuronal expression of *PlxnB3* (Figure 28.3).

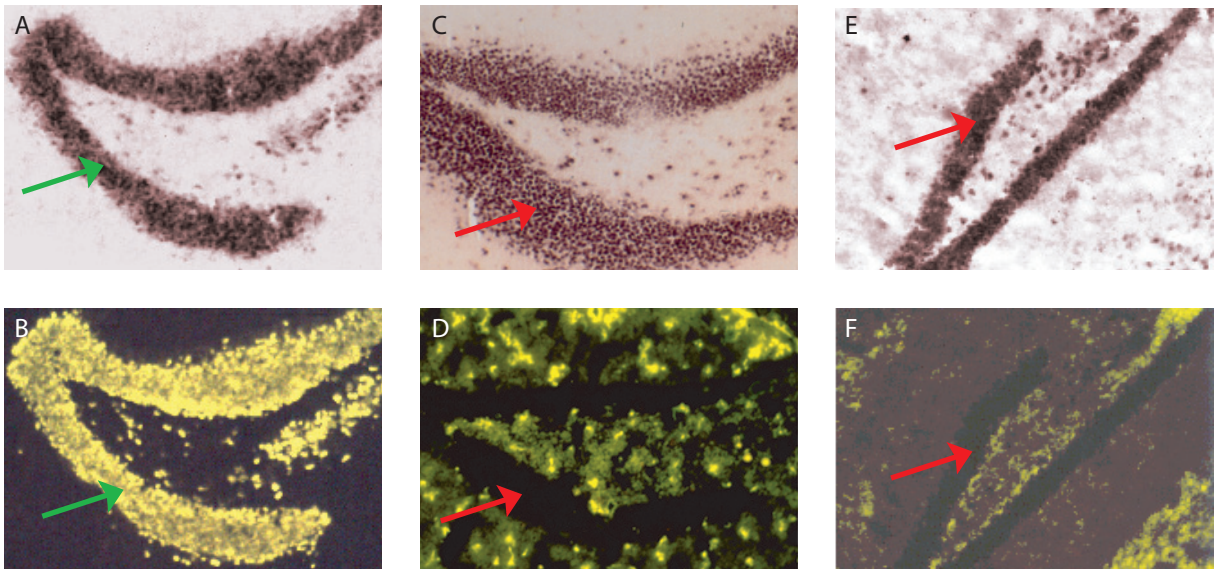

Figure 28.3. *PlxnB3 mRNA is expressed in NeuN-positive cells of the mouse hippocampus but not detectable in GFAP positive cells (astrocytes) and CNPase positive cells (oligodendrocytes). PlxnB3 mRNA (purple) was detected by ISH using DIG-labelled antisense cRNA probe A (A, C, E), followed by immunohistochemistry using NeuN (B), GFAP (D), CNPase (F) antibodies on adult mouse sagittal brain sections. PlxnB3 mRNA-positive cells (A, green arrow) are positively stained using neuronal marker NeuN (B, green arrow). No PlxnB3 mRNA was detected in GFAP-positive astrocytes (C, D, red arrow) and CNPase-positive oligodendrocytes cells (E, F, red arrow). Original magnification 200×.*

28.3 *PlxnB3* is expressed in cultured primary neurons

In order to investigate the cell type-specific expression of *PlxnB3* in primary cultured cells of the nervous system, cerebellar tissue of a six day old mouse was dissociated. Cells of the cerebellar lysate were cultured under cell type-specific selective conditions. After ISH with the *PlxnB3* DIG-labelled antisense probe A, the specimens were immunostained using antibodies against NeuN, neuromodulin, GFAP, and CNPase. Double labelling using anti-NeuN or anti-neuromodulin was performed on neurons grown seven days *in vitro* (DIV), anti-GFAP on astrocytes grown 7 days (DIV), and anti-CNPase on oligodendrocytes selectively grown for 28 days *in vitro* (DIV). Only cells positive for neuron-specific markers NeuN and neuromodulin showed co-localization with cells expressing *PlxnB3*. Cells immunoreactive for GFAP and CNPase show no *PlxnB3* hybridization signal (Figure 28.4).

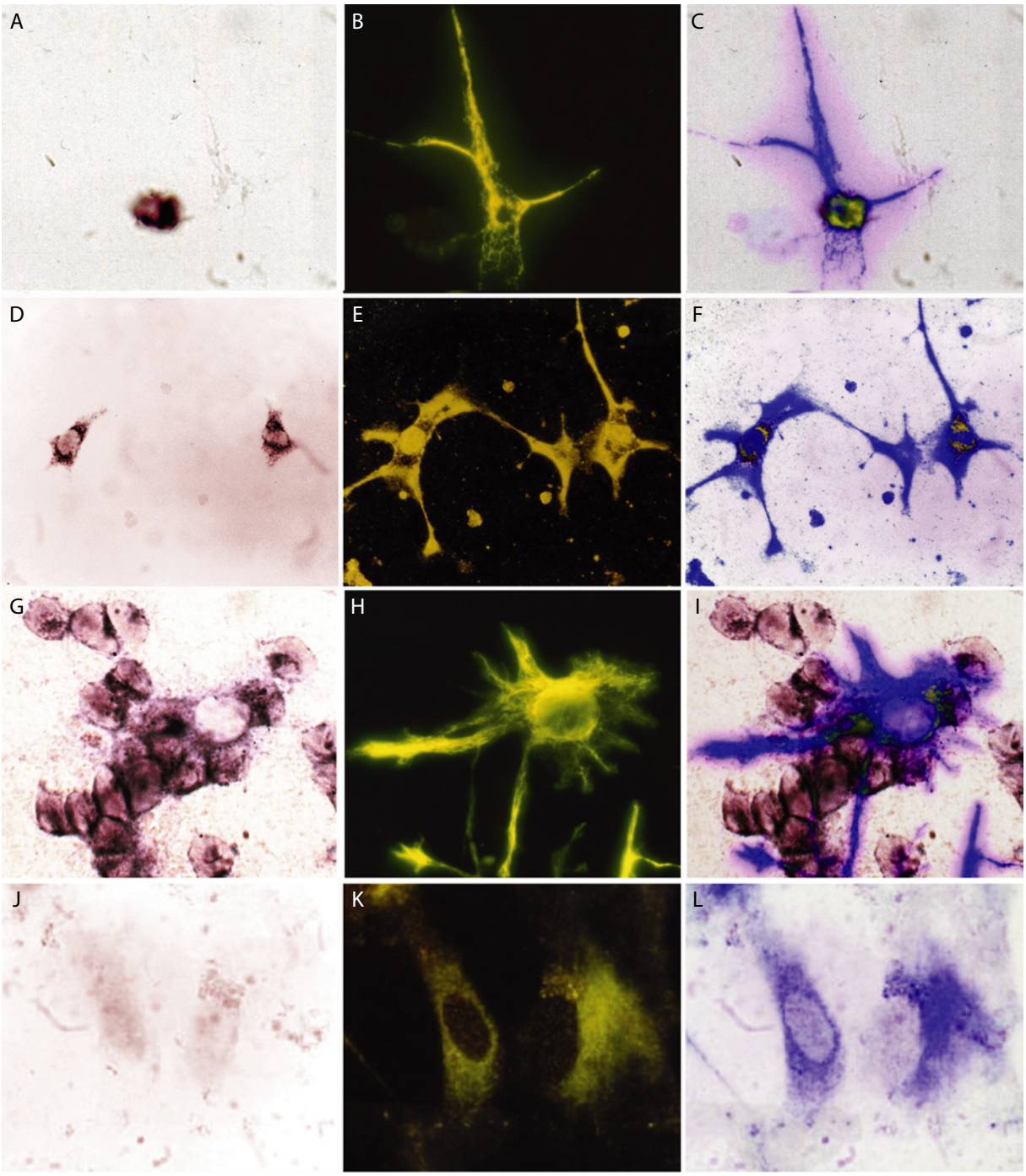

Figure 28.4. *Expression of PlxnB3 in cultivated primary murine cerebellar neurons. Expression of PlxnB3 in cultivated primary cerebellar neurons isolated from four day old c57BL/6J mice (A-F; 400× magnification) but not in astrocytes (G-I) or oligodendrocytes (J-L) (630× magnification). The cells were cultivated from a cerebellar homogenate of a four day old mouse and analyzed by combined in situ hybridization (ISH) using a PlxnB3-specific probe A (A,D,G,J) and immunocytochemistry (IC) using cell type-specific antibodies (B, E, H, K). Overlays of ISH bright field signals and IC signals (blue) are shown in C, F, I, L. The cells were grown under the respective selective conditions for neurons, astrocytes or oligodendrocytes. Following ISH slides were used for IC using primary antibodies against neuromodulin (B) and NeuN (E) for neurons, GFAP for astrocytes (H) or CNPase for oligodendrocytes (K). The Neuromodulin- and NeuN-positive cells (neurons) shown in B and E are positive for PlxnB3 mRNA (A, D)*

29 Developmental expression of *PlxnB3*

29.1 Analysis of the embryonic expression of *PlxnB3* by *in situ* hybridization

To elucidate the spatial and temporal expression of *PlxnB3* during mouse embryonic development, non-radioactive ISH at embryonic stages E8–E15 was performed. The results show an expression of *PlxnB3* in the central nervous system (CNS) throughout all developmental stages studied. Outside the developing nervous system, *PlxnB3* was expressed in the lung bud, bronchus, forelimb bud, primordial follicles of vibrissae, primordium of upper and lower teeth, thymus gland, and all of the epidermis. The expression in the developing liver was not evaluated due to high background signal. The overall expression patterns of *PlxnB3* are presented on sagittal sections of mouse embryo at embryonic stages E8, E9, E10.5, E11, and E15 shown in Figures 29.1 – 29.6.

29.1.1 Stage E8

At stage E8 the headfolds are prominent, and the boundary zone that separates the neural ectoderm (neuroepithelium) from the surface ectoderm becomes clear in both cephalic regions. *PlxnB3*-specific signal is seen in cells of the primordia of the neuroepithelium of the cephalic neural fold (prospective hindbrain region). Cells of the cephalic mesenchyme (prospective midbrain) and cells of the intra-embryonic coelomic cavity (prospective pericardial cavity) remain negative. The trophoblast is highly positive (Figure 29.1).

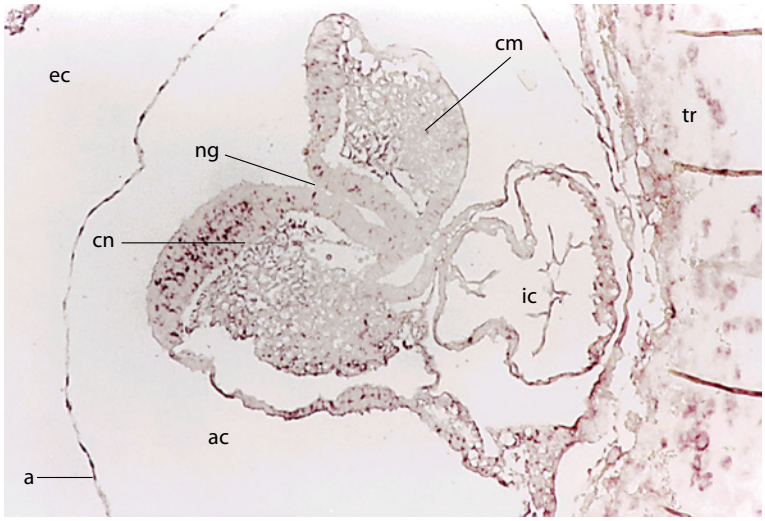

Figure 29.1. *In situ hybridization on E8 mouse embryo section with PlxnB3-specific probe. Positive signal is seen as purple colour. Original magnification 100×. Abbreviations are as follows:* **a**, *amnion;* **ac**, *amniotic cavity;* **cm**, *cephalic mesenchyme tissue;* **cn**, *neuroepithelium of cephalic neural fold;* **ec**, *extra-embryonic coelomic (exocoelomic) cavity;* **ic**, *intra-embryonic coelomic cavity (prospective pericardial cavity);* **ng** *neural groove;* **tr**, *trophoblast.*

29.1.2 Stage E9

At stage E9 the cephalic region of the neural tube begins to close and forms the three primitive brain vesicles. In the forebrain region, the primary optic vesicles become particularly promin-

ent. The sagittal section of the embryo at this stage shows *PlxnB3*-specific signals in the cells of the forebrain, hindbrain and the surface ectoderm (Figure 29.2). A less dense signal is seen in the primary optic vesicle. A strong signal is still present in the extra-embryonic ectoderm (not shown). The cells of the cephalic mesenchyme tissue are negative.

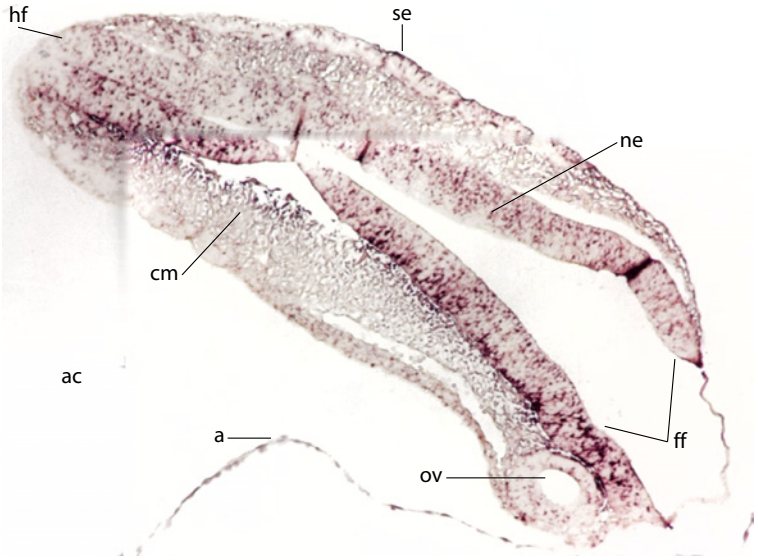

Figure 29.2. *In situ hybridization on E9 mouse embryo section with PlxnB3-specific probe. Original mg 100×. Abbreviations are as follows:* **a**, *amnion;* **ac**, *amniotic cavity;* **cm**, *cephalic mesenchyme tissue;* **ff**, *forebrain of neural fold;* **hf**, *hindbrain of neural fold;* **ne**, *neuroepithelium of prospective rhombomere;* **se**, *surface ectoderm;* **ov**, *optic vesicle.*

29.1.3 Stage E10.5

At stage E10.5 a progressive differentiation of the two telencephalic vesicles becomes evident. The *PlxnB3*-specific signals are visible in cells of the floor plate of the prospective rhombencephalon and at a lower intensity in the mandibular component of the 1st branchial arch and in the otic vesicle. In the heart, a broad region of positive cells in the midline is observed. However, it is unclear, whether this positive signal represents the primordium of the septum primum in the heart (Figure 29.3).

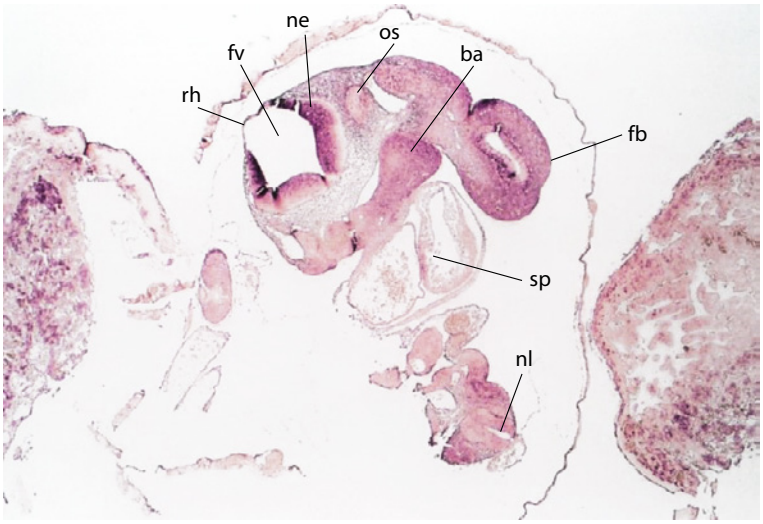

Figure 29.3. *In situ hybridization on E10.5 mouse section with PlxnB3-specific probe. Original magnification 100×. Abbreviations are as follows:* **ba**, *mandibular component of 1*st *branchial arch;* **fb**, *forelimb bud;* **fv**, *fourth ventricle;* **ne**, *neuroepithelium of hindbrain;* **nl**, *neural lumen (dilated region of neural tube in caudal region of the tail);* **os**, *optic stalk;* **rh**, *roof of hindbrain;* **sp**, *putative septum primum.*

29.1.4 Stage E11.5

At this stage the sagittal section shows a distribution of *PlxnB3*-specific signals over various brain areas. *PlxnB3* is expressed in all developing brain regions and in the spinal cord, with the strongest signal in neuroepithelium of the mesencephalic vesicle. Additional signals are observed in the mandibular component of the 1st branchial arch, in the olfactory pit, the main bronchus, and lung bud as well (Figure 29.4).

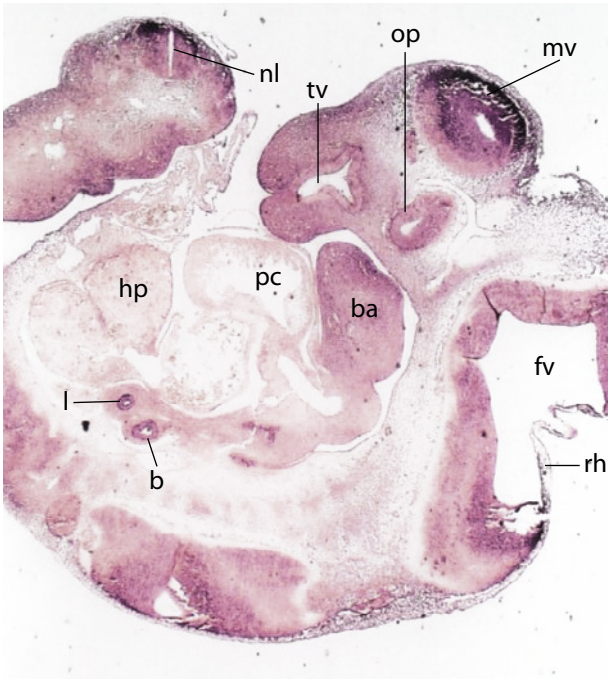

Figure 29.4. *In situ hybridization on E11.5 mouse embryo section with PlxnB3-specific probe. Original magnification 100×. Abbreviations are as follows:* **b**, *main bronchus;* **ba**, *mandibular component of the 1st branchial arch;* **fv**, *fourth ventricle;* **hp**, *hepatic primordium;* **l**, *lung bud;* **nl**, *neuroepithelium of neural tube;* **mv**, *mesencephalic vesicle;* **op**, *olfactory pit;* **pc**, *pericardial cavity;* **rh**, *roof of hindbrain;* **tv**, *third vesicle.*

29.1.5 Stage E15

With respect to CNS development, the principal difference observed between stage E15 and previous stages relates to the increased degree of differentiation of the wall of the telencephalic vesicles. The most marked change relates to the cellular migration from the mantle zone into the overlying marginal zone, a process that forms the primitive cortex. ISH signals are visible as a darkly stained layer of the neopallial cortex rich with cell nuclei and a rather narrow layer of the relatively anuclear marginal zone. The superficial and cortical layers are separated from the mantle layer by a narrow anuclear intermediate zone. Trigeminal and glossopharyngeal ganglions also stain positive for *PlxnB3* (Figure 29.6.A).

In addition, the primordial follicles of the vibrissae associated with the upper lip and the primordia of the upper and lower teeth are clearly positive, particularly the primordia of the upper and lower incisor teeth. With regard to the respiratory tract, positive signals are visible along the length of the trachea and the main bronchus and in the lung lobes (Fig. 29.6.B). Figure 29.5.A shows an overview of a whole sagittal section. No labeling was observed using the sense probe (Figure 29.5.B).

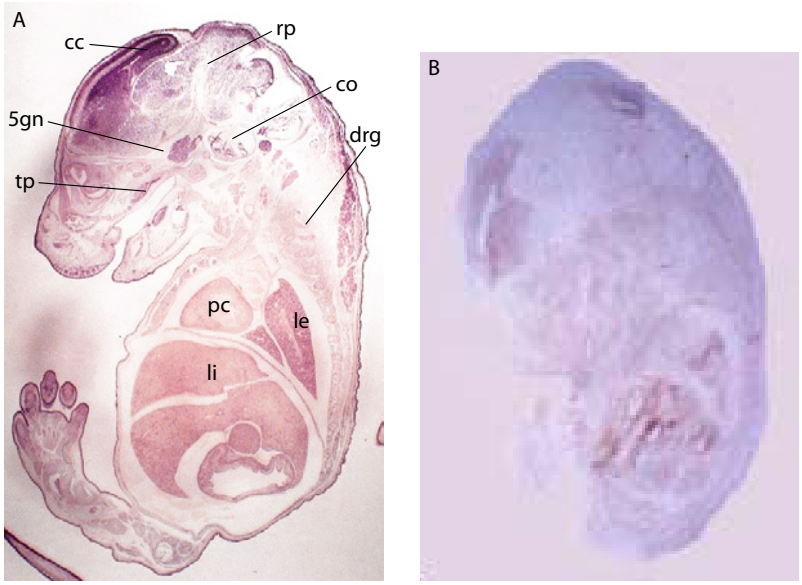

Figure 29.5. *In situ hybridization on E15 mouse embryo sagittal section with PlxnB3-specific probe. (A) Overview; (B) sense probe revealed no detectable signal. Original magnification 25×. Abbreviations are as follows:* **cc**, *cerebral cortex;* **co**, *cochlea;* **drg**, *dorsal root ganglia;* **le**, *lung epithelium;* **li**, *liver;* **pc**, *pericardial cavity;* **rp**, *Rathke's pouch;* **tp**, *tooth primordium;* **5gn**, *trigeminal ganglion.*

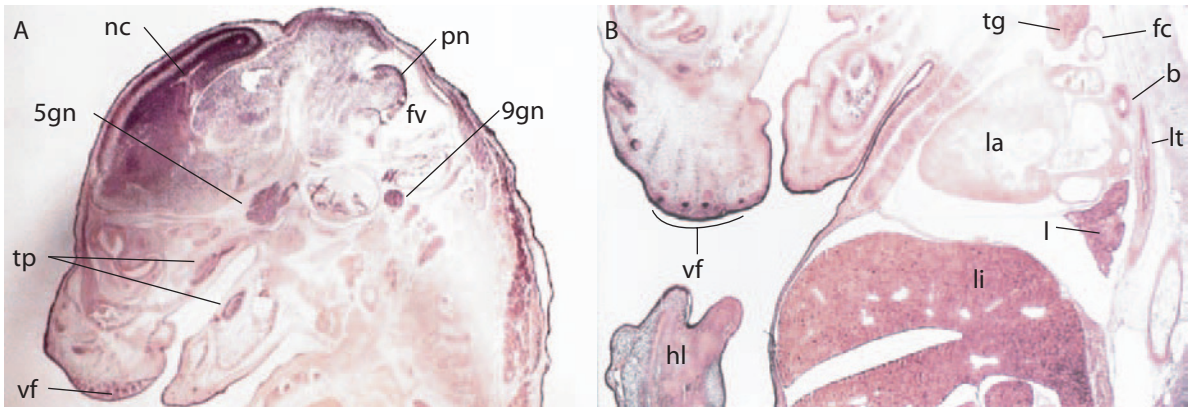

Figure 29.6. *In situ hybridization on E15 mouse embryo sagittal section with PlxnB3-specific probe, detail view on mouse brain and internal organs. Higher magnification of the mouse brain (A) and mouse internal organs (B). Original magnification 40×. Abbreviations are as follows:* **b**, *bronchus;* **fc**, *first costal cartilage;* **fv**, *fourth ventricle;* **hl**, *hindlimb;* **l**, *middle lobe of the lung;* **la**, *lumen of the right atrium;* **li**, *lobe of the liver;* **lt**, *lumen of the caudal part of the trachea;* **nc**, *neopallial cortex (future cerebral cortex);* **pn**, *pontine neuroepithelium;* **tg**, *thymus gland;* **tp**, *primordium of the upper and lower tooth;* **vf**, *primordia of follicles of vibrissae associated with upper lip;* **5gn**, *trigeminal ganglion;* **9gn**, *glossopharyngeal ganglion.*

29.2 Analysis of the expression of *PlxnB3* by whole mount *in situ* hybridization

To further study the expression patterns of *PlxnB3* in the mouse embryo, whole mount ISH was performed at stages E10–E15 using the identical DIG-labelled cRNA probe as for the sagittal sections described above. In the developing brain, whole-mount *in situ* hybridization reveals a complex expression pattern consistent to the one seen on sagittal sections. The whole mount ISH results showed a homogenous expression pattern of *PlxnB3* in the neuroepithelium of all brain areas as shown in the sagittal sections (Figure 29.7).

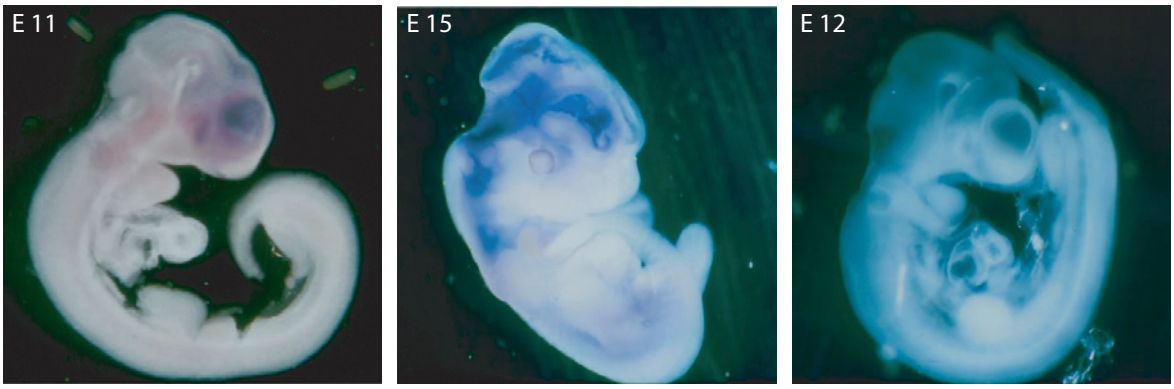

Figure 29.7. *Whole mount in situ hybridization on E11, E15 mouse embryos with PlxnB3-specific probe revealed a prominent expression pattern in the developing brain and spinal cord. At stage E15, PlxnB3 appears to be expressed throughout the central nervous system including the spinal cord (E15), while at stage E11 the most prominent signal is seen in the mesencephalic vesicle (E11). Sense probe at stage E12 revealed no signal. Original magnification 2.5×.*

30 *PLXNB3* expression in human organs

30.1 Northern blot and Multiple RNA dot blot array analysis

Expression of *PLXNB3* was analyzed in various organs by Northern blot and Multiple RNA dot blot array analysis. The *PLXNB3*-specific probe spanning nucleotides 833-1814 (NCBI/GenBank Acc. no. AF14019) was hybridized to normalized Multiple Tissue Northern Blot and poly(A)$^+$ Multiple Tissue Expression Array. Northern blot analysis of twelve human tissues revealed a strong band of ~6.3 kb in the brain sample, and faint hybridization signals in a small number of additional organs such as colon and intestine (Figure 30.1) indicating that *PLXNB3* is expressed not only in the brain. The band observed in brain corresponds to the mature *PLXNB3* mRNA predicted from cloned full-length cDNA. The identical probe was used for hybridization with human multiple RNA dot blot array. Dot blot array confirmed predominant expression of *PLXNB3* in the adult CNS. Most prominent hybridization signals were detected in various human brain regions (putamen, medulla oblongata, corpus callosum, hippocampus, cerebellum), in addition to weak signals in spleen, thymus, lymph node, leukocytes, adrenal and salivary glands (Figure 30.2).

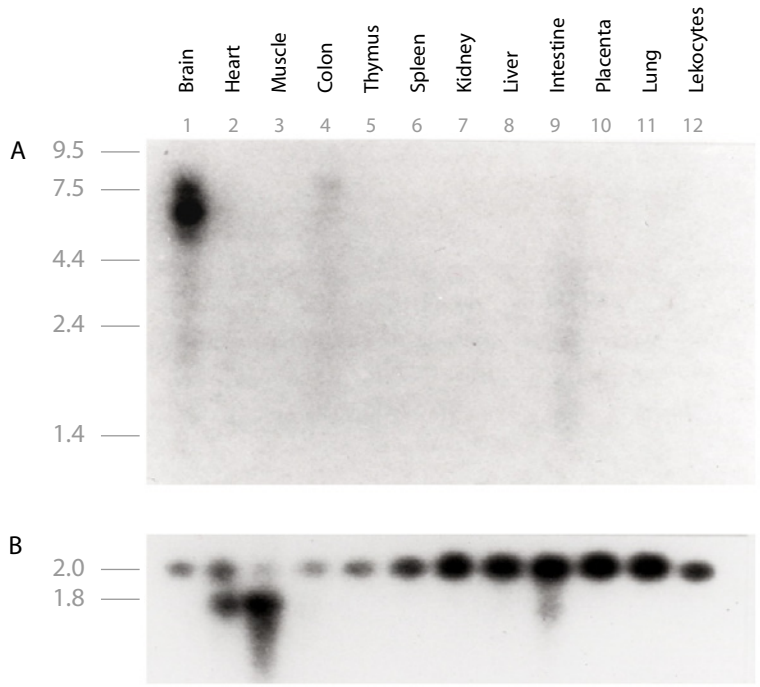

Figure 30.1. *Northern blot analysis of PLXNB3 expression in various human organs. Panel A: Each line was loaded with poly(A)$^+$ mRNA from various human organs as indicated above. Panel B: The membrane was stripped and reprobed with a control β-actin probe. Molecular weight in kb is indicated at the left side.*

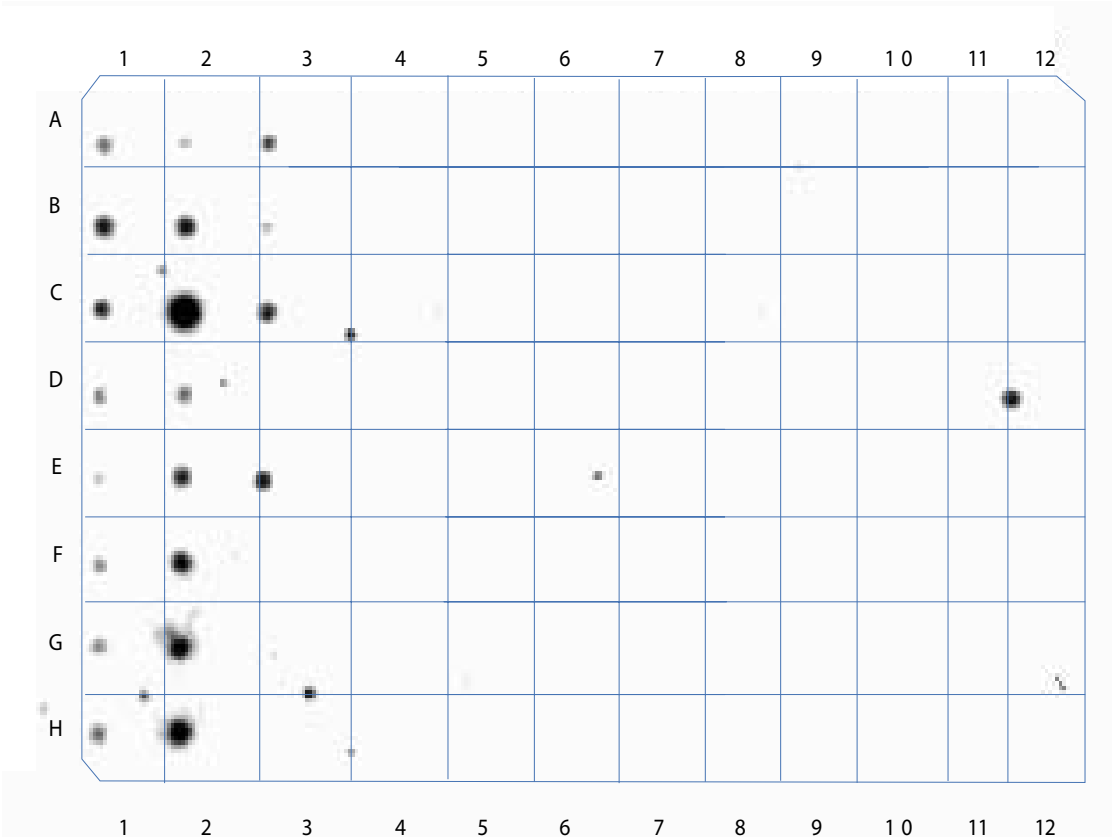

	1	2	3	4	5	6	7	8	9	10	11	12
A	whole brain	cerebellum, left	substantia nigra	heart	esophagus	colon, transverse	kidney	lung	liver	leukemia, HL-60	fetal brain	yeast total RNA
B	cerebral cortex	cerebellum, right	nucleus accumbens	aorta	stomach	colon, desending	skeletal muscle	placenta	pancreas	HeLa S3	fetal heart	yeast tRNA
C	frontal lobe	corpus callosum	thalamus	atrium, left	duodenum	rectum	spleen	bladder	adrenal gland	leukemia, K-562	fetal kidney	*E. coli* rRNA
D	parietal lobe	amygdala	pituitary gland	atrium, right	jejunum		thymus	uterus	thyroid gland	leukemia, MOLT-4	fetal liver	*E. coli* DNA
E	occipital lobe	caudate nucleus	spinal cord	ventricle, left	ileum		peripheral blood leukocyte	prostate	salivary gland	Burkitt's lymphoma, Raji	fetal spleen	poly r(A)
F	temporal lobe	hippo-campus		ventricle, right	ileocecum		lymph node	testis	mammary gland	Burkitt's lymphoma, Daudi	fetal thymus	human C_0t-1 DNA
G	p. g.* of cerebral cortex	medulla oblongata		inter-ventricular septum	appendix		bone morrow	ovary		colorectal adeno-carcinoma, SW480	fetal lung	human DNA 100 ng
H	pons	putamen		apex of the heart	colon, ascending		trachea			lung carcinoma, A549		human DNA 500 ng

Figure 30.2. *Autoradiogram of human poly(A)$^+$ RNA dot blot array. The upper panel shows hybridization of normalized (100-500 ng) human poly(A)$^+$ RNA with the human PLXNB3 cDNA probe. PLXNB3 is expressed predominantly in the human brain, but also in a variety of non-neuronal tissues such as spleen, thymus, lymph node, leukocytes, adrenal and salivary glands. The lower panel lists the type and position of the poly(A)$^+$ RNAs dotted on the membrane.*

30.2 Alternative splicing of *PLXNB3* mRNA in adult human tissues

It is well known, that most of the human genes undergo alternative splicing in order to generate multiple different transcripts, which in turn can give rise to the proteins with very different properties and function. To find out isolated PLXNB3 alternative splicing variants search in human dbEST databank for different PLXNB3 isoforms was performed. This search gave additional data of the *PLXNB3* expression pattern in human tissues.

Screening of human dbEST by full-length *PLXNB3* cDNA revealed 56 fully matching entries, all of them representing the 3'-end of the transcript and two variants (NCBI/GenBank, Acc. no. BF345653 and H51489)). EST BF345653 from oligodendroglioma lacked 246 nucleotides of exon 27 corresponding to bp 4,595–4,840 of AF149019. This gap predicts an in-frame loss of 82 codons (aa 1,495–1,575). EST H51489 from adult brain lacks the 67 3'-terminal nucleotides of exon 27 coresponding to bp 4,774–4,840 of AF149019. This gap predicts a C-terminally truncated isoform of B3 due to a frame-shift predicting nine altered amino acids (aa 1,554–1,563) followed by a premature stop. These findings suggested alternative splicing and the existence of at least three different B3-isoforms due to skipping of various parts of exon 27. Differential expression of the three isoforms in human organs was confirmed by PCR using isoform-specific primers. As shown in Figure 30.3.A the full-length exon 27-isoform was detectable in the majority of the organs analyzed except skeletal muscle and heart. cDNA of the truncated isoform was detectable only in the brain (Figure 30.3.B), whereas the isoform lacking 82 codons was present in skeletal muscle, liver, pancreas, kidney, brain, and heart (Figure 30.3.C). The structures of full length B3 and the two different isoforms are shown in Figure 30.4.

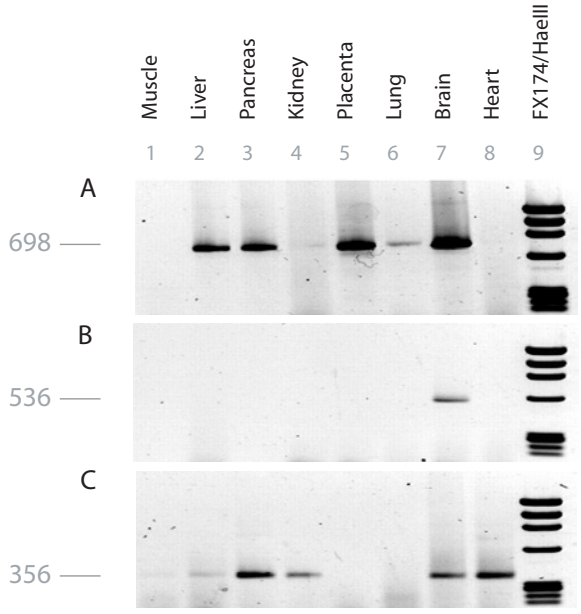

Figure 30.3. *Alternative splicing of PLXNB3 mRNA in adult human tissues. Tissue distribution of three isoforms of PLXNB3 due to alternative splicing of the 3'- part of exon 27. Fragments were amplified by RT-PCR using a common forward primer and isoform-specific reverse primers. Fragment sizes (bp) are given on the right. ϕX174 DNA cleaved by HaeIII was used as size standard. A) 698 bp fragment containing full length exon 27. B) 536 bp fragment lacking the 3'-terminal part of exon 27 and coding for a C-terminally truncated B3. C) 356 bp fragment lacking (in-frame) 246 bp of exon 27.*

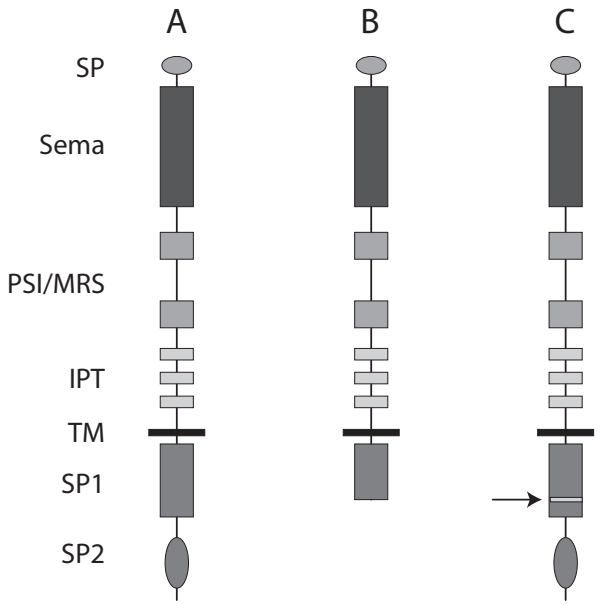

Figure 30.4. *Possible protein structures of B3 predicted by mRNA isoforms generated through alternative splicing of exon 27. D) full length isoform. E) C-terminally truncated B3 predicted by the isoform shown in D. F) structure of the B3 isoform lacking 246 bp of exon 27 (missing 83 amino acids marked by arrow) as shown in E).* **SP**, *signal peptide;* **Sema**, *semaphorin domain;* **MRS**, *Met-related sequences;* **IPT**, *immunoglobulin-like fold shared by plexins and transcription factors;* **TM**, *transmembrane domain;* **SP1/SP2**, *two intracytoplasmatic domains (Sex Plexin).*

30.3 Predominant neuronal expression of *PLXNB3* in the human brain

Various adult human organs were analyzed by ISH using two *PLXNB3*-specific cRNA probes corresponding to *PLXNB3* nucleotides 4515–5552 and 1793–2320 (according to NCBI/GenBank Acc. no. AF14019) (Figure 30.5). The corresponding sense control probes included in every experiment failed to yield signals (Figure 30.5.G). Using both probes covering different part of *PLXNB3* a consistent expression pattern was seen (Figure 30.5.A-F).

Cerebellum *PLXNB3* expression was most prominent in Purkinje cells. These very large neurons at the interface of the molecular and granular layers were amongst the most intensely stained cells. A weaker but consistent staining pattern was observed within the granular layer that is mainly composed of tightly packed granule cells. It could not be excluded that other cell types in this layer, such as Golgi II cells, also express *PLXNB3*. No significant ISH signal was detected within the molecular layer of cerebellum, suggesting that the stellate and others cells in this region do not express *PLXNB3*. Glial cells of the white matter were negative for *PLXNB3* mRNA. Result is shown in Figure 30.5.A.

Hippocampus Neurons of the dentate gyrus were the most prominently stained cells, with tightly packed cell bodies of stratum granulosum displaying strong expression of *PLXNB3*. Figure 30.5.D shows the result of ISH in pyramidal cells of the hippocampus.

Cerebral neocortex In cerebral neocortex, neuronal cell bodies within the grey matter of cortical layers demonstrated positivity for *PLXNB3* mRNA and consequently a six- layered structure could be seen. Very few positive cells could be detected in the molecular layer (layer I), suggesting limited expression or insuficient detection of *PLXNB3* expression in the cells of this region. In the external granular layer (layer II), many positively staining neurons were detected. These cells are primarily pyramidal cells with a small soma. Their staining pattern was variable, some cells were stained more intensely. Similarly, cells of the pyramidal cell layer (layer III) also showed *PLXNB3* mRNA staining. This layer is composed of pyramidal neurons of various sizes with larger cells showing intense staining and smaller cells exhibiting again generally lower and more variable expression. Layer IV (internal granular layer) is largely composed of stellate cells, and does not show sign of *PLXNB3* expression. In the ganglionic layer V, the great majority of pyramidal cells of varying size express *PLXNB3*. In layer VI, fuciform cells, many positive cells were seen, but intensity of expression was generally lower than that seen in layer V. In the subcortical white matter, no *PLXNB3* mRNA was detected, suggesting that astrocytes, oligodendrocytes and other white matter glial cells do not contribute significantly to the production of *PLXNB3* in human brain. Comparable results were obtained in the white matter of all brain regions analyzed. Figure 30.5.E shows the result of ISH in the neocortex.

Thalamus Neurons expressing *PLXNB3* were detected throughout the human thalamus. Due to their large size, the larger thalamic neurons exhibit a relatively homogeneous and very intense cellular cytoplasmatic staining. Figure 30.5.F shows the result of ISH in the thalamus.

Non-neuronal cerebral tissue In addition to neurons, expression of *PLXNB3* was detected in vascular endothelium throughout the brain regions analyzed, including small arteries in the cerebral cortex.

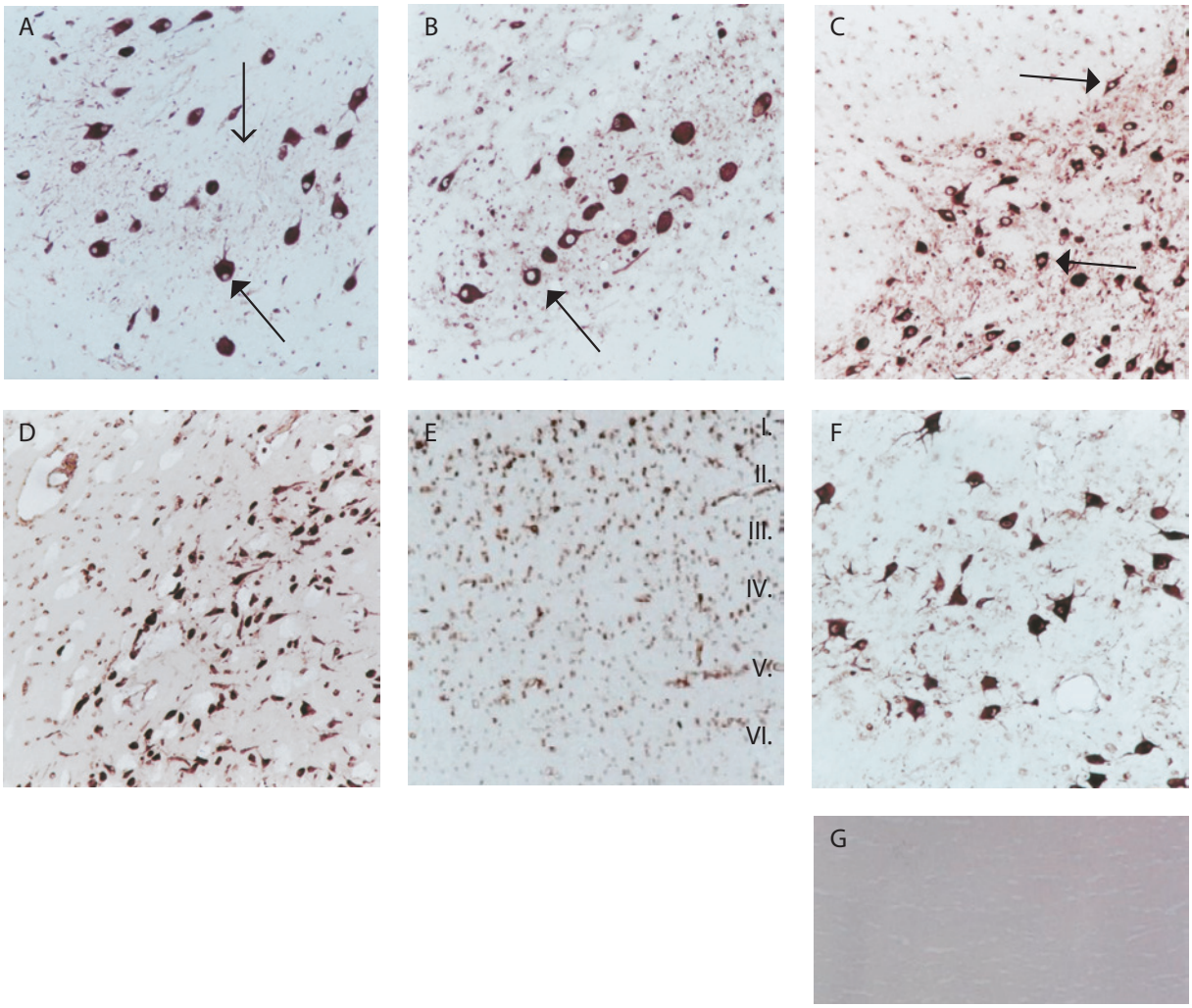

Figure 30.5. *In situ hybridization on paraffin embedded human tissue (Human Normal Tissue set, Novagen) with PLXNB3-specific DIG-labelled cRNA probe. ISH shows the cellular distribution of PLXNB3 mRNA in the human brain. A) Cerebellum: Most intense staining of Purkinje cells (filled arrow) and faint staining of granule cells (open arrow). In the molecular layer, the cell types expressing PLXNB3 are not always distinguishable; some of the positive cells appear to be interneurons likely. B) Spinal cord: Prominent signal in motor neurons (arrow). C) Pons: Intense staining of neurons in the pontine nuclei (arrow). D) Hippocampus: Strong positivity is seen in pyramidal neurons. E) Neocortex: Specific signals of PLXNB3 mRNA throughout all six layers of the grey matter (layers marked by Roman numbers). F) Thalamus: Neurons of various soma sizes show positive signals. G) Negative control using sense probe. Original magnification 100×*

30.4 *PLXNB3* is not expressed in astrocytes and oligondendrocytes

In order to identify the major cell types expressing *PLXNB3* in the adult human brain, ISH was combined with immunohistochemistry (IHC). ISH was followed by cell type-specific fluorescent IHC detecting neuron-specific NeuN, astrocyte-specific GFAP or oligodendrocyte-specific CNPase (Figure 30.6). Neurons were distinguished by monoclonal antibody NeuN that recognizes the neuron-specific nuclear protein NeuN. NeuN labels nuclei and perikarya of most neuronal cells in human brain. Glial fibrillary acidic protein (GFAP) staining was used to identify astrocytes, and cell type-specific marker CNPase (2',3'-cyclic nucleotide 3'-phosphodiesterase) was used for differentiation of oligodendrocytes. The result of combined experiments (ISH followed by IHC) showed that *PLXNB3* is expressed predominantly in neurons, whereas astrocytes and oligondredrocytes remain negative.

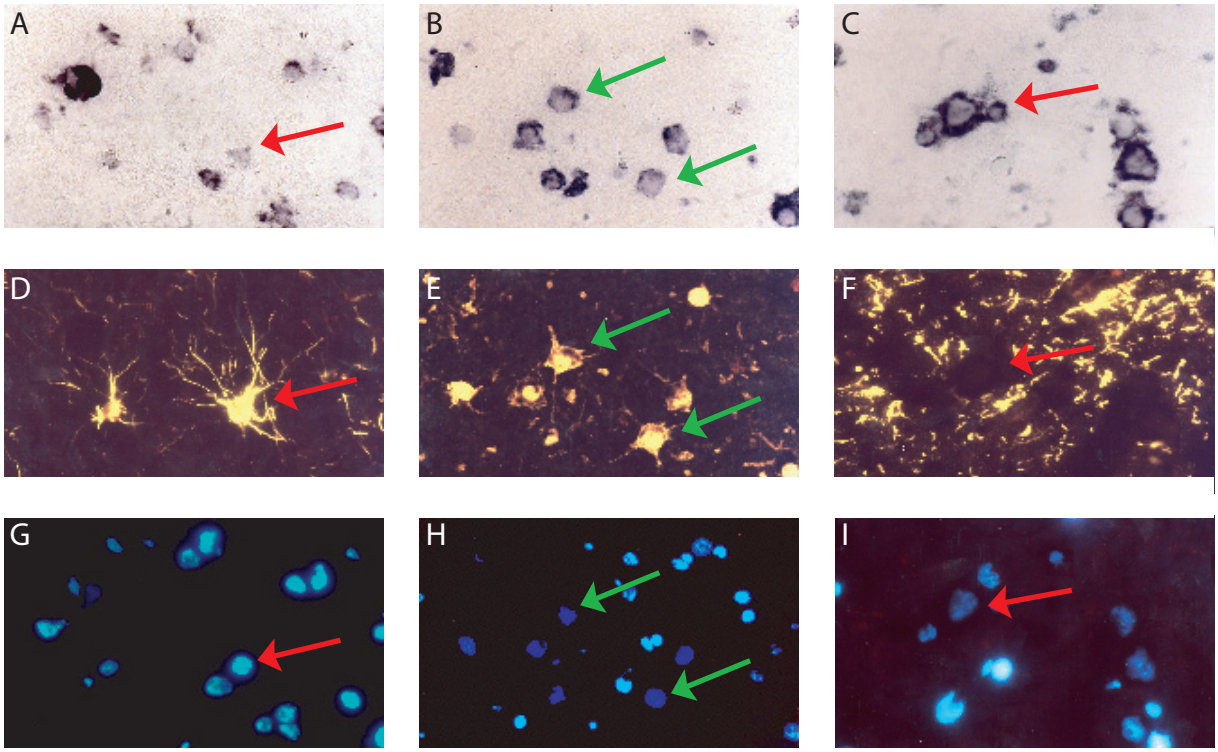

Figure 30.6. *Adult human neocortex showing predominant neuronal expression of PLXNB3. mRNA (purple) was detected by ISH with PLXNB3-specific DIG-labelled antisense cRNA probe (A, B, C) followed by immunodetection of cells with monoclonal antibodies (D, E, F). Astrocytes were visualized with GFAP (D), neurons with NeuN (E), oligodendrocytes with CNPase (F). Nuclear staining was performed with DAPI (G, H, I). Green arrows in B, E and H indicate PLXNB3 mRNA positive / NeuN positive neurons. Red arrows (in A, D and G) indicate PLXNB3 mRNA negative / GFAP positive astrocytes. The red arrows in C, F and I indicate PLXNB3 mRNA negative / CNPase positive oligodendrocytes. Original magnification 630×.*

30.5 Immunolocalization of plexin B3 protein parallels the predominant neuronal distribution of its mRNA in the human brain

Two different rabbit polyclonal antibodies were used to study localization of plexin B3 at the protein level in human adult tissues. The first serum was raised against a synthetic peptide corresponding to the human Plexin B3 sema domain (aa 354-369, pAbB3-A), the second against a region corresponding to aa 1058-1074 (pAbB3-B). pABb3-B antibody yielded better results compared to pAbB3-A, therefore the majority of the results shown here are using antibody pAbB3-B. Positive immunoreaction signal was detected in the cytoplasm of cells. Control immunostaining (with preimmune serum instead of specific antibody or omitting the primary antibody) remained negative. Immunostaining pattern in the human brain corresponded to that observed by ISH with *PLXNB3*-specific cRNA probe. Positive staining was detected in neuronal cell bodies of the cerebral cortex, in cell soma and dendrites of Purkinje cells and in some granule cells as well. In hippocampus, pyramidal neurons of cornu ammonis (CA1, CA2, CA3) gave the most prominent signal. White matter showed no staining along the axons of myelinated tracts or in glial cells. In corpus callosum, faint positive staining was seen along nerve fibres (Figure 30.7.E). No major differences were observed between ISH and IHC in the types of positive cells or intensities of staining. Negative control samples showed no staining (Figure 30.7.B).

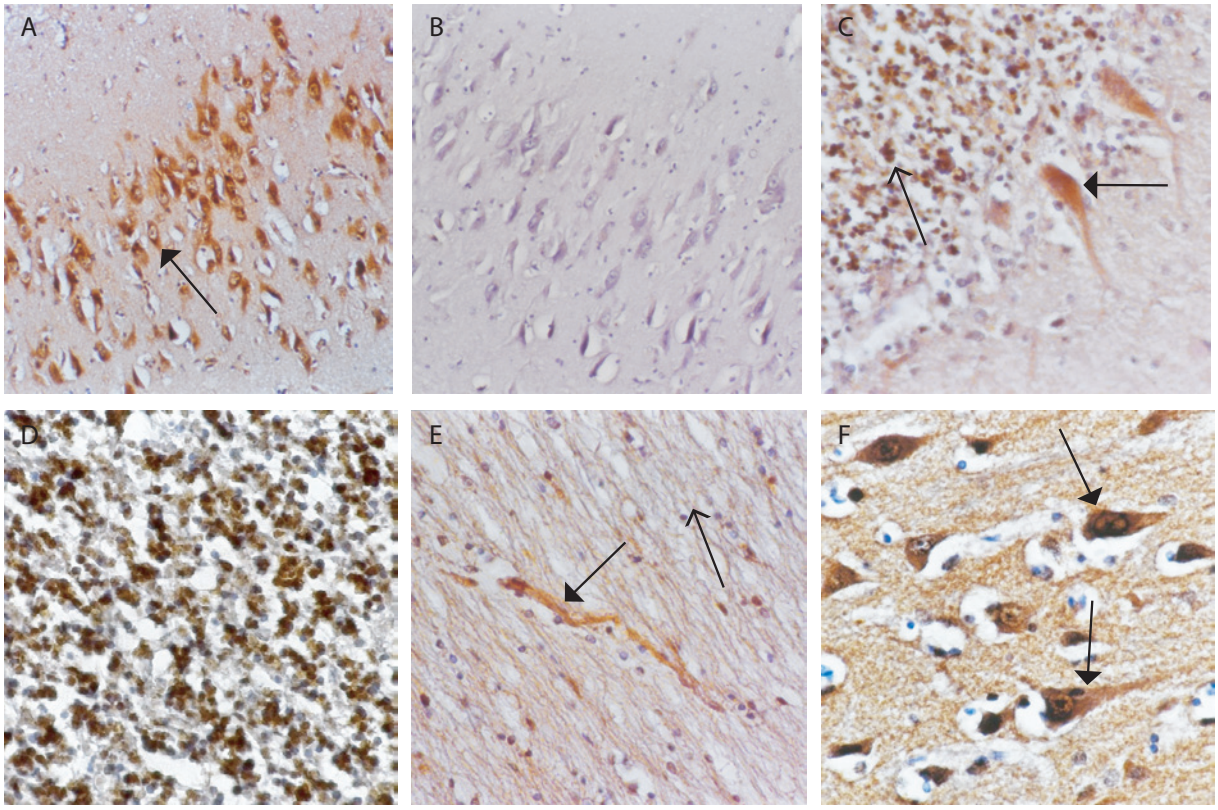

Figure 30.7. *Immunohistochemical detection of plexin B3 in selected areas of human adult brain. Immunostaining was performed using pAbB3-B anti-plexin B3 polyclonal antibody. Positive signal is detected as brown (DAB chromogen) staining, and immunoperoxidase reaction was counterstained with haematoxylin. A) Positive staining of the granular layer of neurons in hippocampus (arrow). B) Negative control of hippocampus without primary antibody. C) Positive staining of cerebellar Purkinje cells (filled arrow) and granular layer (open arrow) D) Detail of the granular cell layer of the cerebellum. E) Detection of PLXNB3 in vascular endothelium (filled arrow) and along the fibres (open arrow) in corpus callosum. F) Positive staining of pyramidal neurons (arrows) of human neocortex. Original magnifications A, B, C 200× and D, E, F 400× .*

30.6 Immunolocalization of human plexin B3 protein in non-neuronal tissues

Widespread expression of plexin B3 protein was detected in normal and tumour tissues. Results of immunohistochemical analysis of plexin B3 in human non-neuronal and various tumour tissues are summarized in Table 30.1. The plexin B3 positive signal was detected as homogenous or granular staining in cytoplasm. High levels of immunoreactivity were observed in skin, digestive tract, kidney, testis, pancreas, liver, adrenal medulla and placenta. No immunoreactivity was detected in adipose tissue, ovary, prostate and thyroid gland. Within the organs evaluated, plexin B3 expression was detected consistently in the epithelial cells while the stromal elements showed no or weak immunoreactivity (Figure 30.8. B).

Skin Widespread strong diffuse plexin B3-specific immunostaining in epithelial cells of epidermis.

Gastrointestinal system In the lamina propria, numerous plasma cells demonstrated positive signal. Positive signals were observed especially on the tips of intestinal villi whereas muscularis and stroma revealed no staining. In colon, immunostaining was observed in epithelial cells lining the crypts (Figure 30.8. A). Plexin B3 was also detected in ganglion cells of Meissner's plexus of the submucosa.

Pancreas High level of plexin B3 was detected in the Islets of Langerhans.

Liver In the liver, high level of plexin B3 immunopositivity was noted in hepatocytes. Among the portal tract elements, bile duct epithelia revealed moderate intensity of immunostaining (Figure 30.8. D).

Heart Cardiac myocytes revealed strong immunoreactivity (Figure 30.8. C).

Respiratory system In the larynx, plexin B3 was found in the squamous epithelium. The identical staining pattern was detected in the bronchial and bronchiolar epithelium. In the lung, diffuse plexin B3 immunostaining was found both in pneumocytes and intraalveolar macrophages (Figure 30.8. E).

Kidney Positive immunostaining was detected in the epithelia of the proximal and distal tubule but not in Henle's loop, collecting ducts, glomeruli, Bowman's capsule, or mesangial cells.

Female and male reproductive tract In the testis, groups of Leydig cells consistently demonstrated strong cytoplasmic immunostaining. Sertoli cells and seminiferous tubules revealed no positive signal (Figure 30.8. F). No plexin B3 signal was detected in the ovary.

Tumor tissues Plexin B3 protein was detected in nearly all tumour tissues studied and listed in Table 30.1, with the exception of thecoma and adenocarcinoma of ovary, and liposarcoma. The most intense staining in tumour tissues were exhibited by astrocytoma, squamous cell carcinoma of the esophagus, hepatocellular carcinoma, and colon adenocarcinoma.

Table 30.1. *Immunohistochemical detection of plexin B3 in paraffin-embedded human adult normal and tumour tissues (Tissue Array Set, BioCat). Immunostaining was performed using pAbB3-B anti-plexin B3 polyclonal antibody. Relative intensity of staining is described as: - no staining, + weak staining, ++ moderate staining, +++ strong staining.*

Organ	Tissue/Cell type	Intensity	Tumour tissue	Intensity
Human placenta	Syncytiotrophoblast	++		
Adrenal medulla	Zona glomerulosa	+	Pheochromocytoma	++
	Zona reticularis	+++		
	Zona fasciculosa	-		
Adipose tissue		-	Liposarcoma	-
Bladder	Epithelial cells	++	Transitional cell carcinoma grade II	++
			Transitional cell carcinoma grade III	++
Brain	Neuronal cells	+	Astrocytoma	+++
Breast	Epithelial cells	+	Invasive ductal carcinoma	+
	Fibroadenoma	+		
Colon	Epithelial cells	+	Adenocarcinoma	+
	Ganglion cells	+		
Duodenum	Mucosa	++	Duodenum tumor	+
Esophagus	Epithelial cells	+++	Squamous cell carcinoma	+++
	Adenocarcinoma	++		
Fallopian tube	Epithelium	++	Adenocarcinoma	+
Gall bladder	Epithelial cells	++	Adenocarcinoma	++
Kidney	Proximal tubulus	+	Granular cell carcinoma	+
	Distal tubulus	++	Clear cell carcinoma	+
Liver	Hepatocytes	+++	Cholangiocellular carcinoma	+
	Endothelium	+++	Hepatocellular carcinoma	+++
Lung	Capillaries	+	Squamous cell carcinoma	+
	Alveolar macrophages	+	Adenocarcinoma	+
			Alveolus cell carcinoma	++
Lymph node		-	Lymphoma	+
			Non-Hodgin's lymphoma	++
Ovary		-	Adenocarcinoma	-
			Thecoma	-
Parotis	Epithelial cells	+	Squamous cell carcinoma	+
Prostate		-	Adenocarcinoma	++
Rectum	Ganglion cells	+	Adenocarcinoma	++
Skin	Epithelium	++	Malignant melanoma	++
Small intestine	Apical cells	++	Adenocarcinoma	++
	Ganglion cells	++		
Smooth muscle	Muscle fibers	+	Soft tissue tumor	+
Stomach	Parietal cells	+	Squamous cell carcinoma	+
			Adenocarcinoma	++
Testis	Leydig cell	++	Seminoma	+
Tongue	Myocytes	+	Squamous cell carcinoma	+
Throat, Pharynx	Epithelium	++	Squamous cell carcinoma	++
Thymus	Hassall's corpuscle	+	Thymoma	+
Thyroid		-	Adenocarcinoma	++
Uterus		-	Leiomyoma	++
			Adenocarcinoma	++

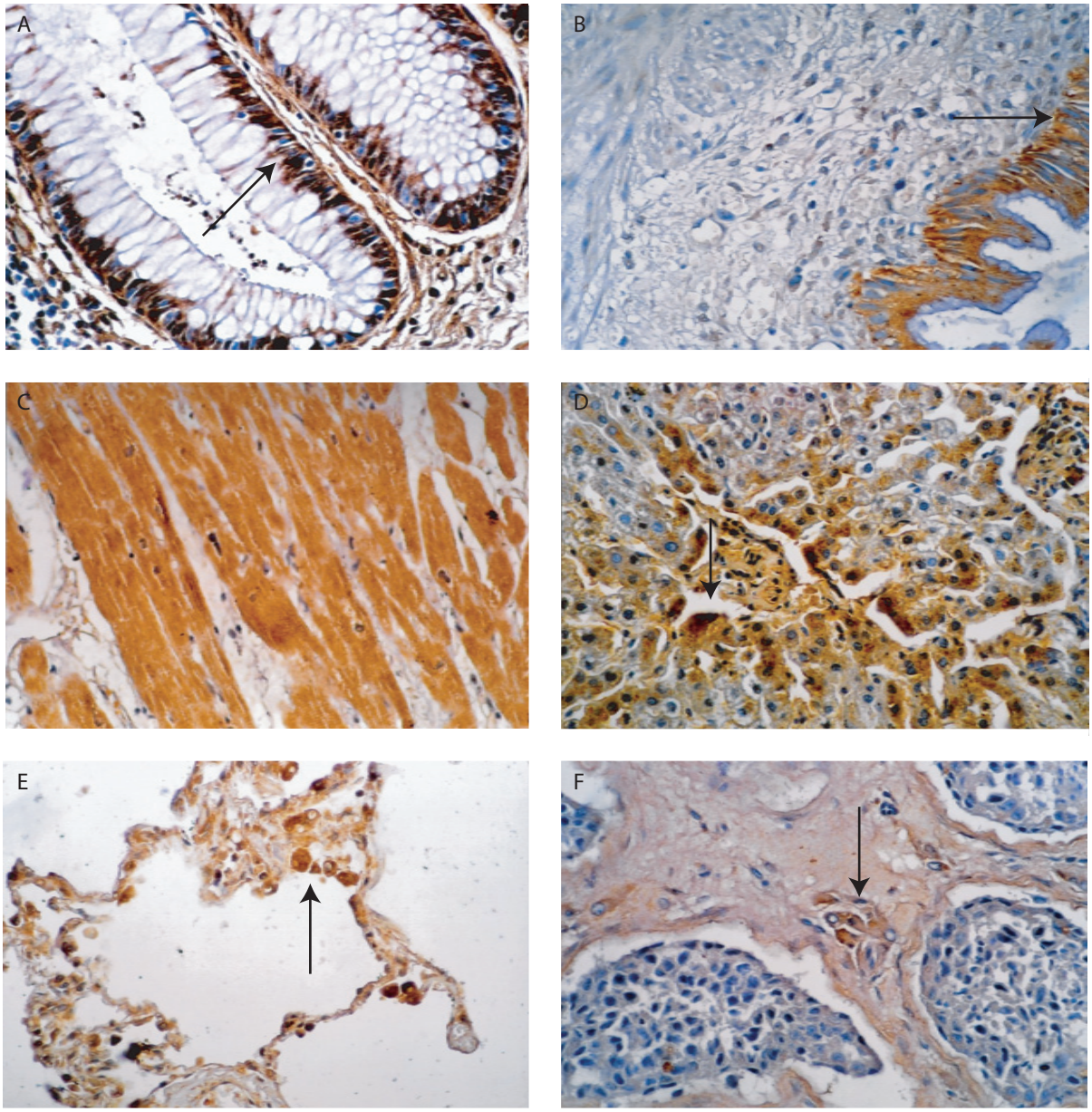

Figure 30.8. *Immunohistochemical distribution of plexin B3 in human non-neuronal tissues. Plexin B3 protein is detected as brown staining (DAB chromogen and immunoperoxidase reaction was counter-stained with haematoxylin. A) Colon: Positive signal of plexin B3 protein in simple columnar epithelial cells (arrow) shaped into the crypts. B) Gallbladder: Simple columnar epithelial cells (arrow) are positive. C) Heart: Longitudinal section of cardiac muscle with positive cardiac muscle fibres. D) Liver: Positive hepatocytes and endothelium, which lines liver sinusoids (arrow). E) Lung: capillaries in alveolar walls and alveolar macrophages (arrow) are positive. F) Testis: Positive staining in cluster of Leydic cells (arrow) within the interstitial stroma of testis. Original magnification 400×.*

31 Mutation screening of *PLXNB3*

For mutation screening 191 male subjects were selected. One group of 166 males with clinicaly diagnosed mental retardation was obtained from the European X-linked Mental Retardation Consortium [XLMR, 2005]. The second group was 17 males with suspected L1 disease but without mutation findings in *L1CAM*, and testing the last group consisted of 8 males with suspected nonsyndromic X-linked mental retardation. From each subject the coding exons of *PLXNB3* together with the exon-intron boundaries, including adjacent intronic sequences (minimum 50 bp on each side), were amplified by PCR. A total of 40 amplicons ranging in size between 176-405 bp were examined by single strand conformation polymorphism (SSCP) analysis using two different conditions to improve mutation detection efficiency. All fragments that showed mobility shifts of SSCP analysis were subsequently sequenced.

31.1 Rare sequence variants

Direct sequencing of amplicons with aberrant migration patterns in SSCP analysis revealed six unique sequence variant. These findings included silent mutations in codons 83, 429, and 1372 and two intronic alterations, and in addition one missense mutation in codon 670 was found in two unrelated patients (Table 31.1). Missense mutation (Glu670Lys) due to a G to A transition at position 2122 was identified in two out of 191 unrelated patients, but not in 412 control X chromosomes (179 females, 54 males). Glu670Lys represents a non-conservative change of an acidic amino acid to an basic residue. However, the healthy brother of one of the patients also carried this mutation. This suggests that Glu670Lys represents a rare polymorphism without pathogenic effect. The first intronic alteration IVS8+19A>G lays outside the known splice consensus sequence and had no effect on the splice efficiency score calculated by several computer programs (data not shown). Therefore, no additional controls were screened.

The second intronic alteration IVS22+21G>A was found in one patient, but not in the group of 412 control X chromosomes (179 females, 54 males). This mutation is located in a region of intron 22, which is almost fully (one nucleotide difference) conserved between chimp and human and appears to be relatively conserved between human and mouse. Alignment of the nucleotide sequences shown in Figure 31.1, and it was assumed that intronic alteration IVS22+21G>A could effect splicing. Due to the lack of patient mRNA, this hypothesis was tested in an Exon Trapping assay. This method allows detection of potentially functional splice sites in genomic DNA fragments, i.e. in this case in intron 22 of *PLXNB3*. The results of the exon trapping experiments are described in section 32. In addition, the nucleotide changes found in the patients and listed in Table 31.1 were also analyzed using splice site prediction programs. The computational analysis using several programs (Putative Alternative Splicing Database, NetGene2 Server, RESCUE-ESE Web Server, SpliceView, Splice Site Prediction by Neural Network, GENIO/splice) did not predict any significant effects on splice efficiency score (data not shown).

```
                                  *
1  GTGAGACCCGCCCACCCCCAGCACACTTCCCTCCTCGCCATTGGC  human
1  GTGAGACCCCCCCACCCCCAGCACACTTCCCTCCTCGCCATTGGC  chimp
1  GTGAGGATGTTCCCTCATCAGCACAT--------------ACGGGC  mouse

46 AAGGGCGCCCTGGCAGGCGGCTGGCCTGGCCCCGGCCCTGGCTGA  human
46 AAGGGCGCCCTGGCAGGCGGCTGGCCTGGCCCCGGCCCTGGCTGA  chimp
33 AAATTTCCCATGGCAGGC------CCTAGGCCAG----TGGCC-A  mouse

91 TGCTGGCCCCGGCCC-TGGCTGATGAAGCTGGCCCCGGGCTGCAG  human
91 TGCTGGCCCCGGCCC-TGGCTGATGAAGCTGGCCCCGGGCTGCAG  chimp
67 TCCTGGTCTGGGCCTGTGGCT-ATGC--CTGGCCTCTTGCTCCAG  mouse
```

Figure 31.1. *Alignment of intron 22 of PLXNB3 with the corresponding intronic regions of chimp and mouse. Position of the mutation IVS22+21G>A is framed and marked by an asterisk. Differences from the human sequence are shaded. Numbers at the left side indicate nucleotide numbers of intron 22, with number +1 corresponding to the first nucleotide of the intron. Alignment was carried out using MegAlign software (ClustalW Method). Sequences are from sequences entries deposited in NCBI/GenBank Acc.no.: PLXNB3 (Homo sapiens), AF149019; PlxnB3 (Mus musculus) NM_019587; PLXNB3 (Pan troglodytes) AC151486. To compare the NCBI entry, the sequence of intron 22 from chimp was confirmed by direct sequencing of genomic chimp DNA amplified by PCR.*

31.2 Polymorphisms in *PLXNB3*

In addition to the rare sequence variants mentioned in the previous section, ten single nucleotide polymorphisms (SNPs) and one 28 bp insertion polymorphism were found (Table 31.2). These changes were found in several of the patients and controls screened. Therefore, they are considered non-pathogenic polymorphisms. The frequencies of polymorphisms keep listed in Table 31.2 and their schematic localization is shown in Figure 31.2. Sequencing and comparison of NCBI/GenBank Acc. no. AF149019 (*Homo sapiens*) and AC151486 (*Pan troglodytes*) revealed a C>G substitution in 5′ upstream region of human *PLXNB3*, located -485 nucleotides upstream from the transcription start site, and was further confirmed to be a SNP by genotyping 30 subjects.

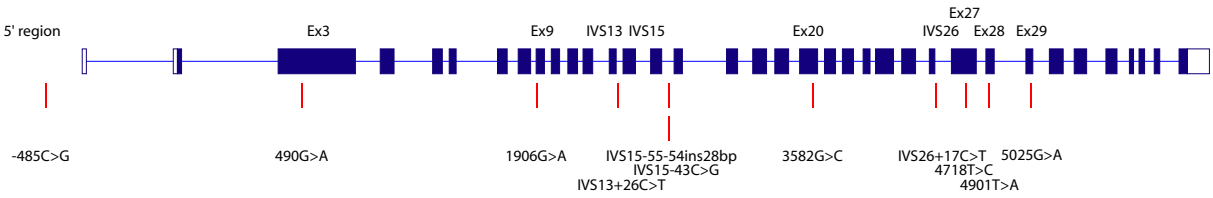

Figure 31.2. *Schematic localization of ten single nucleotide polymorphisms (SNPs) and one insertion polymorphism found in PLXNB3. The exon-intron structure of PLXNB3 is drawn to scale. Positions of the polymorphisms are marked by vertical lines, and numbers of exons, introns and 5′ upstream region containing these variants are shown on top.*

Table 31.1. *Nucleotide changes, found in human PLXNB3 in 191 subjects with mental retardation (MR). Nucleotide numbers are given according to NCBI/GenBank Acc. no. AF149019.*

	Position	Nucleotide Change	Amino Acid Change	Frequency MR	Frequency Controls[a]
1	Exon 3	363 C>T	Leu83	1 / 191	
2	Exon 5	1401G>A	Gln429	1 / 191	
3	Intron 8	IVS8+19A>G	-	1 / 191	
4	Exon 10	2122G>A	Glu670Lys	2[b] / 191	0 / 412
5	Intron 22	IVS22+21G>A	-	1 / 191	0 / 412
6	Exon 24	4227G>A	Thr1372	1 / 191	

[a] Refers to number of X chromosomes in controls
[b] No co-segregation with MR

Table 31.2. *The 11 polymorphic sequence changes found in PLXNB3 and their relative frequencies. Nucleotide numbers are given according to NCBI/GenBank Acc. no. AF149019. In the table are shown numbers of screened subjects with mental retardation (MR), female controls and frequencies (f) of the rare alleles (rare all.).*

Position	Nucleotide Change	Amino Acid Change	Patients MR (n)	Patients Rare all.	Controls Controls (n)	Controls Rare all.
5′ region	-485C>G	-	30	$f_G = 0.12$	-	
Exon 3	490G>A	Ala126Thr	168	$f_A = 0.04$	100 ♀	$f_A = 0.04$
Exon 9	1906G>A	Val598Ile	190	$f_A = 0.41$	-	
IVS 13	IVS13+26C>T	-	187	$f_T = 0.12$	-	
IVS 15	IVS15-54–55ins28bp	-	165	$f_{ins} = 0.14$	80 ♀	$f_{ins} = 0.09$
IVS 15	IVS15-43C>G	-	165	$f_C = 0.19$	80 ♀	$f_C = 0.29$
Exon 20	3582G>C	Glu1156Asp	186	$f_G = 0.25$	-	
IVS 26	IVS26+17C>T	-	190	$f_T = 0.14$	-	
Exon 27	4718T>C	Met1535Thr	190	$f_T = 0.21$	-	
Exon 28	4901T>A	Val1596Glu	184	$f_A = 0.11$	-	
Exon 29	5025G>A	Arg1637	188	$f_G = 0.38$	-	

31.3 Evolution of haplotypes

31.3.1 Genotyping of *PLXNB3*

The six SNPs, -485C>G (5′ region), 1906G>A (Val598Ile, ex.9), 3582G>C (Glu1156Asp, ex.20), 4718T>C (Met1535Thr, ex.27), 4901T>A (Val1596Glu, ex.28) and 5025G>A (Arg1637, ex.29) described in the previous section were used for haplotype analysis (Table 31.3). Three of them, coding for Val598Ile (exon 9), Glu1156Asp (exon 20) and Val1596Glu (exon 28) result in changes of evolutionary conserved amino acids of plexin B3. An extended haplotype analysis was performed in 85 male subjects using six SNPs mentioned above. These polymorphisms cover a genomic interval of 16,606 bp and the physical distances between six SNPs are given in Figure 31.3.

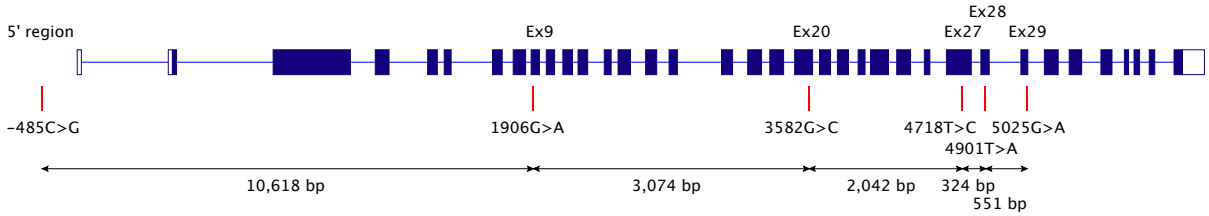

Figure 31.3. *Schematic localization of the six polymorphisms in PLXNB3 used for haplotyping. The exon-intron structure of PLXNB3 are drawn to scale. Vertical lines and numbers of exons above indicate position of SNPs used for haplotyping. The horizontal line indicates physical distances between the SNPs.*

The PCR primers used for amplification of fragments of human *PLXNB3* flanking the SNPs from -485C>G to 5025G>A could also be used to amplify and sequence the homologous fragment of chimp *PLXNB3*. Chimp sequences at the sites corresponding to the positions of the human SNPs were obtained by sequencing and compared with published chimpanzee sequences (NCBI/GenBank Acc. no. AC151486, *Pan troglodytes*) and are listed in Table 31.3 along with corresponding human, rat, and mouse data. Comparison of the complete coding sequence of the published chimp sequence with its human *PLXNB3* homologue revealed six amino acid differences in codons 8, 421, 987, 1016, 1118, and 1535. The non-polymorphic (human) differences between human and chimp affect non-conserved residues (Table 31.4). In human *PLXNB3*, a polymorphism in exon 27 (codon 1535) was found, encoding for threonine (common allele) or methionine (rare allele). The common human allele (Table 31.2) corresponds to the allele found in the sequenced chimp, and entry from NCBI/GenBank Acc. no. AC151486 (*Pan troglodytes*).

31.3.2 Haplotypes based on single nucleotide polymorphisms

Several coding and non-coding SNPs allowed an evolutionary analysis of common haplotypes specific for *PLXNB3*. Under assumption of unique mutation events driving evolution six SNPs described in the previous section (31.3.1) allowed to reconstruct a "phylogenetic" tree describing a possible evolutionary process of human haplotypes. In the initial reconstruction five intragenic SNPs were used. Later, during the screening process an additional extragenic SNP in 5′ region was found, and the haplotype analysis was expanded to six SNPs.

Table 31.3. *Six human polymorphisms identified in coding regions and 5′ region of PLXNB3, predicted amino acid changes and corresponding residues in orthologues in rodents and chimp. Residues encoded by the more frequent allele in human are underlined. The respective frequencies of the human rare alleles (in parenthesis) are given in the last column. SNPs located in exon 9, 20, and 28 affect residues conserved in rodents and chimp and are highlighted in bold. The SNPs shown here were used in haplotype analysis. The SNP denoted number 6 was found last and was therefore given the highest number.*

SNP No.	Position	Nucleotide change	Amino acid change	Mouse	Rat	Chimp	Freq. of rare allele in human
6	5′ region	-485C>G	-	-	-	G	12% (G)
1	Exon 9	1906G>A	Val598Ile	**Val**	**Val**	**Val**	41% (A)
2	Exon 20	3582G>C	Glu1156Asp	**Glu**	**Glu**	**Glu**	25% (G)
3	Exon 27	4718T>C	Met1535Thr	Val	Val	Thr	21% (T)
4	Exon 28	4901T>A	Val1596Glu	**Val**	**Val**	**Val**	11% (A)
5	Exon 29	5025G>A	Arg1637	?	?	Arg	38% (G)

Table 31.4. *Coding differences between human and chimp PLXNB3 along with the corresponding sites in rodents. Positions are given according to NCBI/GenBank Acc. no. AF149019 (Homo sapiens), AC151148 (Pan troglodytes), XM_343841 (Rattus norvegicus) and NM_019587 (Mus musculus). The sequence for the first two exons in rodents is not yet known. In exon 27 codon 1535 the chimp sequence encodes for threonine in contrast to the human sequence where two sequence variants were found (Table 31.2). In the sequence of rodent exon 27, two species specific sequence variants were found; rat* `GTA` *versus mouse* `GTG`*, both encoding for valine.*

	Codon	Human		Chimp		Rat / Mouse	
Exon 1	8	`ACC`	Thr	`ATC`	Ile	?	?
Exon 3	421	`TAC`	Tyr	`CAC`	His	`CAT`	His
Exon 17	987	`GCC`	Ala	`GTC`	Val	`GAG`	Glu
Exon 17	1016	`CAG`	Gln	`CGG`	Arg	`CAA`	Gln
Exon 19	1118	`CAC`	His	`CGC`	Arg	`CTC`	Leu
Exon 27	1535	`ATG/ACG`	Met/Thr	`ACG`	Thr	`GTA / GTG`	Val

Based on the five intragenic and one extragenic SNPs 85 subjects where genotyped and 13 different haplotypes (#) were identified. Two haplotypes (`GGCTG` and `GGTTG`) occured in more than half of the male subjects studied (46.6% and 16.1% respectively), and two haplotypes (`AGTTG` and `GGCTG`) were found only in a single subject each. The inclusion of the polymorphism -485C>G located in 5′ upsteam region revealed basically the same result, but gave rise to a sub-differentiation of two single haplotypes (`GGTTG` and `ACCTA`) into two sub-haplotypes (`CGGTTG` #4, `GGGTTG` #12 and `CACCTA` #6, `GACCTA` #13), respectively yielding a total of 13 different haplotypes. The haplotypes based on the six SNPs and their frequency are shown in Table 31.5. The most frequent haplotype #6 was identified in 41 subjects (48.24%), and the second most frequent haplotype #4 in 13 subjects (15.3%).

Table 31.5. *Summary of 13 haplotypes and their frequency based on the five intragenic SNPs and one SNP found in the 5′ upstream region genotyped in 85 subjects. The numbering system 1-6 used in the table corresponds to the numbering of SNPs in Table 31.3.*

Haplotype	6	1	2	3	4	5	Subjects (n)	Freq. (%)
Mouse/Rat	?	G	G	T	T	?	-	-
Chimp	G	G	G	C	T	G	-	-
Human								
#1	G	G	C	C	T	A	2	2.35
#2	G	A	G	T	T	G	1	1.17
#3	C	G	C	C	A	A	1	1.17
#4	C	G	G	T	T	G	13	15.30
#5	G	G	C	C	T	G	3	3.53
#6	C	A	C	C	T	A	41	48.24
#7	C	A	C	C	A	A	7	8.24
#8	C	A	C	C	T	G	4	4.71
#9	C	A	G	C	T	A	4	4.71
#10	G	G	C	T	T	G	2	2.35
#11	G	G	G	C	T	G	1	1.17
#12	G	G	G	T	T	G	1	1.17
#13	G	A	C	C	T	A	5	5.89
Σ							85	100.00

Comparison of obtained human haplotypes with the corresponding sequences derived from rodents (mouse and rat) and chimp suggested an evolutionary tree of human haplotypes. In 29.41% of the chromosomes analyzed, the evidence of ancestral recombination events within 16,606 bp region covered by the SNPs. Therefore the recombinant haplotypes #2, #3, #4, #9, #8, and #10 were excluded from the phylogenetic tree. These haplotypes are shown in Table 31.6. Gaps between the lines suggest possible recombination sites.

Table 31.6. *Presumed recombinant haplotypes. Gaps with asterisk between the lines suggest possible recombination sites. These haplotypes were excluded from the phylogenetic tree.*

Freq.	Haplotype	6	1	2	3	4	5
1.17%	Human # 2	G	∗ A	∗ G	T	T	G
1.17%	Human # 3	C	G	∗ C	C	A	A
15.3%	Human # 4	C	∗ G	G	T	T	G
4.71%	Human # 9	C	A	∗ G	∗ C	T	A
4.71%	Human # 8	C	A	C	C	∗ T	G
2.35%	Human # 10	G	G	C	∗ T	T	G

31.4 Phylogenetic tree based on human, chimp, rat, and mouse sequences

Based on comparison with published chimpanzee sequences and with respect to the six SNPs used for haplotyping, human haplotype #11 showed no difference to the chimpanzee sequence. Therefore haplotype #11 may represent the archetypal among the primates. According to this hypothesis, haplotype #12 on the one hand evolved from haplotype #11, while on the other hand haplotypes #5, #1, #13, #6, and #7 appear to have evolved by consecutive single mutations from haplotype 11. Haplotypes #3, #4, #9, #8, and #10 most likely resulted from single or various recombination during evolution (Table 31.6). The chimpanzee, mouse/rat and human sequences permitted the reconstruction of a hypothetical phylogenetic tree with ancestral haplotypes and most modern haplotypes as shown schematically in Figure 31.4. 70.59% of the observed haplotypes fit this scheme based on the assumption of single mutation events driving evolution. 29.41% of the haplotypes are most likely results of recombination events. These data suggest that more than 56.48% of present haplotypes fall into the most modern group consisting of haplotypes #6 and #7. Haplotype #12 may be a possible modern haplotype as well, but the data are inconclusive.

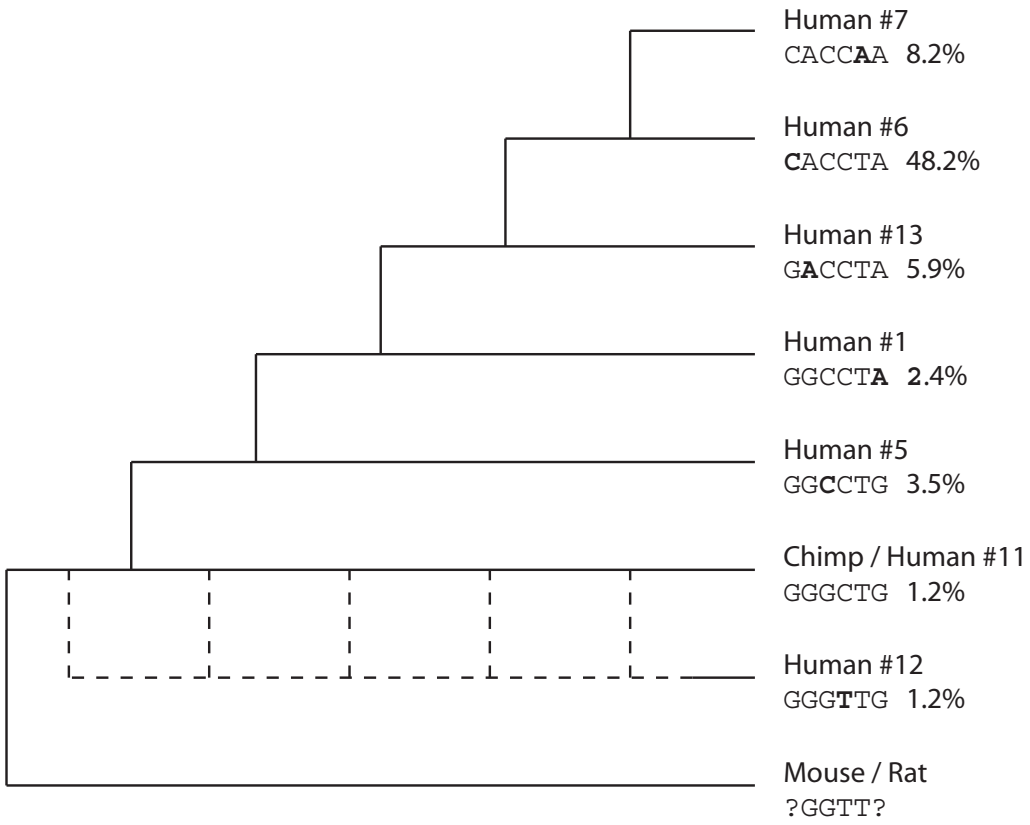

Figure 31.4. *Suggested evolution of human haplotypes. The tree suggests a probable human modern haplotype evolutionary path. Human haplotype #11 being the archetypal haplotype identical to the chimp, and human haplotype #7 being the most modern one (See section 31.4).*

32 Exon trapping

32.1 Exon trapping based on pSPL3 minigene expression

From the patient with the intronic mutation IVS22+21G>A there was no mRNA available for analysis of splicing. Therefore, the possible effect of the mutation on splicing was analysed using Exon Trapping System (Gibco, BRL). The aim was to investigate whether the mutation in intron 22 had a quantitative and/or qualitative influence on splicing. For exon trapping, genomic DNA fragments of *PLXNB3* containing either wild type or the mutated intronic sequence were cloned into vector pSPL3 and transfected into COS-7 cells. The constructs contained 57 bp of intron 19, exon 20, intron 20, exon 21, intron 21, exon 22, intron 22, exon 23, and 72 bp of intron 23 (Figure 32.1). Cytoplasmic mRNA of the transfected COS-7 cells was isolated, and products from reverse transcription were used for analysis of the splicing products by two rounds of PCR. An empty pSPL3 vector with no genomic insert and non-transfected COS-7 cells served as negative controls and were included in each experiment to control for the presence of vector-derived and contamination by PCR-products or genomic DNA.

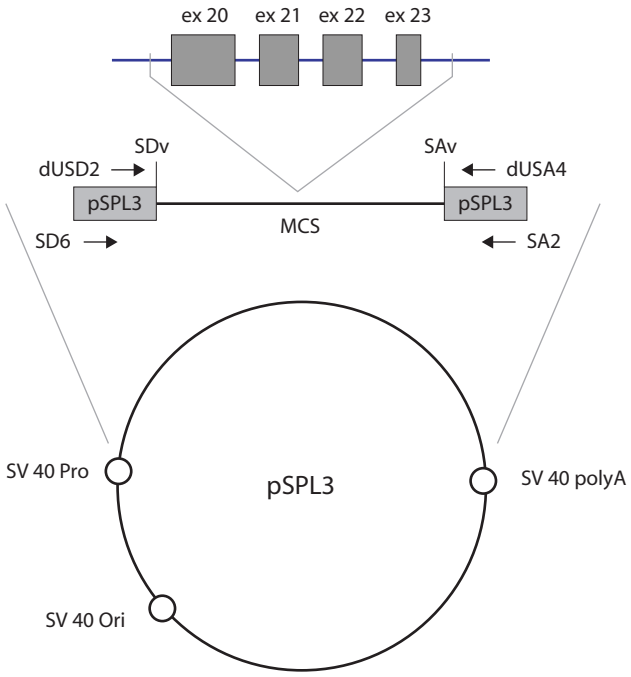

Figure 32.1. *Structure of pSPL3 constructs used for exon trapping experiments. The insert contains either a wild type or the corresponding mutant IVS22+21G>A of a PLXNB3 genomic fragment. The constitutive splicing donor and acceptor sites of the vector are denoted SDv and SAv, respectively. The oligonucleotides SD6 and SD2 were used in primary PCR amplification of spliced transcripts of pSPL3 constructs expressed in the transfected COS-7 cells. For secondary PCR amplification the oligonucleotides dUSA4 and dUSD2 were used.*

Nested-PCR after elimination of vector-derived products with BstX I restriction cleavage revealed major products of 177 bp, 300 bp, and 400 bp and several less abundant larger products (Figure 32.2). PCR amplicons of 177 bp, 300 bp, and 400 bp were seen in products derived from all genomic constructs as well as from the empty control vector. Therefore, these fragments were considered to represent vector-derived products and were eliminated from further ana-

lysis using a subsequent colony PCR analysis of the transformants. PCR fragments of 500 bp, 850 bp, and 900 bp were produced from reactions derived from both wild type and mutant genomic constructs, but not from the vector control. When comparing PCR fragments derived from wild type and mutated constructs, one additional unique band of 600 bp produced exclusively from the mutated construct was trapped. The whole exon trapping experiment was performed in triplicate, including transfection of COS-7 cells, cytoplasmic mRNA extraction, cDNA synthesis, and primary and secondary nested PCR. The trapped 600 bp band was detected in all of the experiments involving the mutant construct but never in the wild type construct (Figure 32.2).

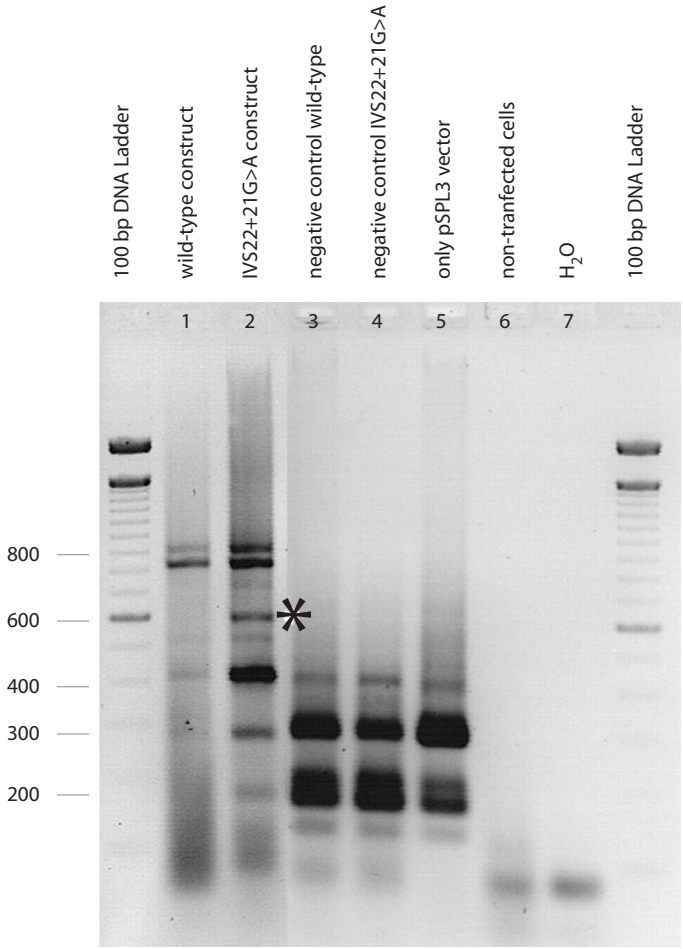

Figure 32.2. *Representative result of exon trapping experiment; second PCR performed with dUSA4 and dUSD2 oligonucleotides of three independent experiments. 10 µl of PCR product were separated on a 2% agarose gel and visualized by ethidium bromide staining. Lanes 1-7 show the secondary PCR products using dUSA4 and dUSD2 oligonucleotides. The asterisk marks an unique additional 600 bp band detected only in mutated construct. 100 bp DNA ladder was used (New England Biolabs).*

32.2 Different splicing isoforms *in vivo*

Putative insert-specific RT-PCR amplification products were subcloned into a pAMP10 vector and plated. Colony PCR products were sequenced using dUSD2- and dUSA4-sequencing primers. Sequencing analysis of the transformants from colony PCR products derived from wild type and mutated constructs revealed different splice variants that are listed in Figure 32.3. In summary, both the wild type and mutated constructs gave rise to various splice variants. Splicing isoforms including exon 22 have been observed only in wild type construct

and never detected in constructs containing mutation. The unique 600 bp PCR product of the mutated construct was analyzed by direct sequencing of bands isolated from the gel using primers dUSA4 or dUSD2 and revealed a variant containing exon 20 spliced together with intron 22 and exon 23. This splice variant was never observed in the products derived from the wild type (Figure 32.3). These results suggest that the mutation IVS22+21G>A can result in aberrant splicing of *PLXNB3* characterized by skipping of exon 22, and possible production of additional various aberrantly spliced isoforms.

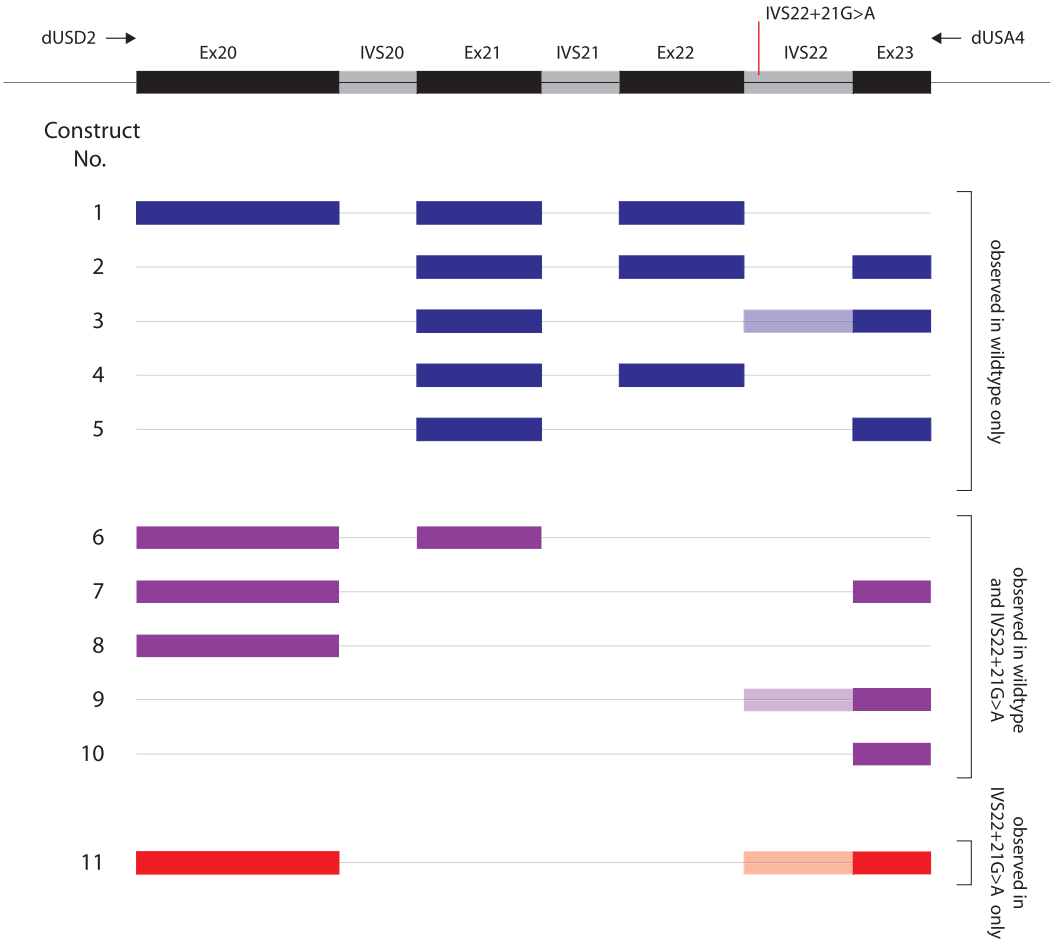

Figure 32.3. *Sequencing analysis of colony PCR products derived from wild type and IVS22+21G>A mutated constructs. Splice variants No. 1, 2, 3, 4 and 5 were observed in wild type construct constitutively and isoforms No. 6, 7, 8, 9 and 10 were observed constitutively in wild type and in constuct containing mutation. Whereas, isoform No. 11 was observed exclusively in mutant-derived products.*

33 Functional characterization of the human *PLXBN3* promoter

During mutation screening a possible pathogenic intronic mutation affecting splicing, but no evidence for pathogenic mutations in the coding region of *PLXNB3*, has been found. However, the 5′ region was neglected in that screen and therefore further investigation of that region was performed. The promoter region is interesting in many aspects. First, this region may well contain pathogenic mutations; second, analysis of this region may help to understand the regulation of transcription of *PLXNB3*.

33.1 Computer-assisted promoter sequence analysis of *PLXNB3*

Initially, a computer assisted promoter analysis of the *PLXNB3* 5′ upstream region using different programs as Promoter Inspector and Genomatix was provided [Genomatix, 2005, Scherf et al., 2000]. This analysis covered 30 kb of the 5′ region of *PLXNB3* (NCBI/GenBank Acc. no. U52111) and revealed no known promoter motif and did not predict any promoter region. The 5′ upstream region of *PLXNB3* lacks a `TATA` box, `CAAT` box, initiator elements or GC-rich regions. *PLXNB3* presumably falls into a class of genes, in which transcriptional control mechanisms are poorly understood.

33.2 Analysis of the 5′ region of *PLXNB3*

A fragment containing the 1117 nucleotides upstream from of *PLXNB3* was examined in detail for the presence of eukaryotic gene regulatory elements using the transcription factor database [Wingender et al., 2000]. This analysis revealed the presence of several putative binding sequences for a number of trans-activating regulatory proteins although the region was devoid of canonical `TATA` or `CAAT` elements. The putative transcription factors and their consensus DNA target sequences are listed in Table 33.1 and their physical positions marked in Figure 33.2.

Using the transcription factor database, 12 different potential transcription factor binding sites (motifs) were predicted. Three motifs were present for myeloid zinc finger protein (MZF1), preferentially expressed in haematopoietic cells. A consensus `CCAAT`/enhancer-binding protein beta (C/EBP-beta) binding site was predicted at position -357 to -367. The `CCAAT`/enhancer-binding protein beta is described as a nuclear factor for IL-6 expression with the consensus binding sequence `RNRTKNNGMAAKNN`. Three delta EF1 repressor boxes were present, each containing the binding consensus `CACCTG` sequence. A binding motif for the muscle regulatory protein MyoD is present at position -1003 to -1014. Interestingly, at position -218 to -226 a motif for RE1/NRSE repressor element /neuron-restrictive silencer element was present. RE1 silencing transcription factor (REST), also known as neuron-restrictive silencer factor, is a zinc finger protein that functions as a transcriptional repressor of neuronal genes in non-neuronal tissues [Thiel et al., 1998]. In the vicinity of the RE1 repressor element, another repressor ele-

ment GATA-1 at position -155 to -162 was found, and at positions -447 to -455 and -926 to -933 two GATA-1 elements were present. GATA-1 element is required and essential for erythropoiesis, and many genes are down regulated by GATA-1 element, highlighting the importance of GATA-1 elements in gene repression.

Other *cis*-acting factor binding motifs for the putative *PLXNB3* promoter were predicted: including a motifs for SOx/sRY-sex/testis determining factors, Activator protein 1, Homeo domain factor Nkx-2.2, RAR-related orphan receptor A1 (RORa1), Upstream stimulating factor and N-myc. Some of these transcription factors are involved in tissue-specific gene expression like the activator protein-1 (AP-1). Nkx-2.2 belongs to the developmentally important homedomain transcription factors of the NK-2 class and is involved in pancreas and central nervous system development. RORa1 is a member of the steroid hormone nuclear receptor superfamily related to the retinoic acid receptors.

33.3 Computational analysis of conserved promoter elements

The availability of extensive sequence data for both the human and mouse genome have provided the opportunity to identify regulatory elements using global sequence alignments, as functionally important sequences are often conserved during evolution [Hardison et al., 1997].

Unfortunately, due to the lack of sequence information and precise localization of the first two exons in rodent *PLXNB3*, comparative alignment of the 5′ region between mice and human could not be performed. Comparison of human and chimp 5′ regions encompassing 1.1 kb from the transcription start site revealed eight nucleotides differences (Figure 33.1). Furthermore comparison of putative transcription factor-binding sites within 1.1 kb of the 5′-flanking region in the chimp, (NCBI/GenBank Acc. no. AC151486) determined by the TFSEARCH and MatInspector databases, revealed one additional transcription binding site in chimp. At position -490 to -505 in the chimp 5′ region transcription factor-binding sites for Arnt element (Aryl hydrocarbon receptor) was present.

33.4 Functional analysis of the *PLXNB3* promoter region

Published data indicates that most of the regulatory DNA elements important for tissue-specific expression are localized within 2 kb upstream from transcription start sites. For functional analysis of the putative *PLXNB3* promoter region the commercially available GreatEscAPE SEAP Reporter System was used. In this system, SEAP, a truncated form of placental alkaline phosphatase is the secreted reporter molecule. This protein lacks the membrane-anchoring domain; thereby the protein is efficiently secreted from the transfected cells into medium and allows monitoring the activity of promoters, enhancers or silencers.

In order to analyze the putative activity of the *PLXNB3* 5′-flanking region a series of five constructs covering up to 1.1 kb of the upstream region and one control construct covering a part of the expressed region of *PLXNB3*, including exon 1 and part of exon 2 were cloned into pSEAP2-basic vector and co-transfected with β-galactosidase plasmid into CHO-K1, HeLa, and HEK cells (Figure 33.3).

The constructs used in the promoter assay were designated as pex1+2 (-249 to +1268), p1 (-1116 to -16), p2 (-907 to -16), p3 (-601 to -16), p4 (-249 to -16) and p5 (-147 to -16) as shown in Figure 33.3. The positive control construct pSEAP2-Control (containing SV40 promoter driving the transcription of the SEAP gene) showed the highest activity in all cell lines. The construct pex1+2 covering untranslated exon 1 and part of exon 2 (covering -16 to +1248) of *PLXNB3* showed the lowest activity of all experiments. The results of the reporter assays in CHO-K1, HeLa and HEK cells are shown in Figure 33.4.

33.5 Comparison of transient expression assays in various cell lines

Compared to the longer reporter constructs p2–p4, short construct p5 (covering -147 to -16) showed significantly stronger reporter activity in all three cell lines. Compared to pBasic, p5 induced mean promoter activity was 5.4-fold in CHO-K1 cells (Figure 33.4 CHO-K1; $p \leq 6.0 \times 10^{-5}$), 4.7-fold in HeLa cells (Figure 33.4 HeLa; $p \leq 0.007$), and 2.8-fold in HEK cells (Figure 33.4 HEK; $p \leq 0.0007$). The construct p4 exceeds p5 by 102 bp and both constructs cover a common genomic fragment of 131 bp (from -147 to -16). Therefore, the findings of the reporter assays suggest a strong promoter or enhancer element within the region -147 to -16, and a possible strong repressor element within the region -249 to -148. Interestingly in this region, binding sites for three repressors were predicted: GATA binding factor (-155 to -162); Delta EF1 (-188 to -196); and interestingly RE-1 repressor (-218 to -226) also known as neuron-restrictive silencer element (RE1/NRSE) (Table 33.1).

Table 33.1. *Potential binding sites for transcription regulatory elements of PLXNB3. Within the 1.1 kb upstream region of PLXNB3 12 different potentional regulatory elements were identified by TFSEARCH. Numbering is based on +1 for transcriptional start site. The scores of similarity to the shown consensus core sequences is given. The sequence characters refer to IUPAC nomenclature [IUPAC, 2005] where* R *is purine (*A *or* G*),* Y *is pyrimidine (*T *or* C*),* W *is (*A *or* T*),* M *is (*A *or* C*), and* N *is any nucleotide.*

Name	Description	Consensus sequence	Core sequence	Position		Score
MZF	Myeloid zinc finger protein [Peterson and Morris, 2000]	AGTGGGGANGT	tgtgggga	-33	-26	95.7
		CGGGNGAGGGG	cacattc	-690	-934	95.7
		AA	cagcccc	-940	-934	90.4
GATA-1	GATA Binding factor 1 [Whitelaw et al., 1990]	WGATAR	atcatgcc	-162	-155	91.4
			catctcctg	-455	-447	91.8
			atcsccst	-926	-933	99.2
Delta E	DeltaEF1 [Sekido et al., 1994]	CACCTG	tctcacctgcc	-196	-188	90.8
			ccccacctga	-600	-591	91.1
			agccaccctga	-977	-968	90.0
RE1	Repressor element 1 [Bruce et al., 2004]	TYAGMRCCNNRGMG/SAG	atgcccacc	-226	-218	91.7
SRY	Sox/sRY-sex/testis determing factors 1 [Harley et al., 1992]	AACAAAG	gtttgtttctg	-298	-288	100.0
C/EBP	CCAAT/enhancer binding protein [Ramji and Foka, 2002]	GATTGCGYAAY	ttgccacata	-367	-357	90.0
AP-1	Activator protein 1 [Angel and Karin, 1991]	TGAGTCANTGASTCAN	ttgactcag	-388	-370	97.7
Nkx-2.2	NKX homeodomain factor [Watada et al., 2000]	TTTTTAAGTGGTTTT	ttaagtg	-400	-394	97.7
RORa1	RAR-related ophan recep. alpha 1 [Giguere et al., 1994]	RGGTCA	ggttcaa	-424	-418	91.7
USF	Upstream stimulating factor [Sato et al., 1990]	CACGTGACCG	ccacgtgg	-504	-497	95.6
N-Myc	N-myc oncogene [Blackwell et al., 1990]	CACGTG	acgtgggcatg	-502	-492	94.0
MyoD	Myoblast determining [Huang et al., 1996]	CANNTG	cacctggccct	-1014	-104	93.0

Figure 33.1. *Comparison of 5′ region of PLXNB3 in human and chimp. Numbering is relative to the transcriptional start site with the guanine residue designated as +1. The eight nucleotide differences between human and chimp are highlighted by bold and the nucleotides in chimp sequence that match with human are not shown but represented by dots. The alignment was generated using ClustalW computer program.*

Figure 33.2. *Putative transcription factor binding sites within the 1.1 kb of the 5′ region of PLXNB3 identified by the TFSEARCH database. Numbering is relative to the transcription start site designated as +1. Sequences with similarity to binding motifs of known transcription factors are underlined. Comparing the human and chimp 5′ region, one additional putative transcription binding site at position -490 to -505 was identified in chimp, namely for Arnt element (Aryl hydrocarbon receptor). The promoter construct p4 is delineated by light and dark gray background and promoter construct p5 by dark gray background only.*

Figure 33.3. *Reporter constructs used in the PLXNB3 promoter assays. Schematic representation of the genomic locus with denoted regions preceding the 5′ upstream region and untranslated exons 1 and exon 2. Top coordinates correspond to basepair offset in sequence of chromosome X in NCBI Build 35 (May 2004) of the Human Genome. Transcription start site is anotated by arrow. Numbering on the below vertical line (from -1116 to +1268) is relative to the transcription start site designated as +1. For functional analysis of the promoter region five constructs were used containing different parts of 5′ region extending from -16 bp to -1116 bp (p1 to p5) and one construct containing exons 1 and 2 extending from -249 bp to +1248 bp (pex1+2) downstream from the transcription start site.*

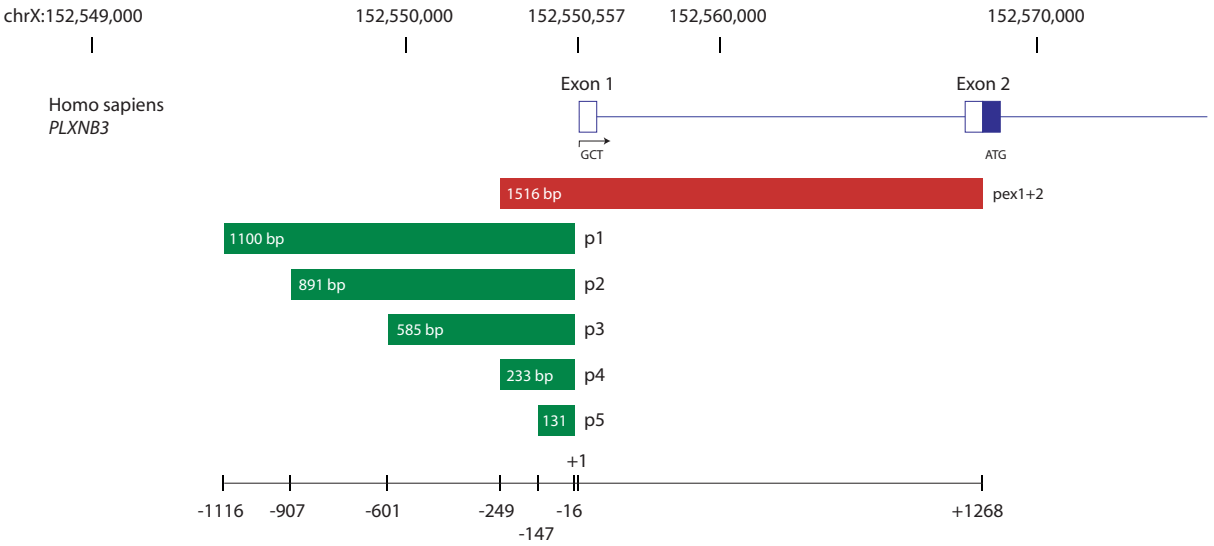

Figure 33.4. *The bar graphs on pages 107-109 represent SEAP activity after transfection with human PLXNB3 promoter constructs in three different cell lines (CHO-K1, HeLa, and HEK). Relative SEAP enzyme activity was measured in fluorescence counts in cells transfected with corresponding reporter gene constructs are given at the bottom of the diagrams in the following abbreviations, pex1+2, p1, p2, p3, p4, p5, pBasic, and pControl (far right).*
In the top left three (for HEK cells two) panels SEAP activity data for three independent experiments I, II, III normalized with β-galactosidase are shown. Each triple bar represents SEAP activity measured 72 h after transient triplicate transfection in one independent experiment. Controls included the pSEAP2-Basic vector, which contained neither SV40 enhancer nor promoter and pSEAP2-Control vector with promoter and enhancer SV40. The highest activity is seen for the pControl construct as expected. The highest activity for all cell lines amongst the PLXNB3-promoter constructs is seen for construct p5, corresponding to nucleotides -147 to -16 upstream from the transcription start site.
The top right three (for HEK cells two) panels show values from triplicate experiments in multiples of the negative control (pBasic=1) including standard error bars.
The mean of all relative values were calculated and are shown in bottom graph including standard error bars. The activity of construct p5 of PLXNB3 is highest compared to constructs pex1+2, p1, p2, p3, and p4 in all cells lines analysed.

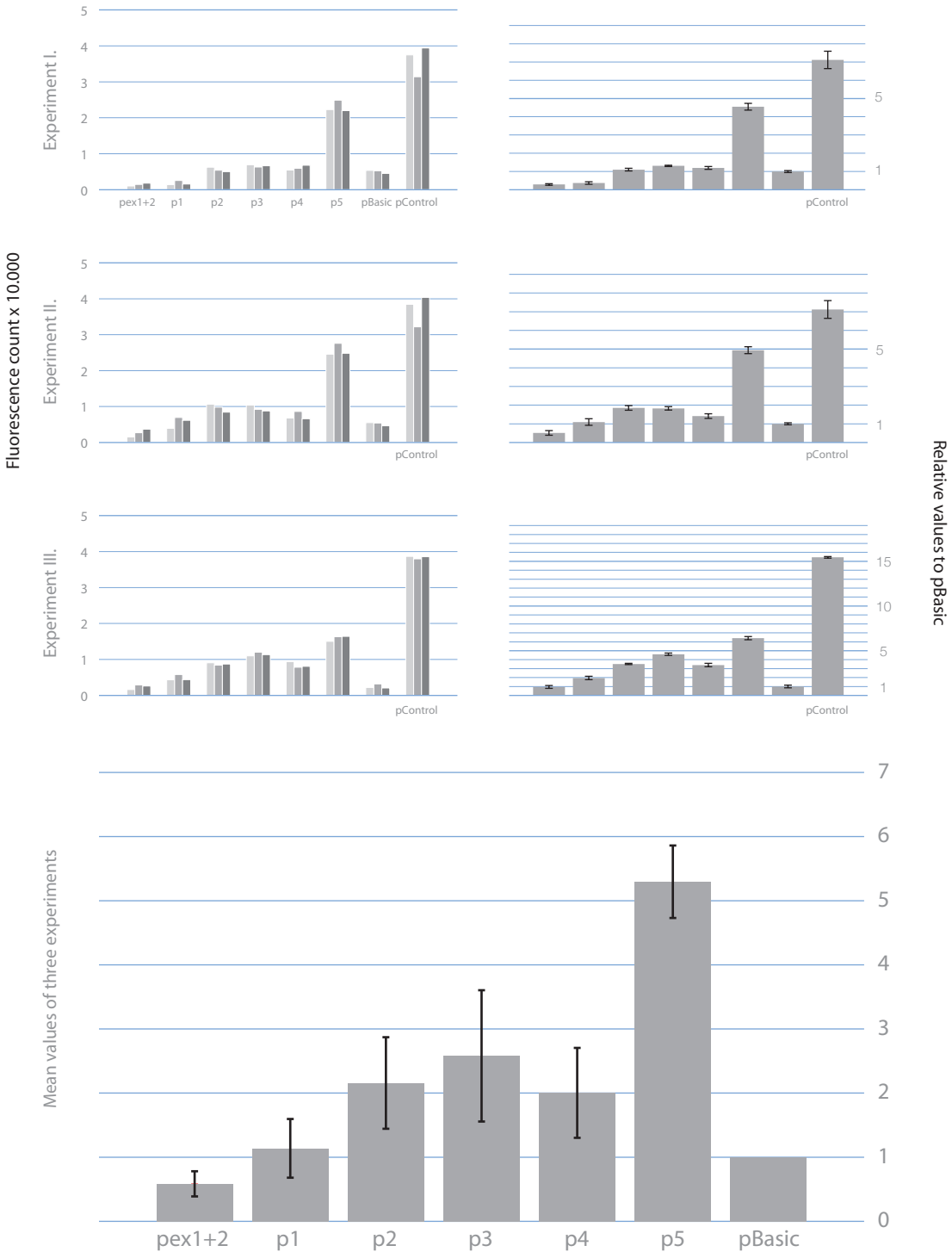
Fluorescence count x 10.000
Relative values to pBasic
Experiment I.
Experiment II.
Experiment III.
Mean values of three experiments
pex1+2
p1
p2
p3
p4
p5
pBasic
pControl

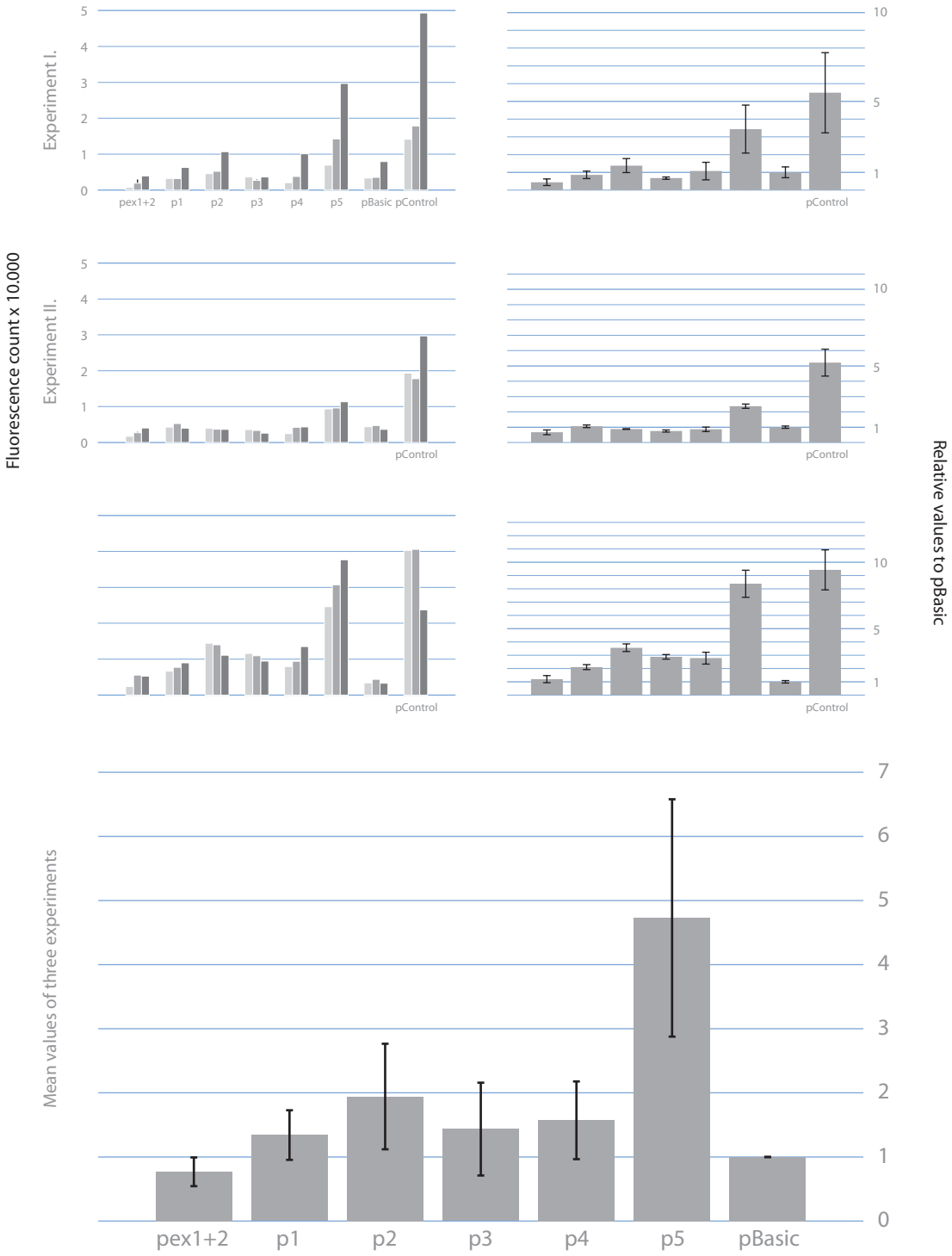
Fluorescence count x 10.000
Relative values to pBasic
Experiment I.
Experiment II.
pex1+2
p1
p2
p3
p4
p5
pBasic
pControl
Mean values of three experiments

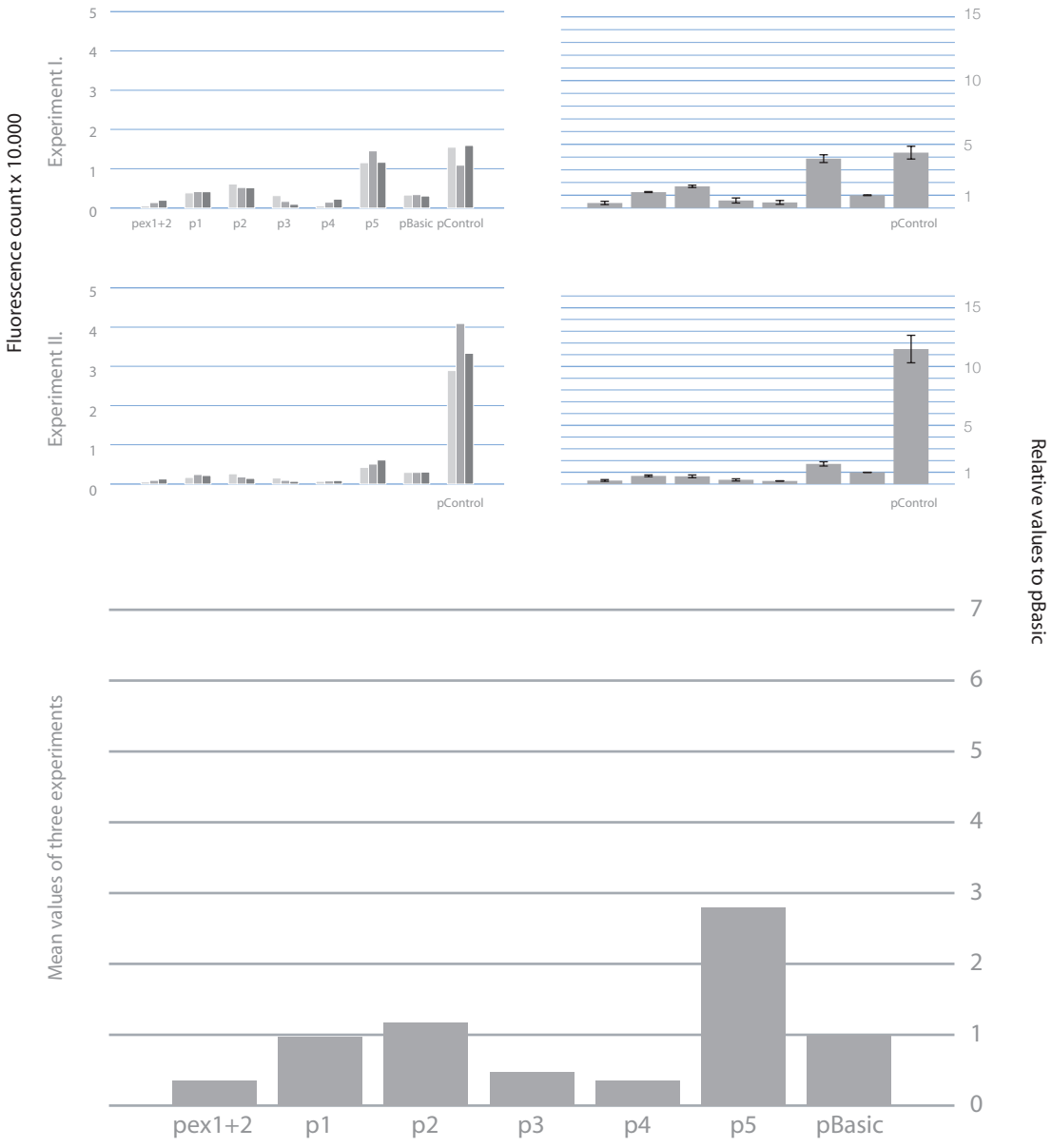
Fluorescence count x 10.000
Experiment I.
Experiment II.
pex1+2
p1
p2
p3
p4
p5
pBasic
pControl
Relative values to pBasic
Mean values of three experiments

Part V

Discussion

34 Disease causing mutation versus polymorphism

One of the aims of this work was to identify a possible relationship between mutations in the *PLXNB3* gene and mental retardation. Before discussing the results obtained by mutation screening it is important clarify two crucial terms; mutation and polymorphism. It might seem unnecessary to define such central and fundamental terms in modern biology and genetics, unfortunately the terms mutation and polymorphism have taken on many different meanings in different fields of science, even within a single field like medical genetics.

A Dictionary of Genetics states three definitions for mutation 1) a process which a gene undergoes structural change, 2) a modified gene resulting from mutation, and 3) by extension, the individual manifesting the mutation [King and Stansfield, 1990]. In addition in 1998 Cotton and Scriver listed three different common use of this term in different scientific fields [Cotton and Scriver, 1998]. In the field of biology, mutation means any change in nucleotide sequence, in applied knowledge of medical genetics it is used to state whether the result of the nucleotide change is neutral or disease-phenotype causing. Whereas, in medical genetics a mutation means a harmful change and a polymorphism is considered harmless. In the work of Cotton and Scriver, which among others things include the initiation of the HUGO (The Human Genome Organisation) mutation database, each 'allelic variant' is defined to be result of a mutation [Cotton and Scriver, 1998].

In the book Human Molecular Genetics 'mutation' is defined as a 'heritable change' [Read and Strachan, 2004]. In the same textbook, a definition of the term 'polymorphism' is given. Strictly, as the existence of two or more variants at significant frequencies in a population, and loosely, among molecular geneticists as either 1) any sequence variant present at a frequency larger than 1% in a population, or 2) any non-pathogenic sequence variant, regardless of frequency. But still Redei states in another book Encyclopedic Dictionary of Genetics, Genomics and Proteomics (2003) that the mutation is heritable change in the genetic material or process of genetic alteration and polymorphism is defined as occurrence of different alleles.

In the field of human genetics, terms like normal, neutral, or harmless refer to commonly accepted standards in the scientific community and are most useful in areas of identifying genetic cause for distinct disease. However, the expansion of genetics research from the area of somatic disorders into non-pathological traits like intelligence, blue-eyed-ness, or even bed-wetting, it has become necessary to introduce a third category or term; normal-variation.

To make a clear and precise definition of the two terms and avoid misinterpretation of my data in regards to the present work, I have chosen and applied the following definitions: Polymorphism: Any sequence change present at a frequency of more than 0.01 (1%) in a general population. Mutation: A sequence variation that is found exclusively in a group of patients with a pathological phenotype (mental retardation) than in a control group of healthy subjects (without pathological phenotype, mental retardation).

In the past couple of years, a number of mutation/polymorphism databases have been established and made available online. The Human Genome Mutation Database is currently holding ~44,000 entries, the HapMap (Haplotypes map) project more than 4,200,000 variants in four different ethnic groups, and the largest NCBI Single Nucleotide Database (dbSNP) contains more the 21,000,000 registered genomic variants. It is clear, that most if not all known genes will be shown to be polymorphic. Whether the polymorphisms are neutral, normal-variance, or disease-causing is a large ongoing project in which this work was intended to contribute.

35 *PLXNB3* is a candidate gene for X-linked mental retardation

There is no formal criteria by which a gene is defined as a candidate gene for the given disease. Below I will discuss a number of reasons why *PLXNB3* was originally considered as a suitable candidate gene for mental retardation.

In a recent article about X-linked mental retardation (XLMR) Ropers et al. have reported some important observations about the distribution of known X chromosomal mutations causing syndromic (S-XLMR) and non-syndromic mental retardation (NS-XLMR) [Ropers et al., 2003]. The main observation was that mutated genes are not evenly distributed along the length of the X chromosome, but seem to cluster in three or four regions. The highest concentration of disease causing genes was seen on the long arm in region q28. [Mitelman, 1995, nomenclature in].

Ropers and Hamel (2005) reported seven genes in which mutations are known to cause S-XLMR (*FMR1*, *IDS*, *ABCD1*, *L1CAM*, *FLNA*, *IKBKG*, *DKC1*) and four genes (*FMR2*, *GDI1*, *MECP2*, *SLC6A8*) where mutations are causing NS-XLMR. However, when evaluating large families with known mutations it has proven difficult to keep a clear distinction between S-XLMR and NS-XMLR [Frints et al., 2002] likewise when investigating groups of subjects for mutation screening a precise clinical description is not always available. For reasons of references and convention I am maintaining a distinction between syndromic and non-syndromic forms of mental retardation, despite the probable overlap.

Expression analysis of 885 known protein-coding genes located on the X chromosome has shown that 40% demonstrate expression in brain tissues and could therefore likely be involved in the development of X-linked mental retardation. As shown on figure 7.1 genes surrounding *PLXNB3* have been demonstrated to play an role in mental retardation. It is likely that there are more then 11 genes in Xq28 that play a role in mental retardation. *PLXNB3* located on Xq28 as a novel gene characterized by our group, by location is a suitable and good candidate gene for the above mentioned group of diseases.

The causative gene for the L1 disease, *L1CAM* has been studied also in our group for a couple of years. Besides location, *PLXNB3* shares a number of characteristics with *L1CAM*. Both proteins are cell adhesion molecules, both undergo homophilic binding, both show expression in neurons, both molecules promote neurite outgrowth and consequently both are involved in axon guidance events [Hartwig et al., 2005]. Therefore *PLXNB3* seems a likely candidate

gene for diseases involving neuronal development and in mental retardation. Recently it was shown that Plexin-B3 is a receptor for semaphorin 5A, a gene located in the region deleted in Cri-du-chat syndrome [Simmons et al., 1998]. Cri-du-chat syndrome is often associated with severe mental retardation. For functional relation to Semaphorin 5A and Plexin B3 could be considered as possible candidate gene for diseases with mental retardation.

36 Sequence variance findings

In the present study, mutation screening of *PLXNB3* by SSCP was performed on 191 male subjects and 17 sequence variants were found. None of the variants were shown to be disease-causing and by the strict definition (above) none of them can be called mutations. Whether they can be called polymorphisms in a strict sense depends on the frequency they are found in our population. Six nucleotide changes shown in Table 31.1 were identified as unique non-disease-causing changes. The eleven nucleotide changes in Table 31.2 are all called polymorphisms because the frequencies of the rare alleles are greater than 1%.

To elucidate whether the sequence variant 2122G>C is a mutation and hence disease-causing or a very rare polymorphism, segregation analysis was performed in the family. The analysis excluded the sequence variation as mutation, because the healthy brother of the patient carried identical allele (2122C) of this sequence variant. Consequently, was suggested that this non-conservative change is a 'harmless' mutation, i.e. a polymorphism.

Even with the relatively large number of subjects in the screening, it can not be ruled out by the methods used, that other possible mutations in *PLXNB3* could be found. The screening was performed on the coding regions of *PLXNB3* and in short ($\sim$50 bp) flanking intronic sequences. Therefore, intronic mutations located more distantly from splicing sites would not have been detected by the mutations analysis performed in this work.

Three unique findings Leu83, Gln429, Thr1372 and one frequent polymorphism Arg1637, were considered as synonymous silent mutations. Silent mutations are by definition DNA mutations that although they alter a particular codon they do not alter the amino acid, and hence do not affect the protein. Because silent mutations do not alter protein function they are thought to be evolutionarily neutral. According to the strict definition of mutation a more correct term might be silent nucleotide changes, but to prevent misunderstandings and follow the convention I am using the term in the above definition.

However, analysis of silent mutations in genes causing hereditary disorders has shown that some silent mutations indeed affect gene transcription leading to the formation of truncated proteins with reduced or even no function. It is known that silent mutations can disrupt exonic splicing enhancer (ESE) or silencer (ESS) motifs, and thus affect the splicing pattern affecting RNA processing [Nissim-Rafinia and Kerem, 2002]. For instance, activation of a splice site mediated by a silent exon mutation in the gene encoding for fibroblast growth factor receptor 2 (*FGFR2*) has been reported to cause Crouzon syndrome. The silent mutation p.A334 creates a new donor splice site, which results in a stable transcript and an altered receptor with a

deletion in the Ig IIIc domain of *FGFR2* [Li et al., 1995]. Another silent mutation p.F208 in *SMN2* (survival motor neuron 2, centromeric) disrupts an ESE motif, promotes skipping of this exon and leads to spinal muscular atrophy, the second most common lethal autosomal recessive disease in Caucasians [Lorson et al., 1999]. Therefore, a further investigation of the effect of silent mutations found in *PLXNB3* on cDNA levels would be interesting.

37 Sensitivity of SSCP

Identification of a causative mutation in all candidate genes has important relevance for human genetics. Searching the entire candidate gene for sequence variants in a large series of patients needs simple, fast, and well-founded methods. Methods based upon direct sequencing have very high sensitivity for mutation detection, but they are still comparatively expensive, technically more demanding and time consuming and therefore not practical for handling a large cohort of samples. Various methods for mutation detection such as denaturing gradient gel electrophoresis (DGGE) analysis [Schwaab et al., 1997], mismatch cleavage [Winter et al., 1985], heteroduplex analysis [Jackson et al., 1997], and dideoxy fingerprinting [Sarkar et al., 1992] have been established. In this study, 191 subjects were screened using a single strand conformation polymorphism (SSCP) analysis as the major detection approach. SSCP is a widely employed method to detect mutation [Orita et al., 1989b], because it is cheap and reasonably sensitive (∼80%) for fragments up to 200 bp. According to the opinion of different authors, the size of the DNA fragments used in the SSCP analysis should not exceed 200 to 300 bp [Hayashi and Yandell, 1993]. The mobility of single strand DNA (ssDNA) in a nondenaturing polyacrylamide gel (PAA) depends on their conformation, which is influenced by the size and the sequence composition.

The pattern of bands is dependent on many parameters such as electrophoresis temperature, ionic strength of the buffer, and additives such as glycerol which all influence the quality of gel resolution. Glycerol acts as a weak denaturant that opens the folded structures of ssDNA resulting in increased resolution of the fragments. ssDNA has a tendency to reanneal before and/or during electrophoresis, and may lead to difficulties in detecting mutations. In order to prevent reannealing of ssDNA, dilution of the PCR samples in buffer containing formamide is recommended.

The results presented in this work were obtained using SSCP under two electrophoretic conditions: 8% PAA gel containing 10% glycerol at 4˚C and 8% PAA gel containing 10% glycerol at room temperature. Under the second conditions the results reveals higher sensitivity, most noticeable in exon 20 and exon 27, where mobility shift of the ssDNA were not detected under the first condition.

Although, a problem in using the SSCP method is that certain single nucleotide changes might be missed, nevertheless, alteration in electrophoretic mobility of analyzed DNA fragments will indicate the existence of mutations. The lack of change in electrophoretic mobility of DNA fragments does not however excluded the existence of mutation in the target DNA.

38 Intronic mutation IVS22+21G>A

Two unique intronic nucleotide changes were found by mutation screening. Both sequence variants, IVS8+19A>G and IVS22+21G>A, were analyzed using splice site prediction software, without any significant effect on splice efficiency score. Nevertheless, both IVS22+21G and the surrounding sequence showed evolutionary conservation in intron 22 in mouse and chimp. Since, no RNA sample of the patient was available, a direct analysis of transcripts produced *in vivo* was not possible. Therefore, the putative effect of IVS22+21G>A on splicing was analyzed using the exon trapping.

In eukaryotes, most genes and their coding sequences are interrupted by intervening sequences, introns. Genes are transcribed as pre-messenger RNA (pre-mRNA), and the introns are removed by splicing in the nucleus [Smith et al., 1989]. The resulting mRNA, composed of spliced exons, is then transported to the cytoplasm. Splicing of exons is performed by the spliceosome, made up of five small nuclear ribonucleoproteins (snRNPs) and >100 other proteins. The spliceosome performs two primary functions of splicing: recognition of exon/intron boundaries, and catalyzing cut-and-join reactions that remove introns and join exons. The accuracy of splicing is dependent on the recognition of donor and acceptor splice sites and branch points. Introns contain highly conserved invariant GT and AG dinucleotides at the 5′ splice donor and 3′ splice acceptor of exon-intron junctions, respectively [Shapiro and Senapathy, 1987]. Approximately 10-15% of disease-causing mutations in human genes affect pre-mRNA splicing [Krawczak et al., 1992], and most of the splicing mutations occur within or around these invariant conserved sequences. Such mutations may lead to exon skipping or retention of whole introns. The abnormal splicing pattern may also exclude part of a normal exon or result in new exonic sequences [Nissim-Rafinia and Kerem, 2002, reviewed in]. To investigate putative effects of the intronic variant IVS22+21G>A on splicing exon trapping assay was performed and the results are discussed in next chapter.

39 Exon trapping assay results in different splicing isoforms *in vivo*

The exon trapping assay relies on the conservation of sequences at the exon-intron boundaries and it has been used for identifying of a genomic DNA fragment that are part of an expressed gene. After cloning a genomic fragment into a trapping vector, flanked by two exons, in a specialized exon trapping vector, the construct is expressed through a strong promoter. Exons encoded by the genomic fragment will be spliced into the resulting mRNA, changing its size and allowing its detection. General splicing machinery present in all cells can act with precision upon endogenous as well as foreign transcripts. Exon trapping has been used to characterize a number of genes, i.e. including the *ATP7A* gene (ATPase, Cu++ transporting, alpha polypeptide; Menkes syndrome) [Vulpe et al., 1993], or *NF2* gene (neurofibromatosis, type 2) [Trofatter et al., 1993].

Mutation screening revealed two intronic alterations. Using the Exon Trapping System, one intronic sequence variant IVS22+21G>A was further investigated for possible effects on splicing. Both wild type and mutated constructs used in exon trapping gave rise to various splice variants in transfected cells. The transcript containing exons 20, 21, 22, 23 has never been observed using exon trapping assay, neither from a wild type or from construct containing the mutation. Different transcripts were found, whereas splicing isoforms containing *PLXNB3* exon 22 never have been trapped for constructs with the mutation IVS22+21G>A. These data suggest that the intronic mutation IVS22+21G>A may possibly result in pathological skipping of exon 22.

The exon trapping assay can lead to artifacts. One example is the case of the transcript containing exon 20 and intron 22 with exon 23 observed exclusively in constructs with the mutation (figure 32.3, transcript no.11). In this case, the mutation would have an effect on aberrant splicing causing skipping of exon 22, but also missing exon 21 would be highly unlikely.

However, even that exon trapping assay is a sophisticated protocol, *in vitro* experiments never exactly recapitulates what occurs during splicing events *in vivo*. Obtained data suggests that the intronic mutation IVS22+21G>A may results in change of splicing pattern of (constitutively) spliced exon 22. Whether this aberrant splicing occur *in vivo*, has effect on downstream exons, or associated with a phenotypic change is in general uncertain. Taken together the results from trapping assay suggest that this particular method for investigation of sequence variant IVS22+21G>A and its putative effect on splicing was not generally helpful and it did not unmask fully all distinctly possible combinations of correctly or aberrantly spliced exons.

40 Alternative splicing

Nearly all eukaryotic genes contain introns that are 'spliced out' during processing of transcripts to mature mRNA. A common mechanism for altering the properties of protein products is to modify the pattern of splicing. Alternative splicing means that certain exons are included in the protein and some others are not by joining different 5' and 3' splice sites, allowing individual genes to express multiple mRNAs that encode proteins with diverse or even antagonistic functions. Alternative splicing can insert or remove amino acids, shift the reading frame, or introduce a termination codon, and also affect gene expression by removing or inserting regulatory elements controlling translation, mRNA stability, or tissue localization. Very often this mechanism is controlled in a tissue specific manner: e.g. muscle protein Troponin T and cardiac protein Tropomyosin occur in many different alternatively spliced forms [Breitbart et al., 1985, Graham et al., 1992]. In some cases, different peptide sequences have different biological functions and they are present or absent in different tissue. Between one-third and two-third of human genes are estimated to undergo AS [Modrek and Lee, 2002]. The disruption of specific AS events has been implicated in several human genetic diseases [Faustino and Cooper, 2003, reviewed in], whereas mutations that affect an alternative splice site shift the ratio of natural isoforms rather than create an aberrant splicing product with the usual associated loss of function. Several human diseases associated with such mutations were reported: familial isolated

growth hormone deficiency type II (GH-1) [Cogan et al., 1997], frontotemporal dementia and Parkinsonism linked to Chromosome 17 (MAPT) [Hong et al., 1998], inactivation of the Wilms tumor suppressor gene (WT1), [Miles et al., 1998] and three additional disorders associated with abnormalities in WT1 expression, WAGR Syndrome (Wilms tumor, aniridia, genitourinary abnormalities, mental retardation), Denys-Drash syndrome, and Frasier syndrome [Melo et al., 2002].

In this study, EST analysis and RT-PCR were performed, to investigate the splice patterns of PLXNB3. Allele-specific RT-PCR elucidated at least four differentially spliced isoforms of human PLXNB3 *in vivo* due to skipping of various 3'-parts of exon 27 [Hartwig et al., 2005]. These isoforms are expressed differentially in various tissues suggesting the existence of isoform-specific proteins with functionally distinct roles during ontogenesis. The first isoform containing the complete exon 27 was not detectable in heart, whereas an isoform detected in brain, heart and other tissues contains a frameshift predicting a C-terminally truncated plexin B3. This isoform may be not able to interact with PDZ-RhoGEF/LARG as the critical last three amino acids are missing [Swiercz et al., 2002]. An isoform lacking an 82 residues encoded by exon 27 appeared to be expressed exclusively in brain, suggesting another isoform-specific function.

As mentioned before plexins are transmembrane receptors that interact with semaphorins through their extracellular domains [Tamagnone et al., 1999]. The intracellular part of the B3 molecule contains two Ras GAP-like domains, the cytoplasmic domains which are highly conserved during evolution within and across species and show sequence similarity to Ras family-specific GTPase activating proteins (GAPs), especially R-Ras GAP [Rohm et al., 2000, Hu et al., 2001]. Several members of the plexin family (e.g. plexin A1 or B1) are known to bind directly to Rho-type small GTPases, e.g. Rac1 and Rnd1. It will be interesting to study the influence of different splicing isoforms of plexin B3 on binding to various intracellular adaptor molecules if the protein is truncated or altered.

There are several examples in literature showing that alternative splicing may influence receptor-mediated signal transduction pathways [Schlessinger, 2000, Adjei, 2001, reviewed in]. One of the examples described that has similar alternative splicing as seen with plexin B3 is neurofibromin (NF1). Neurofibromatosis type 1 is a disorder caused by a mutation in *NF1*, which encodes the Ras GAP-related protein neurofibromin expressed in the central nervous system. Neurofibromin is a protein that is involved in many of biological processes, including cells growth, tissue differentiation, learning, and memory. The NF1 protein contains a domain, which is related to the GTPase-activating protein (GAP) and accelerates the switch of GTP-bound form of Ras to inactivate GDP-bound form of Ras. Alternative splicing of *NF1* mRNA gives rise to four isoforms (I–IV), of which isoforms I and II are expressed exclusively in the brain [Costa et al., 2001]. Both isoforms I and II of NF1 protein have been shown to affect Ras inhibition [Sweatt, 2001]. A recent study of the knock-out mouse that lacks exon 23a of *Nf1* following selective targeting shows, that splice variant II of neurofibromin is important for brain function, but not for embryological development. The mouse lacking isoform type II revealed learning impairments similar to those of people with neurofibromatosis, indicating that

modification of the GAP domain of NF1 modulated Ras pathways important for learning and memory [Costa et al., 2001]. This study provides interesting paralles with plexin B3, that has different isoforms responsible for different biological functions. The corresponding proteins can be associated with different signaling pathways, with different responses to stimuli.

41 *PlxnB3* mRNA expression pattern

The plexin family consists of nine mammalian genes A1–A4, B1–B3, C1, and D1 [Tamagnone et al., 1999, van der Zwaag et al., 2002] that encode large single-pass transmembrane proteins. Plexins are receptors for different semaphorins either alone or in combination with neuropilins. Plexins play important roles in patterning and connectivity of the developing nervous system, and recent data suggests that members of the plexin-B family and their semaphorin receptors may be involved in axon guidance. However, subtype-specific functions of the majority of the nine members of the mammalian plexin family are largely unknown. In order to investigate the expression pattern of plexin B3 *in situ* hybridization (ISH), immunohistochemistry, and immunocytochemistry on human and murine tissues and cells was performed.

For murine *PlxnB3*, both neuronal and glial expression have been demonstrated. Using combined *in situ* hybridization and immunocytochemistry *PlxnB3* mRNA was detected in cultured primary cerebellar neurons of six days old mice. *PlxnB3* mRNA was also observed in adult murine cerebellum and prominent with neuronal B3-specific immunostaining in adult human cerebellum. For detection of murine *PlxnB3* two cRNA probes were used (Figure 41.1). The ISH probe A used in this work and a similar probe used by Cheng (2001) [Cheng et al., 2001], both cover major parts of the 3′ UTR of *PlxnB3*. Using these probes neuronal expression was detected. The ISH probe B hybridising more upstream was identical to the probe used by Worzfeld (2004) [Worzfeld et al., 2004] and appeared to detect a lower level of neuronal and more pronounced non-neuronal expression of *PlxnB3*. These data suggest the existence of cell-type specific isoforms of plexin B3 with different 3′ ends of the mRNA. In human organs, evidence was found for the expression of such isoforms [Hartwig et al., 2005]. However in the mouse EST database (NCBI dbEST), the 3′-end of *PlxnB3* transcripts is strongly overrepresented while the more upstream sequences are represented very rarely and thus do not allow the rapid detailed analysis of tissue-specific expression of B3 isoforms.

Expression studies of the plexin A-subfamily have focused on the later developmental stages of the nervous system, nearly all from embryonic day 16.5 to adult [Maestrini et al., 1996, Murakami et al., 2001, Suto et al., 2003, Takahashi et al., 1999, Tamagnone et al., 1999]. Plexin-A1 has been shown to have a role during lung and cardiac morphogenesis with expression observed in the epithelium and mesenchyme of the mouse lung at E11.5–E17.5 [Kagoshima and Ito, 2001], as well as in the heart at E10.5 [Toyofuku et al., 2004]. *PlxnD1* mRNA is most prominently expressed in the vascular endothelium (including the capillaries of the kidney glomeruli) and in the central nervous system in the developing murine embryo [Gitler et al., 2004, van der Zwaag et al., 2002].

Figure 41.1: Position of the PlxnB3-specific DIG-labelled cRNA probes relative to the PlxnB3.

Expression of plexin B-subfamily members has also been studied in the developing murine nervous system. *PlxnB1* and *PlxnB2* are widely expressed outside of the nervous system at E14 where they show highly specific patterns starting from embryonic day 13.5 to adult stages [Worzfeld et al., 2004]. By using semi-quantitative reverse transcription-PCR, *PlxnB3* expression has been shown in the dorsal root ganglia, heart, lung, optic bulb, brain and liver [Artigiani et al., 2004].

In this work I demonstrated constant expression of *PlxnB3* during mouse development from embryonic day 8 to 15, mainly in the neuroepithelium of the developing nervous system, which is at variance with the results published by Perälä (2005). In this work no *PlxnB3* mRNA by in situ hybridisation was detected at E14. The ISH probe A used for detection of mRNA during murine embryonic development by me and the probe used by Perälä et al. differ greatly with respect to location in the mRNA. My probe A covered major parts of the 3' UTR of *PlxnB3*, in contrast to the cRNA probe used by Perälä et al. which mainly covered the 5' coding region (figure 41.1).

PlxnB3 expression was found in cultured primary cerebellar neurons of six day old mice. The success of combining ISH and immunohisto(cyto)chemistry on one specimen is dependent on a number of factors: the type and sensitivity of antigen to be detected, tissue fixation, access of probes to the nucleic acid sequence, stability of the colour precipitate and fluorescent signal, and crossreactivity. Several steps in the ISH procedure, including enzymatic digestion, postfixation, denaturation at high temperatures, and hybridization in formamide, may destroy antigenic determinants.

A procedure starting with immunohisto(cyto)chemistry followed by ISH is preferred in most cases [Speel et al., 1999]. There are existing reports, where very poor correlation between the existence of particular mRNA and corresponding protein was observed. In the present study, both approaches were used, immunohisto(cyto)chemistry followed by ISH or vice versa, and both, comparable results were obtained. In the present study neurons were distinguished using monoclonal antibodies NeuN [Wolf et al., 1996] and neuromodulin [Schreyer and Skene, 1991], astrocytes by GFAP (glial fibrilar acidic protein) [Weinstein et al., 1991] and oligodendrocytes by CNPase [Reynolds et al., 1989].

42 *PLXNB3* expression pattern

Levels of *PLXNB3* mRNA expression in different human organs and tissues were determined to gain insight about *PLXNB3*'s expression pattern. Tissue expression profiling by mRNA tissue array and Northern blot showed that *PLXNB3* is expressed at highest levels in the brain, and especially in those areas which are neuron rich, such as the thalamus. ISH and immunohistochemistry (IHC) on various brain regions also indicated that neurons and vascular endothelium are the most likely places of abundant *PLXNB3* mRNA expression.

Gene expression studies involved post-mortem brain tissues. Compared generally with single-cell organisms or cell lines, the biological environment and handling of human subjects can not be well controlled. This is confounded with time delay between death and post-mortem collection of specimens (24-96 h in this study). The stability and of mRNA is influenced by several heterogeneous factor, i.e. the lower pH of brain tissue samples exhibited a systematic decrease in expression of genes involved in energy metabolism and proteolytic activities, while a consistent increase of genes encoding stress-response proteins and transcription factors [Li et al., 2004].

The widespread detection of plexin B3 protein was demonstrated by IHC in normal neuronal and non-neuronal tissues and in tumors tissues as well. High levels of immunoreactivity in non-neuronal tissues were observed in skin, digestive tract, kidney, testis, pancreas, liver, adrenal medulla, and placenta. In all organs evaluated, plexin B3 protein was found consistently in the epithelial cells while the stromal tissue was negative. IHC and ISH were performed on paraffin embedded human neuronal and various non-neuronal tissues on commercially available Tissue Array Sets and also on archived human neocortex and corpus callosum (Department of Neurosurgery, UKE, Hamburg). The results showed that in the human nervous system, *PLXNB3* mRNA and protein were detected within neurons in all regions analyzed, while was not expressed in astrocytes or oligodendrocytes *in vivo*. The results obtained were similar to the expression patterns of plexin D1 and plexin B1 reported by van der Zwaag et al. (2002). Combined ISH and IHC clarified that PLXNB3 is expressed predominantly in neurons in various parts of human brain, and the data suggest a role of the plexin B3 molecule in development of and function in nervous and vascular systems.

43 Non-neuronal expression of *PLXNB3* was not detected

Similarity between ORF of *PlxnB3* and *PLXNB3* is 82.8%, reaching 83.8% of the amino acid level. These two orthologues have high homology and they are highly conserved. ISH performed on adult mouse specimens demonstrated apparent *PlxnB3* expression in neurons and in oligodendrocytes. Nevertheless, investigation of cell type-specific expression of *PlxnB3* on cultured mouse cerebellar cells showed expression in solely neurons. After ISH immunocytochemistry was performed on the same slide using monoclonal antibodies against neurons including NeuN and neuromodulin, against astrocytes using GFAP, and against oligodendrocytes using CNPase was performed. Only cells positive for neuron-specific markers NeuN and neuromodulin showed expression of *PlxnB3*, whereas cells immunoreacting for GFAP and CNPase showed no *PlxnB3* hybridization signal. Also, exclusive expression on cultured neurons, and no expression in astrocytes and oligodendrocytes was demonstrated by this experiment. However this later work was performed on cells *in vitro*, which may behave differently when removed from their natural environment and their intimate relationships with neurons [Brown, 1999]. Results showed that *PlxnB3* expression was detected primarily in neurons. Worzfeld (2004) work suggested that glia cells do indeed express *PlxnB3 in vivo*, but the samples used in such analyses were fresh frozen rodent tissues, cut on a cryostat. It is possible that glia cells, in addition to inaccessibility of the detection, have higher levels of nucleases relative to surrounding neurons. This can cause loss of detection because of the post-mortem delay and specimens manipulation.

Additional experiments in our group relied on Western blot and RT-PCR detected *PLXNB3* in human adult neocortex but no signal in corpus callosum. These results also suggest that plexin B3 is expressed predominantly in neurons.

44 General aspects of *in situ* hybridization protocol

In situ hybridization (ISH) has become an indispensable tool for studies of gene expression in cells and tissues, and was first introduced for the localization of distinct repetitive DNA sequences and later adapted for the detection of mRNA transcripts. There are several procedures in the ISH protocol, which were found to be of critical importance to achieve high sensitivity and high specificity, and high-resolution. It is important to empirically optimize the various experimental parameters of ISH, such as Proteinase K digestion, size, concentration, and localization of the probe. Additional parameters include hybridization temperature, stringency of washing, and methods of detection have to be optimized as well. Fixation is one of the critical steps in the ISH procedure in preserving good morphology, and retaining cellular RNAs. A cross-linking fixative, e.g. buffered paraformaldehyde (pH 7.4) has been recommended by several authors [Moorman et al., 1993, Wilcox, 1993].

In the present study, paraformaldehyde fixation at room temperature was used, with a higher pH (pH 9) allowing faster penetration and stronger action of the fixative [Basyuk et al., 2000]. A problem of the ISH technique lies in the fact that nucleic acids are bound inside a complex matrix of cellular structures, so target sequences may not be readily accessible to the labelled probes. Proteinase K has been accepted as the standard enzyme used for proteolytic digestion in ISH. However, in cases of too intense digestion membranes and protein structures may lose integrity, and the template RNA or hybrid complex may leak from the cells and make surroundings cells falsely positive. Another adverse consequence can be high background and poor target tissue morphology. In our hands, digestion with 10 μg/ml Proteinase K for 15 min at 37˚C led to complete loss of cell morphology. Therefore no Proteinase K treatment was used on mouse and human specimens, and omitting Proteinase K digestion did not reveal any significant influence. On the other hand, in whole mount ISH experiments, Proteinase K was effectively used (1 μg/ml of Proteinase K incubation for 1 min × days of embryo age).

Additional parameters should be considered when calculating optimal hybridization conditions including the probe length and concentration. The choice of length depended on the intended target. Problems arise with probe penetration using intact cells or tissues. Shorter probes give more rapid hybridization, as they can more easily gain access to targets, but they are more prone to homology with other gene sequences and risk cross-hybridization, bona fide problem with mouse plexins B1 and B2. The control hybridization with the corresponding sense probes showed no specific staining, confirming the specificity of hybridization.

The advantage of cRNA probes providing a more sensitive detection of RNA by ISH [Cox et al., 1984], has been supported by this work. Hybridization performed at 55˚C or 65˚C and stringent washing conditions using 0.2×SSC and 0.2×SSC/50% (v/v) formamide (3 times 1 hour) at 65˚C improved the signal-to-noise ratio. In addition, low salt concentration in the hybridization mixture or washing solution was used to enhance stringency. Non-specific probe binding was reduced by Rnase treatment after hybridization. Visualization of probes can be carried out using specific antibodies conjugated to reporter molecules such as horseradish peroxidase, alkaline phosphatase, fluorochrome, or gold particles.

The alkaline phosphatase-based system is increasingly favoured for ISH detection for several reasons, but mostly because it allows detection of hybridization signals with high sensitivity and excellent morphological resolution. For alkaline phosphatase, the most convenient substrate is BCIP, which reacts with NBT and generates an intense dark blue/purple or brownish precipitate. The development of the alkaline phosphatase-conjugated anti-digoxigenin antibody with the NBT/BCIP substrate can be prolonged without giving rise to background staining. Indeed, the time to obtain an exceptional signal-to-noise ratio is dependent on the abundance of the RNA molecules of interest in the tissue and can therefore be inspected microscopically in the course of incubation. For detection of mouse *PlxnB3* mRNAs the staining was carried out 4–6 h, and for human *PLXNB3* mRNA the developing time was 1–2 h. The stability of alkaline phosphatase, which remains active even after 122 h of colour development [Emson, 1993], is a prerequisite for the high sensitivity of this mRNA detection protocol.

The differences in ISH protocols presented in this work and that of Worzfeld et al. (2004) concern the permeability step, and different compositions of hybridization mixtures. Moreover, the subsequent washing in Worzfeld's et al. work was likely less stringent. 7 min at 50˚C compared to 3 hours (3×1 hour) at 65˚C in this study.

In summary, in the present study, a detailed protocol for non-radioactive ISH detection of mRNAs encoding human and mouse plexin B3 was established using digoxigenin-labelled cRNA probes. Exclusive localization of mRNA transcripts was observed in the cytoplasm of cells with absence of nuclear and nucleolar staining. The importance of different steps in the ISH procedure, such as fixation, tissue permeability, and detection of the digoxigenin-labelled cRNA probes based on an alkaline phosphatase-system revealed results with very good sensitivity and reproducibility.

45 Functional analysis of the *PLXNB3* promoter region

The promoter is the most important gene element for the control of expression. In most cases, promoters are located immediately upstream of the expressed sequence, although elements regulating cell specific expression patterns are not necessarily located in this region. The presence or absence of enhancer sequences, and the interaction of multiple activator and inhibitor proteins are important regulatory elements of transcription initiation. The number and type of regulatory elements found are different for every gene. Different combinations of transcription factors can also have differential regulatory effects upon transcription initiation. RNA polymerase II is responsible for transcription of protein-coding genes in eukaryotes. Primary targets of RNA polymerase II are DNA motifs, generally called the core promoter, located around -40 to +40 bp relative to the transcription initiation site of the gene. The basic function of the core promoter is to guide the enzyme to initiate transcription from the correct position. Generally there are three kinds of core promoters [Arkhipova, 1995,Burke and Kadonaga, 1996,Burke and Kadonaga, 1997].

The TATA box is an A/T-rich sequence, typically located about 20 to 30 nucleotides upstream of the transcription start site. By consensus, the TATA box is typically designed `TATAAA` and is bound by a TATA-binding protein (TBP) subunit of the TFIID (transcription factor) complex.

Transcription factor TFIID is a multiprotein complex composed of the TATA box-binding protein (TBP) and multiple TBP-associated factors (TAFs). TFIID plays an essential role in mediating transcriptional activation by gene-specific activators.

The Initiator (Inr) was originally identified as a sequence that encompasses the transcription start site, and is sufficient to direct accurate initiation in the absence of a TATA element [Smale, 1997]. However, it is present in both TATA containing and TATA-deficient promoters. A downstream core promoter element (DPE) is located downstream +34 to +38 from the transcription start point (TSP). By consensus, it is designated `(A/G)G(A/T)CGTG` and is bound by TFIID but not TBP [Burke and Kadonaga, 1996].

DPE functions cooperatively with Inr to bind TFIID and to direct accurate and efficient initiation of transcription in TATA-less promoters. The space between DPE and Inr is very strict, in which any deletion or insertion of a single nucleotide would cause a reduction of TFIID binding and transcriptional activity [Kutach and Kadonaga, 2000].

In the present study, 1.1 kb of the 5'-flanking region, and 1.5 kb downstream from the transcription start site of the human gene were cloned. Promoter function was characterized using deletion analysis of six SEAP (SEcreted Alkaline Phosphatase) reporter molecule fusion constructs transiently expressed in various cell lines. Analysis of regulatory motifs in the 5' region of PLXNB3 reveals that the expression of *PLXNB3* involves complex interactions of positive and negative regulatory elements. Unfortunately, due to the lack of information and precise localization of the first two exons in rodents, comparative alignment of the 5' region between mice and human could not be performed.

46 Promoter assays analysis showed two major results

The first, promoter construct p5 show significantly higher promoter activity, and secondly in promoter construct p4 three repressor motifs were predicted. The region showing minimal promoter activity extends to -130 bp in the *PLXNB3* gene; it lacks a classical promoter factor like a TATA or CAAT box or GC-rich region. Database analysis of elements associated with experimental reporter repression revealed three elements known as repressors in the region from -155 to -226, that repressed promoter activity by interacting with cis-acting regulatory elements located in that region. At position -155 to -162 a GATA-1 binding factor, from -188 to -196 the Delta EF1, and most interestingly at position -218 to -226 a motif for a RE-1 repressor element (also known as neuron-restrictive silencer element, RE1/NRSE) were discovered. Patterns of gene expression in multicellular organisms are established and maintained primarily through the interaction of transcription factors with target genes and subsequent transcription regulation. However the target genes for most transcription factors are still unknown. Regulatory elements of gene expression are also important in the developmental process of neurons. Genes encoding transcriptional regulatory proteins have been revealed by many of the mutants affecting neuronal development in organisms such as *Drosophila melanogaster* and *Caenorhabitis elegans* [Way and Chalfie, 1989, Jan and Jan, 1994, reviewed in]. Overexpression of transcription factors in *Xenopus laevis* oocytes and targeted mutagenesis of transcription factor genes in mice have also shown the importance of transcriptional regulation during vertebrate neuronal determination and differentiation [Guillemot et al., 1993]. To understand the biological role of a transcription factor, it is important to determine the complement of genes it regulates. For example, in pituitary cells, *Pit-1* is essential for proper pituitary development and is known to activate its own gene as well as other pituitary-specific genes, such as *prolactin* [Ingraham et al., 1990]. Similarly, a target for *mec-3* and *unc-86*, two proteins necessary for neurogenesis in *Caenorhabitis elegans*, is the *mec-3* gene itself [Xue et al., 1993] as well as the *mec-7 tubulin* [Hamelin et al., 1992]. For most genes, however, target genes for other transcriptional regulators implicated in neural development have not yet been identified.

While most transcription factors thought to be involved in neurogenesis act positively, the importance of negative regulation in this process is becoming increasingly clear [Schoenherr and Anderson, 1995, Simpson, 1995] RE1-silencing transcription factor (REST), also known as neuron-restrictive silencer factor (NRSF), was one of the first negative-acting transcriptional regulators found to be implicated in vertebrate neuronal development. RE1 was originally found in the 5' flanking region of a neuron-specific gene *SCG10* (superior cervical ganglion 10) [Schoenherr and Anderson, 1995] and at least 40% of these genes identified are expressed in nervous system [Bruce et al., 2004]. This 21 bp element has been identified in the regulatory regions of more than 30 genes including neuron-specific *L1CAM* where, RE1 is present twice within 30 bp from the original RE1 element. Neuron-restrictive silencer factor represents the first example of a vertebrate silencer protein that potentially regulates a large series of cell type-specific genes, and functions as a negative regulator of neurogenesis. The proposed role of REST is the restriction of the expression of neuronal genes by silencing expression of these genes in non-neuronal tissue [Chong et al., 1995, Schoenherr and Anderson, 1995].

In summary, various cell types express characteristic combinations of transcription factors; this is the major mechanism for cell-type specificity in the regulation of gene expression. The fact that the same short genomic element of 131 bp (-147 to -16) was the strongest inducer of reporter expression in three different cell lines, two human ones and in a rodent cell line, suggests that the (structurally unknown) promoter of *PLXNB3* is also located immediately upstream the expressed region of the gene. Interestingly, I found strong evidence of a repressor within the 102 bp immediately upstream the promoter region.

Conclusion

I would like to conclude the results of this thesis by looking back to the aims of the study described in the introduction.

Northern blot and multiple tissue RNA array demonstrated the expression of *PLXNB3* predominantly in nervous system, but also in colon and small intestine. By *in situ* hybridization (ISH) expression was detected predominantly in central nervous system particularly in neurons, and in addition in vascular endothelium.

ESTs analysis and allele-specific RT-PCR revealed alternative splicing and the existence of at least four different B3-isoforms of PLXNB3 *in vivo* due to skipping various part of exon 27. These isoforms were differentially expressed in various tissues.

The mouse *PlxnB3* was expressed in neurons and glial cells. Furthermore the expression of *PlxnB3* has been detected in cultivated primary murine neurons. During mouse development (E8–E15 p.c.) *PlxnB3* was shown to be expressed in the central nervous system and in some additional non-neuronal tissues like tooth, epidermis, lung bud, throughout all developmental stages analysed.

Using polyclonale antibodies the plexin B3 protein was detected widespread in human normal and tumor tissues. Plexin-B3 was detected in neurons of CNS and in non-neuronal tissues as well, immunoreactivity was observed in different cell types like Islet of Langerhans, cardiac myocytes, Leydig cells, hepatocytes, epithelial cells and also in some tumour tissues like astrocytoma, hepatocellular carcinoma and, colon adenocarcinoma.

Mutation screening of *PLXNB3* on 191 male subjects with X-linked mental retardation revealed 17 nucleotide changes. These sequence variants include 10 single nucleotide polymorphisms (SNPs), one 28 bp insertion, and six unique sequence variants. None of them appear to be causative mutations for mental retardation. 85 male subjects were genotyped using six SNPs, and 13 human hapotypes were identified.

The region harboring the promoter of *PLXNB3* was characterized using promoter activity reporter assays. The region spans from -16 to -147 upstream from transcription start site demonstrated highest promoter activity, and the region from -16 to -249 a repressor activity and three binding motifs for known repressor elements were predicted.

Publication list

Scientific work by Šárka Krejčová / Veske.

Original Articles

Rujescu D, Meisenzahl EM, **Krejcova S**, Giegling I, Zetzsche T, Reiser M, Born C, Möller HJ, Veske A, Gal A and Finckh U (2005)
Plexin B3 is genetically associated with verbal performance and white matter volume in human brain
Molecular Psychiatry; submitted

Hartwig C, Veske A, **Krejcova S**, Rosenberger G and Finckh U. (2005)
Plexin B3 promotes neurite outgrowth, interacts homophilically, and interacts with Rin
BMC Neuroscience; 2005 Aug 25;6(1):53

Abstracts and Posters

Veske S, Veske A, Hartwig C, Finckh U (2003)
Expression of mouse and human plexin B3, and mutation analysis of it PLXNB3
13th Annual Meeting of the German Society of Human Genetics, September 29–October 2, 2002, Leipzig, Germany

Hartwig C, **Veske S**, Veske A and Finckh U (2003)
Plexin B3 promotes neurite outgrowth and shows homophilic binding mediated through the sema domain
Special FEBS 2003 Meeting of Signal Transduction, Juli 6–10, 2003, Brussels, Belgium

Krejcova S, Veske A, Michelson P, Schachner M, Finckh U (2001)
Molecular characterization of human plexin B3 and demonstration of its gene (PLXNB3) expression in brain.
International Human Genetics Conference, June 12–15, 2001, Wien, Austria

Veske A, Michelson P, Ueckert S, **Krejcova S**, Schachner M, Gal A, Finckh U (2000)
Characterization and expression of plexin 6 cDNA encoded by a novel candidate gene for X-linked neurological disorders
12. Meeting of the German Society of Human Genetics, March 22–25, 2000, Lübeck, Germany

Oral presentations

Veske S, Veske A, Hartwig C, Finckh U (2003)
Expression and mutation analysis of PLXNB3, a candidate gene for neurologic disorders
14th Annual Meeting of the German Society of Human Genetics, October 1–4, 2003, Marburg, Germany

Veske S, Veske A, Hartwig C, Schachner M, Finckh U (2001)
Cloning and characterization of human plexin-B3
21. Treffen der Norddeutschen Humangenetiker, November 3, 2001, Greiswald, Germany

Acknowledgement

I would like to thank a lot of peole whom wihout this work will never has seen the day of light.

First of all I wish to thank to PD Dr. Uli Finkch for giving me the opportunity to do my Ph.D. in his working group. I appreciated the creative space and the possibility to follow my own ideas. I remember his critical discussion and interest of my written work and the checking language style (for) so many times. We have spend time on many valuable constructive discussion together as well as 'speculative' scientific ideas, which sometimes make science more fruity and juicy and suddenly life without 'Sarko let's speculate' will be somehow 'different'.

I would like to warmly thank my supervisor Prof. Dr. Andreas Gal. I have great respect for his critical attitude and aproach to science and I am grateful for his time as well for the way how he showed me and tought me how to formulate and express the precise and essential points of my work. Thank you for helping me to put things into scientific perspective and above all now I know more about the science of genetics and how to deal generally with my future career. Thank you for your guidance and always making time even when there was none.

To Prof. Dr. Alexander Rodewald for his supervision of my thesis. His scientific interest and kindness and many questions focused not only on scientific point of my life helped me to keep going on.

To Prof. Andres Veske Ph.D. , who was Post-doc in our working group, for initiating this work. It was a long but finally fruitfull process. He showed me and introduced to me the magic world of molecular biology. Sometimes a very interesting and harvesting field but also complicated, complex and sometimes even frustrating. I will always remember his response after unexpectable and not optimistics results; 'forwards!'. I am sorry that we were not able to finish this work together.

To Prof. Dr. Schäfer for his help and time he spend to checked and re-evaluated my histochemistry results and our late evening histology discussion at the microscope.

To Prof. Dr. Kerstin Kutche for help and answers many questions and for beeing the person who knows in our institute for sure the right answer.

To Mads Hjorth for his excellent technical assistance and introducing me to the complicated world of LaTeX, the programming language in which this work was typeset. I have learned to deal with problems through his geek eyes.

I want to thank all members of Institute of Human Genetics for the joyful times we spent together not only in lab and our 'a bit noisy doctorand office'. Thank you for helpfull cooperation and enjoyable times among other Ph.D. students going through sometimes hard times with smiles, even the tears, but always able to express humor and appreciate a joke. Thank you Köms, Alex, Stefan, Christine, Ben, Verena, Georg, Isabella...

My warmest and heartfelt thanks go to my family, my mother Helenka, my father Jan, and my beloved brother Hynek. I am thankful for their enduring love, encouragement and never-ending patience with me during the long time when I was 'mentaly and physically' away from home because I was writing and writing..... Without your amazing support, trust and confidence in many days, when you have not see me at all, this work would not be never accomplish.

Šárka Krejčová

References

[Adjei, 2001] Adjei, A. A. (2001). Blocking oncogenic Ras signaling for cancer therapy. *J Natl Cancer Inst*, 93(14):1062–1074.

[Altschul et al., 1990] Altschul, S. F., Gish, W., Miller, W., Myers, E. W., and Lipman, D. J. (1990). Basic local alignment search tool. *J Mol Biol*, 215(3):403–10.

[Angel and Karin, 1991] Angel, P. and Karin, M. (1991). The role of Jun, Fos and the AP-1 complex in cell-proliferation and transformation. *Biochim Biophys Acta*, 1072(2-3):129–57.

[Aradhya et al., 2002] Aradhya, S., Woffendin, H., Bonnen, P., Heiss, N. S., Yamagata, T., Esposito, T., Bardaro, T., Poustka, A., D'Urso, M., Kenwrick, S., and Nelson, D. L. (2002). Physical and genetic characterization reveals a pseudogene, an evolutionary junction, and unstable loci in distal Xq28. *Genomics*, 79(1):31–40.

[Arkhipova, 1995] Arkhipova, I. R. (1995). Promoter elements in Drosophila melanogaster revealed by sequence analysis. *Genetics*, 139(3):1359–69.

[Artigiani et al., 1999] Artigiani, S., Comoglio, P. M., and Tamagnone, L. (1999). Plexins, semaphorins, and scatter factor receptors: a common root for cell guidance signals? *IUBMB Life*, 48(5):477–82.

[Artigiani et al., 2004] Artigiani, S., Conrotto, P., Fazzari, P., Gilestro, G. F., Barberis, D., Giordano, S., Comoglio, P. M., and Tamagnone, L. (2004). Plexin-B3 is a functional receptor for semaphorin 5A. *EMBO Rep*, 5(7):710–4.

[Bagnard et al., 1998] Bagnard, D., Lohrum, M., Uziel, D., Püschel, A. W., and Bolz, J. (1998). Semaphorins act as attractive and repulsive guidance signals during the development of cortical projections. *Development*, 125(24):5043–53.

[Basyuk et al., 2000] Basyuk, E., Bertrand, E., and Journot, L. (2000). Alkaline fixation drastically improves the signal of in situ hybridization. *Nucleic Acids Res*, 28(10):E46.

[Behar et al., 1996] Behar, O., Golden, J. A., Mashimo, H., Schoen, F. J., and Fishman, M. C. (1996). Semaphorin III is needed for normal patterning and growth of nerves, bones and heart. *Nature*, 383(6600):525–8.

[Billard et al., 2000] Billard, C., Delaire, S., Raffoux, E., Bensussan, A., and Boumsell, L. (2000). Switch in the protein tyrosine phosphatase associated with human CD100 semaphorin at terminal B-cell differentiation stage. *Blood*, 95(3):965–72.

[Birnboim and Doly, 1979] Birnboim, H. C. and Doly, J. (1979). A rapid alkaline extraction procedure for screening recombinant plasmid DNA. *Nucleic Acids Res*, 7(6):1513–23.

[Blackwell et al., 1990] Blackwell, T. K., Kretzner, L., Blackwood, E. M., Eisenman, R. N., and Weintraub, H. (1990). Sequence-specific DNA binding by the c-Myc protein. *Science*, 250(4984):1149–51.

[Breitbart et al., 1985] Breitbart, R. E., Nguyen, H. T., Medford, R. M., Destree, A. T., Mahdavi, V., and Nadal-Ginard, B. (1985). Intricate combinatorial patterns of exon splicing generate multiple regulated troponin T isoforms from a single gene. *Cell*, 41(1):67–82.

[Brose et al., 1999] Brose, K., Bland, K. S., Wang, K. H., Arnott, D., Henzel, W., Goodman, C. S., Tessier-Lavigne, M., and Kidd, T. (1999). Slit proteins bind Robo receptors and have an evolutionarily conserved role in repulsive axon guidance. *Cell*, 96(6):795–806.

[Brown et al., 2001] Brown, C. B., Feiner, L., Lu, M. M., Li, J., Ma, X., Webber, A. L., Jia, L., Raper, J. A., and Epstein, J. A. (2001). PlexinA2 and semaphorin signaling during cardiac neural crest development. *Development*, 128(16):3071–80.

[Brown, 1999] Brown, D. R. (1999). Prion protein peptide neurotoxicity can be mediated by astrocytes. *J Neurochem*, 73(3):1105–13.

[Bruce et al., 2004] Bruce, A. W., Donaldson, I. J., Wood, I. C., Yerbury, S. A., Sadowski, M. I., Chapman, M., GŽttgens, B., and Buckley, N. J. (2004). Genome-wide analysis of repressor element 1 silencing transcription factor/neuron-restrictive silencing factor (REST/NRSF) target genes. *Proc Natl Acad Sci U S A*, 101(28):10458–63.

[Burge and Karlin, 1997] Burge, C. and Karlin, S. (1997). Prediction of complete gene structures in human genomic DNA. *J Mol Biol*, 268(1):78–94.

[Burke and Kadonaga, 1996] Burke, T. W. and Kadonaga, J. T. (1996). Drosophila TFIID binds to a

conserved downstream basal promoter element that is present in many TATA-box-deficient promoters. *Genes Dev*, 10(6):711–24.

[Burke and Kadonaga, 1997] Burke, T. W. and Kadonaga, J. T. (1997). The downstream core promoter element, DPE, is conserved from Drosophila to humans and is recognized by TAFII60 of Drosophila. *Genes Dev*, 11(22):3020–31.

[Castellani et al., 2002] Castellani, V., Angelis, E. D., Kenwrick, S., and Rougon, G. (2002). Cis and trans interactions of L1 with neuropilin-1 control axonal responses to semaphorin 3A. *EMBO J*, 21(23):6348–57.

[Charron et al., 2003] Charron, F., Stein, E., Jeong, J., McMahon, A. P., and Tessier-Lavigne, M. (2003). The morphogen sonic hedgehog is an axonal chemoattractant that collaborates with netrin-1 in midline axon guidance. *Cell*, 113(1):11–23.

[Chen et al., 2000] Chen, H., Bagri, A., Zupicich, J. A., Zou, Y., Stoeckli, E., Pleasure, S. J., Lowenstein, D. H., Skarnes, W. C., Ch?dotal, A., and Tessier-Lavigne, M. (2000). Neuropilin-2 regulates the development of selective cranial and sensory nerves and hippocampal mossy fiber projections. *Neuron*, 25(1):43–56.

[Chen et al., 1998] Chen, H., He, Z., and Tessier-Lavigne, M. (1998). Axon guidance mechanisms: semaphorins as simultaneous repellents and anti-repellents. *Nat Neurosci*, 1(6):436–9.

[Cheng et al., 2001] Cheng, H. J., Bagri, A., Yaron, A., Stein, E., Pleasure, S. J., and Tessier-Lavigne, M. (2001). Plexin-A3 mediates semaphorin signaling and regulates the development of hippocampal axonal projections. *Neuron*, 32(2):249–63.

[Chong et al., 1995] Chong, J. A., Tapia-Ramirez, J., Kim, S., Toledo-Aral, J. J., Zheng, Y., Boutros, M. C., Altshuller, Y. M., Frohman, M. A., Kraner, S. D., and Mandel, G. (1995). REST: a mammalian silencer protein that restricts sodium channel gene expression to neurons. *Cell*, 80(6):949–57.

[Cogan et al., 1997] Cogan, J. D., Prince, M. A., Lekhakula, S., Bundey, S., Futrakul, A., McCarthy, E. M., and Phillips, J. A. (1997). A novel mechanism of aberrant pre-mRNA splicing in humans. *Hum Mol Genet*, 6(6):909–12.

[Cohen et al., 1998] Cohen, N. R., Taylor, J. S., Scott, L. B., Guillery, R. W., Soriano, P., and Furley, A. J. (1998). Errors in corticospinal axon guidance in mice lacking the neural cell adhesion molecule L1. *Curr Biol*, 8(1):26–33.

[Colamarino and Tessier-Lavigne, 1995] Colamarino, S. A. and Tessier-Lavigne, M. (1995). The axonal chemoattractant netrin-1 is also a chemorepellent for trochlear motor axons. *Cell*, 81(4):621–9.

[Comoglio et al., 1999] Comoglio, P. M., Tamagnone, L., and Boccaccio, C. (1999). Plasminogen-related growth factor and semaphorin receptors: a gene superfamily controlling invasive growth. *Exp Cell Res*, 253(1):88–99.

[Costa et al., 2001] Costa, R. M., Yang, T., Huynh, D. P., Pulst, S. M., Viskochil, D. H., Silva, A. J., and Brannan, C. I. (2001). Learning deficits, but normal development and tumor predisposition, in mice lacking exon 23a of Nf1. *Nat Genet*, 27(4):399–405.

[Cotton and Scriver, 1998] Cotton, R. G. and Scriver, C. R. (1998). Proof of "disease causing" mutation. *Hum Mutat*, 12(1):1–3.

[Cox et al., 1984] Cox, K. H., DeLeon, D. V., Angerer, L. M., and Angerer, R. C. (1984). Detection of mrnas in sea urchin embryos by in situ hybridization using asymmetric RNA probes. *Dev Biol*, 101(2):485–502.

[Don et al., 1991] Don, R. H., Cox, P. T., Wainwright, B. J., Baker, K., and Mattick, J. S. (1991). 'Touchdown' PCR to circumvent spurious priming during gene amplification. *Nucleic Acids Res*, 19(14):4008.

[Driessens et al., 2001] Driessens, M. H., Hu, H., Nobes, C. D., Self, A., Jordens, I., Goodman, C. S., and Hall, A. (2001). Plexin-B semaphorin receptors interact directly with active Rac and regulate the actin cytoskeleton by activating Rho. *Curr Biol*, 11(5):339–44.

[Dugaiczyk et al., 1975] Dugaiczyk, A., Boyer, H. W., and Goodman, H. M. (1975). Ligation of EcoRI endonuclease-generated DNA fragments into linear and circular structures. *J Mol Biol*, 96(1):171–84.

[Fan and Raper, 1995] Fan, J. and Raper, J. A. (1995). Localized collapsing cues can steer growth cones without inducing their full collapse. *Neuron*, 14(2):263–74.

[Faustino and Cooper, 2003] Faustino, N. A. and Cooper, T. A. (2003). Pre-mRNA splicing and human disease. *Genes Dev*, 17(4):419–37.

[Feiner et al., 2001] Feiner, L., Webber, A. L., Brown, C. B., Lu, M. M., Jia, L., Feinstein, P., Mombaerts, P., Epstein, J. A., and Raper, J. A. (2001). Targeted disruption of semaphorin 3C leads to persistent truncus arteriosus and aortic arch interruption. *Development*, 128(16):3061–70.

[Fiore and Püschel, 2003] Fiore, R. and Püschel, A. W. (2003). The function of semaphorins during nervous system development. *Front Biosci*, 8:s484–99.

[Fiore et al., 2005] Fiore, R., Rahim, B., Christoffels, V. M., Moorman, A. F. M., and Püschel, A. W. (2005). Inactivation of the Sema5a gene results in embryonic lethality and defective remodeling of the cranial vascular system. *Mol Cell Biol*, 25(6):2310–9.

[Fishburn et al., 1983] Fishburn, J., Turner, G., Daniel, A., and Brookwell, R. (1983). The diagnosis and frequency of X-linked conditions in a cohort of moderately retarded males with affected brothers. *Am J Med Genet*, 14(4):713–24.

[Fransen et al., 1997] Fransen, E., Camp, G. V., Vits, L., and Willems, P. J. (1997). L1-associated diseases: clinical geneticists divide, molecular geneticists unite. *Hum Mol Genet*, 6(10):1625–1632.

[Frints et al., 2002] Frints, S. G. M., Froyen, G., Marynen, P., and Fryns, J.-P. (2002). X-linked mental retardation: vanishing boundaries between non-specific (MRX) and syndromic (MRXS) forms. *Clin Genet*, 62(6):423–32.

[Fujii et al., 2002] Fujii, T., Nakao, F., Shibata, Y., Shioi, G., Kodama, E., Fujisawa, H., and Takagi, S. (2002). Caenorhabditis elegans PlexinA, PLX-1, interacts with transmembrane semaphorins and regulates epidermal morphogenesis. *Development*, 129(9):2053–63.

[Gauthier and Robbins, 2003] Gauthier, L. R. and Robbins, S. M. (2003). Ephrin signaling: One raft to rule them all? One raft to sort them? One raft to spread their call and in signaling bind them? *Life Sci*, 74(2-3):207–16.

[Gecz et al., 1996] Gecz, J., Gedeon, A. K., Sutherland, G. R., and Mulley, J. C. (1996). Identification of the gene FMR2, associated with FRAXE mental retardation. *Nat Genet*, 13(1):105–8.

[Genomatix, 2005] Genomatix (2005). Promoterinspector. Online Service, http://www.genomatix.de.

[Giger et al., 1998] Giger, R. J., Pasterkamp, R. J., Holtmaat, A. J., and Verhaagen, J. (1998). Semaphorin III: role in neuronal development and structural plasticity. *Prog Brain Res*, 117:133–49.

[Giguere et al., 1994] Giguere, V., Tini, M., Flock, G., Ong, E., Evans, R. M., and Otulakowski, G. (1994). Isoform-specific amino-terminal domains dictate DNA-binding properties of ROR alpha, a novel family of orphan hormone nuclear receptors. *Genes Dev*, 8(5):538–53.

[Giordano et al., 2002] Giordano, S., Corso, S., Conrotto, P., Artigiani, S., Gilestro, G., Barberis, D., Tamagnone, L., and Comoglio, P. M. (2002). The semaphorin 4D receptor controls invasive growth by coupling with Met. *Nat Cell Biol*, 4(9):720–4.

[Gitler et al., 2004] Gitler, A. D., Lu, M. M., and Epstein, J. A. (2004). PlexinD1 and semaphorin signaling are required in endothelial cells for cardiovascular development. *Dev Cell*, 7(1):107–16.

[Gluzman, 1981] Gluzman, Y. (1981). SV40-transformed simian cells support the replication of early SV40 mutants. *Cell*, 23(1):175–82.

[Graham et al., 1992] Graham, I. R., Hamshere, M., and Eperon, I. C. (1992). Alternative splicing of a human alpha-tropomyosin muscle-specific exon: identification of determining sequences. *Mol Cell Biol*, 12(9):3872–3882.

[Gu et al., 2005] Gu, C., Yoshida, Y., Livet, J., Reimert, D. V., Mann, F., Merte, J., Henderson, C. E., Jessell, T. M., Kolodkin, A. L., and Ginty, D. D. (2005). Semaphorin 3E and plexin-D1 control vascular pattern independently of neuropilins. *Science*, 307(5707):265–8.

[Gu et al., 1996] Gu, Y., Shen, Y., Gibbs, R. A., and Nelson, D. L. (1996). Identification of FMR2, a novel gene associated with the FRAXE CCG repeat and CpG island. *Nat Genet*, 13(1):109–13.

[Guillemot et al., 1993] Guillemot, F., Lo, L. C., Johnson, J. E., Auerbach, A., Anderson, D. J., and Joyner, A. L. (1993). Mammalian achaete-scute homolog 1 is required for the early development of olfactory and autonomic neurons. *Cell*, 75(3):463–76.

[Hamelin et al., 1992] Hamelin, M., Scott, I. M., Way, J. C., and Culotti, J. G. (1992). The mec-7 beta-tubulin gene of Caenorhabditis elegans is expressed primarily in the touch receptor neurons. *EMBO J*, 11(8):2885–93.

[Hanahan, 1983] Hanahan, D. (1983). Studies on transformation of Escherichia coli with plasmids. *J Mol Biol*, 166(4):557–80.

[Hardison et al., 1997] Hardison, R. C., Oeltjen, J., and Miller, W. (1997). Long human-mouse sequence alignments reveal novel regulatory elements: a reason to sequence the mouse genome. *Genome Res*, 7(10):959–66.

[Harley et al., 1992] Harley, V. R., Jackson, D. I., Hextall, P. J., Hawkins, J. R., Berkovitz, G. D., Sockanathan, S., Lovell-Badge, R., and Goodfellow, P. N. (1992). DNA binding activity of recombinant SRY from normal males and XY females. *Science*, 255(5043):453–6.

[Hartwig et al., 2005] Hartwig, C., Veske, A., Krejcova, S., Rosenberger, G., and Finckh, U. (2005). Plexin B3 promotes neurite outgrowth, interacts homophilically, and interacts with Rin. *BMC Neurosci*, 6(1):53.

[Hayashi and Yandell, 1993] Hayashi, K. and Yandell, D. W. (1993). How sensitive is PCR-SSCP? *Hum Mutat*, 2(5):338–46.

[Heffner et al., 1990] Heffner, C. D., Lumsden, A. G., and O'Leary, D. D. (1990). Target control of collateral extension and directional axon growth in the mammalian brain. *Science*, 247(4939):217–20.

[Hong et al., 1998] Hong, M., Zhukareva, V., Vogelsberg-Ragaglia, V., Wszolek, Z., Reed, L., Miller, B. I., Geschwind, D. H., Bird, T. D., McKeel, D., Goate, A., Morris, J. C., Wilhelmsen, K. C., Schellenberg, G. D., Trojanowski, J. Q., and Lee, V. M. (1998). Mutation-specific functional impairments in distinct tau isoforms of hereditary FTDP-17. *Science*, 282(5395):1914–7.

[Hu et al., 2001] Hu, H., Marton, T. F., and Goodman, C. S. (2001). Plexin B mediates axon guidance in Drosophila by simultaneously inhibiting active Rac and enhancing RhoA signaling. *Neuron*, 32(1):39–51.

[Huang et al., 1996] Huang, J., Blackwell, T. K., Kedes, L., and Weintraub, H. (1996). Differences between MyoD DNA binding and activation site requirements revealed by functional random sequence selection. *Mol Cell Biol*, 16(7):3893–900.

[Ingraham et al., 1990] Ingraham, H. A., Flynn, S. E., Voss, J. W., Albert, V. R., Kapiloff, M. S., Wilson, L., and Rosenfeld, M. G. (1990). The POU-specific domain of Pit-1 is essential for sequence-specific, high affinity DNA binding and DNA-dependent Pit-1-Pit-1 interactions. *Cell*, 61(6):1021–33.

[Isbister et al., 1999] Isbister, C. M., Tsai, A., Wong, S. T., Kolodkin, A. L., and O'Connor, T. P. (1999). Discrete roles for secreted and transmembrane semaphorins in neuronal growth cone guidance in vivo. *Development*, 126(9):2007–19.

[Ito et al., 2000] Ito, T., Kagoshima, M., Sasaki, Y., Li, C., Udaka, N., Kitsukawa, T., Fujisawa, H., Taniguchi, M., Yagi, T., Kitamura, H., and Goshima, Y. (2000). Repulsive axon guidance molecule Sema3A inhibits branching morphogenesis of fetal mouse lung. *Mech Dev*, 97(1-2):35–45.

[Itoh et al., 2000] Itoh, K., Sakurai, Y., Asou, H., and Umeda, M. (2000). Differential expression of alternatively spliced neural cell adhesion molecule L1 isoforms during oligodendrocyte maturation. *J Neurosci Res*, 60(5):579–586.

[IUPAC, 2005] IUPAC (2005). Abbreviations and symbols for nucleic acids, polynucleotides and their constituents. http://www.chem.qmul.ac.uk/iupac/misc/naabb.html. Commission on Biochemical Nomenclature, CBN.

[Jackson et al., 1997] Jackson, H. A., Bowen, D. J., and Worwood, M. (1997). Rapid genetic screening for haemochromatosis using heteroduplex technology. *Br J Haematol*, 98(4):856–9.

[Jan and Jan, 1994] Jan, Y. N. and Jan, L. Y. (1994). Neuronal cell fate specification in Drosophila. *Curr Opin Neurobiol*, 4(1):8–13.

[Kagoshima and Ito, 2001] Kagoshima, M. and Ito, T. (2001). Diverse gene expression and function of semaphorins in developing lung: positive and negative regulatory roles of semaphorins in lung branching morphogenesis. *Genes Cells*, 6(6):559–71.

[Kaibuchi et al., 1999] Kaibuchi, K., Kuroda, S., and Amano, M. (1999). Regulation of the cytoskeleton and cell adhesion by the Rho family GTPases in mammalian cells. *Annu Rev Biochem*, 68:459–86.

[Kameyama et al., 1996a] Kameyama, T., Murakami, Y., Suto, F., Kawakami, A., Takagi, S., Hirata, T., and Fujisawa, H. (1996a). Identification of a neuronal cell surface molecule, plexin, in mice. *Biochem Biophys Res Commun*, 226(2):524–9.

[Kameyama et al., 1996b] Kameyama, T., Murakami, Y., Suto, F., Kawakami, A., Takagi, S., Hirata, T., and Fujisawa, H. (1996b). Identification of plexin family molecules in mice. *Biochem Biophys Res Commun*, 226(2):396–402.

[Kawasaki et al., 1999] Kawasaki, T., Kitsukawa, T., Bekku, Y., Matsuda, Y., Sanbo, M., Yagi, T., and Fujisawa, H. (1999). A requirement for neuropilin-1 in embryonic vessel formation. *Development*, 126(21):4895–902.

[Kennedy et al., 1994] Kennedy, T. E., Serafini, T., de la Torre, J. R., and Tessier-Lavigne, M. (1994). Netrins are diffusible chemotropic factors for commissural axons in the embryonic spinal cord. *Cell*, 78(3):425–35.

[Kenwrick et al., 2000] Kenwrick, S., Watkins, A., and Angelis, E. D. (2000). Neural cell recognition molecule L1: relating biological complexity to human disease mutations. *Hum Mol Genet*, 9(6):879–86.

[Kerr et al., 1991] Kerr, B., Turner, G., Mulley, J., Gedeon, A., and Partington, M. (1991). Non-specific X linked mental retardation. *J Med Genet*, 28(6):378–82.

[King and Stansfield, 1990] King, R. C. and Stansfield, W. D. (1990). *A dictionary of genetics*. Oxford University Press.

[Kolodkin and Ginty, 1997] Kolodkin, A. L. and Ginty, D. D. (1997). Steering clear of semaphorins: neuropilins sound the retreat. *Neuron*, 19(6):1159–62.

[Kolodkin et al., 1993] Kolodkin, A. L., Matthes, D. J., and Goodman, C. S. (1993). The semaphorin genes encode a family of transmembrane and secreted growth cone guidance molecules. *Cell*, 75(7):1389–99.

[Kolodkin et al., 1992] Kolodkin, A. L., Matthes, D. J., O'Connor, T. P., Patel, N. H., Admon, A., Bentley, D., and Goodman, C. S. (1992). Fasciclin IV: sequence, expression, and function during growth cone guidance in the grasshopper embryo. *Neuron*, 9(5):831–45.

[Krawczak et al., 1992] Krawczak, M., Reiss, J., and Cooper, D. N. (1992). The mutational spectrum of single base-pair substitutions in mRNA splice junctions of human genes: causes and consequences. *Hum Genet*, 90(1-2):41–54.

[Kumanogoh and Kikutani, 2003] Kumanogoh, A. and Kikutani, H. (2003). Immune semaphorins: a new area of semaphorin research. *J Cell Sci*, 116(Pt 17):3463–70.

[Kutach and Kadonaga, 2000] Kutach, A. K. and Kadonaga, J. T. (2000). The downstream promoter element DPE appears to be as widely used as the TATA box in Drosophila core promoters. *Mol Cell Biol*, 20(13):4754–64.

[Lazarini et al., 2003] Lazarini, F., Tham, T. N., Casanova, P., Arenzana-Seisdedos, F., and Dubois-Dalcq, M. (2003). Role of the alpha-chemokine stromal cell-derived factor (SDF-1) in the developing and mature central nervous system. *Glia*, 42(2):139–48.

[Lehrke, 1974] Lehrke, R. G. (1974). X-linked mental retardation and verbal disability. *Birth Defects Orig Artic Ser*, 10(1):1–100.

[Leonard and Wen, 2002] Leonard, H. and Wen, X. (2002). The epidemiology of mental retardation: challenges and opportunities in the new millennium. *Ment Retard Dev Disabil Res Rev*, 8(3):117–34.

[Letourneau, 1975] Letourneau, P. C. (1975). Possible roles for cell-to-substratum adhesion in neuronal morphogenesis. *Dev Biol*, 44(1):77–91.

[Li et al., 2004] Li, J. Z., Vawter, M. P., Walsh, D. M., Tomita, H., Evans, S. J., Choudary, P. V., Lopez, J. F., Avelar, A., Shokoohi, V., Chung, T., Mesarwi, O., Jones, E. G., Watson, S. J., Akil, H., Bunney, W. E., and Myers, R. M. (2004). Systematic changes in gene expression in postmortem human brains associated with tissue pH and terminal medical conditions. *Hum Mol Genet*, 13(6):609–16.

[Li et al., 1995] Li, X., Park, W. J., Pyeritz, R. E., and Jabs, E. W. (1995). Effect on splicing of a silent FGFR2 mutation in Crouzon syndrome. *Nat Genet*, 9(3):232–3.

[Lorson et al., 1999] Lorson, C. L., Hahnen, E., Androphy, E. J., and Wirth, B. (1999). A single nucleotide in the SMN gene regulates splicing and is responsible for spinal muscular atrophy. *Proc Natl Acad Sci U S A*, 96(11):6307–11.

[Lumsden and Davies, 1983] Lumsden, A. G. and Davies, A. M. (1983). Earliest sensory nerve fibres are guided to peripheral targets by attractants other than nerve growth factor. *Nature*, 306(5945):786–8.

[Maestrini et al., 1996] Maestrini, E., Tamagnone, L., Longati, P., Cremona, O., Gulisano, M., Bione, S., Tamanini, F., Neel, B. G., Toniolo, D., and Comoglio, P. M. (1996). A family of transmembrane proteins with homology to the MET-hepatocyte growth factor receptor. *Proc Natl Acad Sci U S A*, 93(2):674–8.

[Matthes et al., 1995] Matthes, D. J., Sink, H., Kolodkin, A. L., and Goodman, C. S. (1995). Semaphorin II can function as a selective inhibitor of specific synaptic arborizations. *Cell*, 81(4):631–9.

[McPherson et al., 2001] McPherson, J. D., Marra, M., Hillier, L., more, ., and Consortium, I. H. G. M. (2001). A physical map of the human genome. *Nature*, 409(6822):934–41.

[Melo et al., 2002] Melo, K. F. S., Martin, R. M., Costa, E. M. F., Carvalho, F. M., Jorge, A. A., Arnhold, I. J. P., and Mendonca, B. B. (2002). An unusual phenotype of Frasier syndrome due to IVS9 +4C>T mutation in the WT1 gene: predominantly male ambiguous genitalia and absence of gonadal dysgenesis. *J Clin Endocrinol Metab*, 87(6):2500–5.

[Miao et al., 2000] Miao, H. Q., Lee, P., Lin, H., Soker, S., and Klagsbrun, M. (2000). Neuropilin-1 expression by tumor cells promotes tumor angiogenesis and progression. *FASEB J*, 14(15):2532–9.

[Miao et al., 1999] Miao, H. Q., Soker, S., Feiner, L., Alonso, J. L., Raper, J. A., and Klagsbrun, M. (1999). Neuropilin-1 mediates collapsin-1/semaphorin III inhibition of endothelial cell motility: functional competition of collapsin-1 and vascular endothelial growth factor-165. *J Cell Biol*, 146(1):233–42.

[Michelson et al., 2002] Michelson, P., Hartwig, C., Schachner, M., Gal, A., Veske, A., and Finckh, U. (2002). Missense mutations in the extracellular domain of the human neural cell adhesion molecule L1 reduce neurite outgrowth of murine cerebellar neurons. *Hum Mutat*, 20(6):481–2.

[Miles et al., 1998] Miles, C., Elgar, G., Coles, E., Kleinjan, D. J., van Heyningen, V., and Hastie, N. (1998). Complete sequencing of the Fugu WAGR region from WT1 to PAX6: dramatic compaction and conservation of synteny with human chromosome 11p13. *Proc Natl Acad Sci U S A*, 95(22):13068–72.

[Mitelman, 1995] Mitelman, F., editor (1995). *An International System for Human Cytogenetic Nomenclature (1995)*. Karger.

[Modrek and Lee, 2002] Modrek, B. and Lee, C. (2002). A genomic view of alternative splicing. *Nat Genet*, 30(1):13–9.

[Moorman et al., 1993] Moorman, A. F., Boer, P. A. D., Vermeulen, J. L., and Lamers, W. H. (1993). Practical aspects of radio-isotopic in situ hybridization on RNA. *Histochem J*, 25(4):251–66.

[Mueller, 1999] Mueller, B. K. (1999). Growth cone guidance: first steps towards a deeper understanding. *Annu Rev Neurosci*, 22:351–88.

[Mullis and Faloona, 1987] Mullis, K. B. and Faloona, F. A. (1987). Specific synthesis of DNA in vitro via a polymerase-catalyzed chain reaction. *Methods Enzymol*, 155:335–50.

[Murakami et al., 2001] Murakami, Y., Suto, F., Shimizu, M., Shinoda, T., Kameyama, T., and Fujisawa, H. (2001). Differential expression of plexin-A subfamily members in the mouse nervous system. *Dev Dyn*, 220(3):246–58.

[Nadeau et al., 2001] Nadeau, J. H., Balling, R., Barsh, G., Beier, D., Brown, S. D., Bucan, M., Camper, S., Carlson, G., Copeland, N., Eppig, J., Fletcher, C., Frankel, W. N., Ganten, D., Goldowitz, D., Goodnow, C., Guenet, J. L., Hicks, G., de Angelis, M. H., Jackson, I., Jacob, H. J., Jenkins, N., Johnson, D., Justice, M., Kay, S., Kingsley, D., Lehrach, H., Magnuson, T., Meisler, M., Poustka, A., Rinchik, E. M., Rossant, J., Russell, L. B., Schimenti, J., Shiroishi, T., Skarnes, W. C., Soriano, P., Stanford, W., Takahashi, J. S., Wurst, W., Zimmer, A., and Consortium, I. M. M. (2001). Sequence interpretation. Functional annotation of mouse genome sequences. *Science*, 291(5507):1251–5.

[Nakamura et al., 2000] Nakamura, F., Kalb, R. G., and Strittmatter, S. M. (2000). Molecular basis of semaphorin-mediated axon guidance. *J Neurobiol*, 44(2):219–29.

[Neufeld et al., 2005] Neufeld, G., Shraga-Heled, N., Lange, T., Guttmann-Raviv, N., Herzog, Y., and Kessler, O. (2005). Semaphorins in cancer. *Front Biosci*, 10:751–60.

[Nissim-Rafinia and Kerem, 2002] Nissim-Rafinia, M. and Kerem, B. (2002). Splicing regulation as a potential genetic modifier. *Trends Genet*, 18(3):123–7.

[Oakley and Tosney, 1993] Oakley, R. A. and Tosney, K. W. (1993). Contact-mediated mechanisms of motor axon segmentation. *J Neurosci*, 13(9):3773–92.

[Ohta et al., 1995] Ohta, K., Mizutani, A., Kawakami, A., Murakami, Y., Kasuya, Y., Takagi, S., Tanaka, H., and Fujisawa, H. (1995). Plexin: a novel neuronal cell surface molecule that mediates cell adhesion via a homophilic binding mechanism in the presence of calcium ions. *Neuron*, 14(6):1189–99.

[Oinuma et al., 2004] Oinuma, I., Ishikawa, Y., Katoh, H., and Negishi, M. (2004). The Semaphorin 4D receptor Plexin-B1 is a GTPase activating protein for R-Ras. *Science*, 305(5685):862–865.

[Orita et al., 1989a] Orita, M., Iwahana, H., Kanazawa, H., Hayashi, K., and Sekiya, T. (1989a). Detection of polymorphisms of human DNA by gel electrophoresis as single-strand conformation polymorphisms. *Proc Natl Acad Sci U S A*, 86(8):2766–70.

[Orita et al., 1989b] Orita, M., Suzuki, Y., Sekiya, T., and Hayashi, K. (1989b). Rapid and sensitive detection of point mutations and DNA polymorphisms using the polymerase chain reaction. *Genomics*, 5(4):874–9.

[Pasterkamp and Kolodkin, 2003] Pasterkamp, R. J. and Kolodkin, A. L. (2003). Semaphorin junction: making tracks toward neural connectivity. *Curr Opin Neurobiol*, 13(1):79–89.

[Perälä et al., 2005] Perälä, N. M., Immonen, T., and Sariola, H. (2005). The expression of plexins during mouse embryogenesis. *Gene Expr Patterns*, 5(3):355–62.

[Peterson and Morris, 2000] Peterson, M. J. and Morris, J. F. (2000). Human myeloid zinc finger gene MZF produces multiple transcripts and encodes a SCAN box protein. *Gene*, 254(1-2):105–18.

[Polleux et al., 2000] Polleux, F., Morrow, T., and Ghosh, A. (2000). Semaphorin 3A is a chemoattractant for cortical apical dendrites. *Nature*, 404(6778):567–73.

[Puck, 1965] Puck, T. T. (1965). Cell turnover in mammalian tissues: use of cell depletion measurements to calculate x-ray reproductive survival curves in vivo. *Proc Natl Acad Sci U S A*, 54(6):1797–803.

[Ramji and Foka, 2002] Ramji, D. P. and Foka, P. (2002). CCAAT/enhancer-binding proteins: structure, function and regulation. *Biochem J*, 365(Pt 3):561–75.

[Rao et al., 2002] Rao, Y., Wong, K., Ward, M., Jurgensen, C., and Wu, J. Y. (2002). Neuronal migration and molecular conservation with leukocyte chemotaxis. *Genes Dev*, 16(23):2973–84.

[Read and Strachan, 2004] Read, A. and Strachan, T. (2004). *Human Molecular Genetics*. Garland Science, 2. edition edition.

[Reynolds et al., 1989] Reynolds, R., Carey, E. M., and Herschkowitz, N. (1989). Immunohistochemical localization of myelin basic protein and 2',3'-cyclic nucleotide 3'-phosphohydrolase in flattened membrane expansions produced by cultured oligodendrocytes. *Neuroscience*, 28(1):181–8.

[Rohm et al., 2000] Rohm, B., Ottemeyer, A., Lohrum, M., and Püschel, A. W. (2000). Plexin/neuropilin complexes mediate repulsion by the axonal guidance signal semaphorin 3A. *Mech Dev*, 93(1-2):95–104.

[Ropers and Hamel, 2005] Ropers, H.-H. and Hamel, B. C. J. (2005). X-linked mental retardation. *Nat Rev Genet*, 6(1):46–57.

[Ropers et al., 2003] Ropers, H.-H., Hoeltzenbein, M., Kalscheuer, V., Yntema, H., Hamel, B., Fryns, J.-P.,

Chelly, J., Partington, M., Gecz, J., and Moraine, C. (2003). Nonsyndromic X-linked mental retardation: where are the missing mutations? *Trends Genet*, 19(6):316–20.

[Rothberg et al., 1990] Rothberg, J. M., Jacobs, J. R., Goodman, C. S., and Artavanis-Tsakonas, S. (1990). slit: an extracellular protein necessary for development of midline glia and commissural axon pathways contains both EGF and LRR domains. *Genes Dev*, 4(12A):2169–87.

[Roy et al., 2000] Roy, P. J., Zheng, H., Warren, C. E., and Culotti, J. G. (2000). mab-20 encodes Semaphorin-2a and is required to prevent ectopic cell contacts during epidermal morphogenesis in Caenorhabditis elegans. *Development*, 127(4):755–67.

[Sahay et al., 2005] Sahay, A., Kim, C.-H., Sepkuty, J. P., Cho, E., Huganir, R. L., Ginty, D. D., and Kolodkin, A. L. (2005). Secreted semaphorins modulate synaptic transmission in the adult hippocampus. *J Neurosci*, 25(14):3613–20.

[Sambrook and Russell, 2001] Sambrook, J. and Russell, D. (2001). *Molecular cloning: a laboratory manual*. Cold Spring Harbor Laboratory Press, Cold Spring Harbor, New York, 3rd edition.

[Sanger et al., 1977] Sanger, F., Nicklen, S., and Coulson, A. R. (1977). DNA sequencing with chain-terminating inhibitors. *Proc Natl Acad Sci U S A*, 74(12):5463–7.

[Sarkar et al., 1992] Sarkar, G., Yoon, H. S., and Sommer, S. S. (1992). Dideoxy fingerprinting (ddE): a rapid and efficient screen for the presence of mutations. *Genomics*, 13(2):441–3.

[Sato et al., 1990] Sato, M., Ishizawa, S., Yoshida, T., and Shibahara, S. (1990). Interaction of upstream stimulatory factor with the human heme oxygenase gene promoter. *Eur J Biochem*, 188(2):231–7.

[Scherf et al., 2000] Scherf, M., Klingenhoff, A., and Werner, T. (2000). Highly specific localization of promoter regions in large genomic sequences by PromoterInspector: a novel context analysis approach. *J Mol Biol*, 297(3):599–606.

[Schlessinger, 2000] Schlessinger, J. (2000). Cell signaling by receptor tyrosine kinases. *Cell*, 103(2):211–225.

[Schoenherr and Anderson, 1995] Schoenherr, C. J. and Anderson, D. J. (1995). The neuron-restrictive silencer factor (NRSF): a coordinate repressor of multiple neuron-specific genes. *Science*, 267(5202):1360–3.

[Schreyer and Skene, 1991] Schreyer, D. J. and Skene, J. H. (1991). Fate of GAP-43 in ascending spinal axons of DRG neurons after peripheral nerve injury: delayed accumulation and correlation with regenerative potential. *J Neurosci*, 11(12):3738–51.

[Schwaab et al., 1997] Schwaab, R., Oldenburg, J., Lalloz, M. R., Schwaab, U., Pemberton, S., Hanfland, P., Brackmann, H. H., Tuddenham, E. G., and Michaelides, K. (1997). Factor VIII gene mutations found by a comparative study of SSCP, DGGE and CMC and their analysis on a molecular model of factor VIII protein. *Hum Genet*, 101(3):323–32.

[Schwab et al., 1983] Schwab, M., Alitalo, K., Klempnauer, K. H., Varmus, H. E., Bishop, J. M., Gilbert, F., Brodeur, G., Goldstein, M., and Trent, J. (1983). Amplified DNA with limited homology to myc cellular oncogene is shared by human neuroblastoma cell lines and a neuroblastoma tumour. *Nature*, 305(5931):245–8.

[Sekido et al., 1994] Sekido, R., Murai, K., Funahashi, J., Kamachi, Y., Fujisawa-Sehara, A., Nabeshima, Y., and Kondoh, H. (1994). The delta-crystallin enhancer-binding protein delta EF1 is a repressor of E2-box-mediated gene activation. *Mol Cell Biol*, 14(9):5692–700.

[Serafini et al., 1994] Serafini, T., Kennedy, T. E., Galko, M. J., Mirzayan, C., Jessell, T. M., and Tessier-Lavigne, M. (1994). The netrins define a family of axon outgrowth-promoting proteins homologous to C. elegans UNC-6. *Cell*, 78(3):409–24.

[Shapiro and Senapathy, 1987] Shapiro, M. B. and Senapathy, P. (1987). RNA splice junctions of different classes of eukaryotes: sequence statistics and functional implications in gene expression. *Nucleic Acids Res*, 15(17):7155–74.

[Shi et al., 2000] Shi, W., Kumanogoh, A., Watanabe, C., Uchida, J., Wang, X., Yasui, T., Yukawa, K., Ikawa, M., Okabe, M., Parnes, J. R., Yoshida, K., and Kikutani, H. (2000). The class IV semaphorin CD100 plays nonredundant roles in the immune system: defective B and T cell activation in CD100-deficient mice. *Immunity*, 13(5):633–42.

[Simmons et al., 1998] Simmons, A. D., Püschel, A. W., McPherson, J. D., Overhauser, J., and Lovett, M. (1998). Molecular cloning and mapping of human semaphorin F from the Cri-du-chat candidate interval. *Biochem Biophys Res Commun*, 242(3):685–91.

[Simpson, 1995] Simpson, P. (1995). Positive and negative regulators of neural fate. *Neuron*, 15(4):739–42.

[Smale, 1997] Smale, S. T. (1997). Transcription initiation from TATA-less promoters within eukaryotic protein-coding genes. *Biochim Biophys Acta*, 1351(1-2):73–88.

[Smith et al., 1989] Smith, C. W., Patton, J. G., and Nadal-Ginard, B. (1989). Alternative splicing in the control of gene expression. *Annu Rev Genet*, 23:527–77.

[Smith and Birnstiel, 1976] Smith, H. O. and Birnstiel, M. L. (1976). A simple method for DNA restriction site mapping. *Nucleic Acids Res*, 3(9):2387–98.

[Song et al., 1998] Song, H., Ming, G., He, Z., Lehmann, M., McKerracher, L., Tessier-Lavigne, M., and Poo, M. (1998). Conversion of neuronal growth cone responses from repulsion to attraction by cyclic nucleotides. *Science*, 281(5382):1515–8.

[Song and Poo, 2001] Song, H. and Poo, M. (2001). The cell biology of neuronal navigation. *Nat Cell Biol*, 3(3):E81–8.

[Stein and Tessier-Lavigne, 2001] Stein, E. and Tessier-Lavigne, M. (2001). Hierarchical organization of guidance receptors: silencing of netrin attraction by slit through a Robo/DCC receptor complex. *Science*, 291(5510):1928–38.

[Suto et al., 2003] Suto, F., Murakami, Y., Nakamura, F., Goshima, Y., and Fujisawa, H. (2003). Identification and characterization of a novel mouse plexin, plexin-A4. *Mech Dev*, 120(3):385–96.

[Sweatt, 2001] Sweatt, J. D. (2001). The neuronal MAP kinase cascade: a biochemical signal integration system subserving synaptic plasticity and memory. *J Neurochem*, 76(1):1–10.

[Swiercz et al., 2002] Swiercz, J. M., Kuner, R., Behrens, J., and Offermanns, S. (2002). Plexin-B1 directly interacts with PDZ-RhoGEF/LARG to regulate RhoA and growth cone morphology. *Neuron*, 35(1):51–63.

[Takagi et al., 1987] Takagi, S., Tsuji, T., Amagai, T., Takamatsu, T., and Fujisawa, H. (1987). Specific cell surface labels in the visual centers of Xenopus laevis tadpole identified using monoclonal antibodies. *Dev Biol*, 122(1):90–100.

[Takahashi et al., 1999] Takahashi, T., Fournier, A., Nakamura, F., Wang, L. H., Murakami, Y., Kalb, R. G., Fujisawa, H., and Strittmatter, S. M. (1999). Plexin-neuropilin-1 complexes form functional semaphorin-3A receptors. *Cell*, 99(1):59–69.

[Takahashi and Strittmatter, 2001] Takahashi, T. and Strittmatter, S. M. (2001). Plexina1 autoinhibition by the plexin sema domain. *Neuron*, 29(2):429–39.

[Tamagnone et al., 1999] Tamagnone, L., Artigiani, S., Chen, H., He, Z., Ming, G. I., Song, H., Chedotal, A., Winberg, M. L., Goodman, C. S., Poo, M., Tessier-Lavigne, M., and Comoglio, P. M. (1999). Plexins are a large family of receptors for transmembrane, secreted, and GPI-anchored semaphorins in vertebrates. *Cell*, 99(1):71–80.

[Taniguchi et al., 1997] Taniguchi, M., Yuasa, S., Fujisawa, H., Naruse, I., Saga, S., Mishina, M., and Yagi, T. (1997). Disruption of semaphorin III/D gene causes severe abnormality in peripheral nerve projection. *Neuron*, 19(3):519–30.

[Tessier-Lavigne and Goodman, 1996] Tessier-Lavigne, M. and Goodman, C. S. (1996). The molecular biology of axon guidance. *Science*, 274(5290):1123–33.

[Tessier-Lavigne and Placzek, 1991] Tessier-Lavigne, M. and Placzek, M. (1991). Target attraction: are developing axons guided by chemotropism? *Trends Neurosci*, 14(7):303–10.

[Thiel et al., 1998] Thiel, G., Lietz, M., and Cramer, M. (1998). Biological activity and modular structure of RE-1-silencing transcription factor (REST), a repressor of neuronal genes. *J Biol Chem*, 273(41):26891–9.

[Toyofuku et al., 2004] Toyofuku, T., Zhang, H., Kumanogoh, A., Takegahara, N., Yabuki, M., Harada, K., Hori, M., and Kikutani, H. (2004). Guidance of myocardial patterning in cardiac development by Sema6D reverse signalling. *Nat Cell Biol*, 6(12):1204–11.

[Trofatter et al., 1993] Trofatter, J. A., MacCollin, M. M., Rutter, J. L., Murrell, J. R., Duyao, M. P., Parry, D. M., Eldridge, R., Kley, N., Menon, A. G., and Pulaski, K. (1993). A novel moesin-, ezrin-, radixin-like gene is a candidate for the neurofibromatosis 2 tumor suppressor. *Cell*, 72(5):791–800.

[Trusolino and Comoglio, 2002] Trusolino, L. and Comoglio, P. M. (2002). Scatter-factor and semaphorin receptors: cell signalling for invasive growth. *Nat Rev Cancer*, 2(4):289–300.

[Turner et al., 1970] Turner, G., Turner, B., and Collins, E. (1970). Renpenning's syndrome–X-linked mental retardation. *Lancet*, 2(7668):365–6.

[van der Zwaag et al., 2002] van der Zwaag, B., Hellemons, A. J. C. G. M., Leenders, W. P. J., Burbach, J. P. H., Brunner, H. G., Padberg, G. W., and Bokhoven, H. V. (2002). PLEXIN-D1, a novel plexin family member, is expressed in vascular endothelium and the central nervous system during mouse embryogenesis. *Dev Dyn*, 225(3):336–43.

[Verkerk et al., 1991] Verkerk, A. J., Pieretti, M., Sutcliffe, J. S., Fu, Y. H., Kuhl, D. P., Pizzuti, A., Reiner, O., Richards, S., Victoria, M. F., and Zhang, F. P. (1991). Identification of a gene (FMR-1) containing a CGG repeat coincident with a breakpoint cluster region exhibiting length variation in fragile X syndrome. *Cell*, 65(5):905–14.

[Vikis et al., 2000] Vikis, H. G., Li, W., He, Z., and Guan, K. L. (2000). The semaphorin receptor plexin-B1 specifically interacts with active Rac in a ligand-dependent manner. *Proc Natl Acad Sci U S A*, 97(23):12457–62.

[Vulpe et al., 1993] Vulpe, C., Levinson, B., Whitney, S., Packman, S., and Gitschier, J. (1993). Isolation of a candidate gene for Menkes disease and evidence that it encodes a copper-transporting ATPase. *Nat Genet*, 3(1):7–13.

[Walsh and Doherty, 1997] Walsh, F. S. and Doherty, P. (1997). Neural cell adhesion molecules of the immunoglobulin superfamily: role in axon growth and guidance. *Annu Rev Cell Dev Biol*, 13:425–56.

[Watada et al., 2000] Watada, H., Mirmira, R. G., Leung, J., and German, M. S. (2000). Transcriptional and translational regulation of beta-cell differentiation factor Nkx6.1. *J Biol Chem*, 275(44):34224–30.

[Way and Chalfie, 1989] Way, J. C. and Chalfie, M. (1989). The mec-3 gene of Caenorhabditis elegans requires its own product for maintained expression and is expressed in three neuronal cell types. *Genes Dev*, 3(12A):1823–33.

[Weinstein et al., 1991] Weinstein, D. E., Shelanski, M. L., and Liem, R. K. (1991). Suppression by antisense mRNA demonstrates a requirement for the glial fibrillary acidic protein in the formation of stable astrocytic processes in response to neurons. *J Cell Biol*, 112(6):1205–13.

[Whitelaw et al., 1990] Whitelaw, E., Tsai, S. F., Hogben, P., and Orkin, S. H. (1990). Regulated expression of globin chains and the erythroid transcription factor GATA-1 during erythropoiesis in the developing mouse. *Mol Cell Biol*, 10(12):6596–606.

[Wilcox, 1993] Wilcox, J. N. (1993). Fundamental principles of in situ hybridization. *J Histochem Cytochem*, 41(12):1725–33.

[Winberg et al., 1998] Winberg, M. L., Mitchell, K. J., and Goodman, C. S. (1998). Genetic analysis of the mechanisms controlling target selection: complementary and combinatorial functions of netrins, semaphorins, and IgCAMs. *Cell*, 93(4):581–91.

[Winberg et al., 2001] Winberg, M. L., Tamagnone, L., Bai, J., Comoglio, P. M., Montell, D., and Goodman, C. S. (2001). The transmembrane protein Off-track associates with Plexins and functions downstream of Semaphorin signaling during axon guidance. *Neuron*, 32(1):53–62.

[Wingender et al., 2000] Wingender, E., Chen, X., Hehl, R., Karas, H., Liebich, I., Matys, V., Meinhardt, T., Prüß M., Reuter, I., and Schacherer, F. (2000). TRANSFAC: an integrated system for gene expression regulation. *Nucleic Acids Res*, 28(1):316–9.

[Winter et al., 1985] Winter, E., Yamamoto, F., Almoguera, C., and Perucho, M. (1985). A method to detect and characterize point mutations in transcribed genes: amplification and overexpression of the mutant c-Ki-ras allele in human tumor cells. *Proc Natl Acad Sci U S A*, 82(22):7575–9.

[Withers et al., 2000] Withers, G. S., Higgins, D., Charette, M., and Banker, G. (2000). Bone morphogenetic protein-7 enhances dendritic growth and receptivity to innervation in cultured hippocampal neurons. *Eur J Neurosci*, 12(1):106–16.

[Wolf et al., 1996] Wolf, H. K., Buslei, R., Schmidt-Kastner, R., Schmidt-Kastner, P. K., Pietsch, T., Wiestler, O. D., and Blümcke, I. (1996). NeuN: a useful neuronal marker for diagnostic histopathology. *J Histochem Cytochem*, 44(10):1167–71.

[Wong et al., 1999] Wong, J. T., Wong, S. T., and O'Connor, T. P. (1999). Ectopic semaphorin-1a functions as an attractive guidance cue for developing peripheral neurons. *Nat Neurosci*, 2(9):798–803.

[Worzfeld et al., 2004] Worzfeld, T., Püschel, A. W., Offermanns, S., and Kuner, R. (2004). Plexin-B family members demonstrate non-redundant expression patterns in the developing mouse nervous system: an anatomical basis for morphogenetic effects of Sema4D during development. *Eur J Neurosci*, 19(10):2622–32.

[XLMR, 2005] XLMR (2005). The European XLMR Consortium. http://www.molgen.mpg.de/~abt_rop/mr/mrx.html.

[Xue et al., 1993] Xue, D., Tu, Y., and Chalfie, M. (1993). Cooperative interactions between the Caenorhabditis elegans homeoproteins UNC-86 and MEC-3. *Science*, 261(5126):1324–8.

[Yoshikawa et al., 2003] Yoshikawa, S., McKinnon, R. D., Kokel, M., and Thomas, J. B. (2003). Wnt-mediated axon guidance via the Drosophila Derailed receptor. *Nature*, 422(6932):583–8.

[Zanata et al., 2002] Zanata, S. M., Hovatta, I., Rohm, B., and Püschel, A. W. (2002). Antagonistic effects of Rnd1 and RhoD GTPases regulate receptor activity in Semaphorin 3A-induced cytoskeletal collapse. *J Neurosci*, 22(2):471–7.